12-2017

Study of 2,5-Diaminoimidazolone, a Mutagenic Product of Oxidation of Guanine in DNA

Hannah Catherine J. Pollard
East Tennessee State University

Study of 2,5-Diaminoimidazolone, a Mutagenic Product of Oxidation of Guanine in DNA

A thesis
presented to
the Faculty of the Department of Chemistry
East Tennessee State University

In partial fulfillment
of the requirements for the degree
Master of Science in Chemistry

---

by
Hannah Catherine Janson Pollard
December 2017

Dr. Marina Roginskaya, Chair
Dr. Scott Kirkby
Dr. Abbas Shilabin

Keywords: DNA damage, oxidative stress, one-electron oxidant, imidazolone

ABSTRACT

Study of 2,5-Diaminoimidazolone, a Mutagenic Product of Oxidation of Guanine in DNA

by

Hannah Catherine Janson Pollard

2,5-diaminoimidazolone (Iz) is an important product of a 4-electron oxidation of guanine. The present research focuses on the mechanisms of formation of Iz via pathways initiated by guanine oxidation by one-electron oxidants (OEOs) generated by X-ray radiolysis in aqueous solutions. The kinetics of formation and yields of Iz in reactions of native highly polymerized DNA with different OEOs have been compared using an HPLC-based quantitative analysis of low-molecular products generated from the reaction of DNA-bound Iz with primary amines. Mechanisms of Iz formation in DNA have been investigated including oxygen and superoxide dependence as well as the hypothesis that 8-oxo-G, another product of guanine oxidation, is not a major precursor to Iz. Results indicate Iz is produced in significant quantities in DNA from guanine oxidation and the efficiency of its formation correlates with the reduction potential and selectivity of a given OEO.

DEDICATION

To my husband, Kyle, for his unwavering love, support, and encouragement. Thank you for being my best friend.

To my parents, Gus and Darcy, who taught me the value of an education from an early age and have always encouraged me to pursue my dreams.

To my in-laws, Steve and Glenda, who have treated me like family since the moment I met them.

This accomplishment would not have been possible without each of you.

ACKNOWLEDGEMENTS

I am forever indebted to Dr. Marina Roginskaya for her tireless dedication and outstanding mentorship during my graduate studies at ETSU and for accepting me into her research group. I owe many thanks to Drs. Scott Kirkby and Abbas Shilabin for their time serving on my advisory committee as well as their guidance and suggestions. I am beholden to Drs. David Close and Yuriy Razskazovskiy for use of their laboratory spaces and to Dr. Yuriy Razskazovskiy for his input and knowledge regarding my research.

To the faculty and staff of the Chemistry Department for their advice, knowledge, and dedication to all students at East Tennessee State University, I am endlessly grateful for all that you do. I am also appreciative to all my fellow graduate students in the Chemistry Department as well as all previous students in Dr. Roginskaya's research group for their commitment to their education. I know I will continuously be amazed by all your future successes and accomplishments.

TABLE OF CONTENTS

LIST OF TABLES

Table Page

LIST OF FIGURES

Figure Page

LIST OF ABBREVIATIONS

1MeC.....1-methyl cytosine

5-MF 5-methylene-2-furanone

8-oxo-G.....2′-deoxy-8-oxo-7,8-dihydroguanosine

A..... adenine

AIz.....2-amino-5-alkylamino-4H-imidazol-4-one

C..... cytosine

Ctrl-DNA ..... non-pre-oxidized DNA

dIz ..... 2-amino-5-[(2-deoxy-β-D-erythropentofuranosyl)-amino]-4H-imidazol-4-one

DNA..... deoxyribonucleic acid

EA .....ethanolamine

ELISA ..... enzyme-linked immunosorbent assay

FapyG..... 2,6-diamino-4-hydroxy-5-formamidopyrimidine

FBR..... free base release

Fur..... furfural

G.....guanine

GABA ..... γ-aminobutyric acid

HPLC-ESI-MS/MS ..... high-performance liquid chromatography/electrospray ionization tandem mass spectrometry

Iz .....2-amino-5-[(2-deoxy-β-D-erythro-pentofuranosyl)-amino]-4H-imidazol-4-one

Lac..... 1-N-oxycarbonylmethyl-5-methyleneazacyclopent-3-ene

LC-MS ..... liquid chromatography-mass spectrometry

LMP ..... low-molecular-weight product

NHE ..... normal hydrogen electrode

OEO ..... one-electron oxidant

Oz..... 2,2-diamino-4-[(2-deoxy- β-D-erythro-pentofuranosyl)-amino]-2,5-dihydrooxazol-5-one

ROS..... reactive oxygen species

TCA.....tricholoroacetate

Ox-DNA..... pre-oxidized DNA

PDA..... photodiode array

Sp ..... sprioiminodihydantion

ST DNA ..... salmon testes DNA

T ..... thymine

CHAPTER 1

INTRODUCTION

Oxidative Stress and DNA

Oxidation of biological molecules is necessary for the survival of aerobic organisms, as it has been shown to promote cellular signaling and other important processes. However, excessive oxidation of molecules may result in a condition of *oxidative stress*, which can potentially harm the organism. Species capable of inducing oxidative stress are called reactive oxygen species (ROS) and include: the hydroxyl radical ($^{\bullet}OH$), the superoxide radical ($O_2^{\bullet-}$), hydrogen peroxide (H_2O_2), nitric oxide (NO), among others. Oxidative stress is the result of an imbalance between the production of ROS and the body's ability to remove the species or repair the resulting damage.

While ROS are by-products of normal metabolic processes, the overproduction of ROS in the human body has been associated with several diseases and conditions including various cancers,[1] stroke,[2] respiratory diseases,[3] aging,[1] inflammatory diseases,[1,2] and even neurodegenerative diseases such as Huntington's disease,[4] and Alzheimer's disease.[5,6] This overproduction of ROS may be the result of both internal and external factors. Internal factors include abnormal metabolism, infection, and pathological conditions.[7-9] External factors include environmental pollution,[5] UV light,[10] and ionizing radiation.[11,12]

Since deoxyribonucleic acid (DNA) is the major hereditary molecule for most biological organisms, damage to the DNA structure due to oxidative stress plays an important role in all major pathologies associated with oxidative stress. Oxidative damage to DNA due to oxidative stress has been thoroughly investigated. In particular, the effect of ionizing radiation has been of particular interest as an important source of oxidative stress in aerobic organisms.[13-15] This radiation damage to DNA can occur via two routes: direct- and indirect-type damage. Direct-type damage is due to direct ionizations of DNA. An initial event in direct damage is the removal of an electron from DNA (ionization), which leads to the production of DNA electron-loss centers (holes). The electron then rapidly attaches to DNA to form electron-gain centers. Indirect-type damage, which is a dominating process *in vivo*, forms radicals in the surrounding medium, which then attack the DNA. Ionization of water or biomolecules creates oxidative substances including various ROS such as the hydroxyl radical, hydrogen peroxide, and the superoxide radical.

Types of Oxidative Damage to DNA

DNA consists of two major components, a deoxyribose (5-carbon sugar) attached to a phosphate group (commonly referred to as the sugar-phosphate backbone) and four nucleobases (adenine, guanine, thymine, and cytosine). Interactions with ROS can produce a number of oxidative modifications in DNA including damage to the deoxyribose component of the sugar-phosphate backbone, base modifications, single- and double-strand breaks, and DNA-protein or DNA-DNA crosslinks.[1] Under normal metabolic conditions, oxidative damage to DNA is typically repaired by cellular mechanisms. However, during oxidative stress the number of DNA lesions is too large to be handled properly by cellular repair machinery and therefore, some DNA modifications are left unrepaired. These unrepaired lesions are believed to be the cause of many

of the diseases and conditions listed above. In the case of cancers, the oxidative damage to DNA is believed to lead to the activation of oncogenes and the inactivation of tumor suppressor genes, resulting in unregulated cell growth.[16]

Damage to DNA occurs when ROS attack the DNA at either the deoxyribose-phosphate (sugar damage) or the nucleobase (base damage). It has been estimated that 2/3 of the damage occurs at the nucleobases while sugar damage accounts for the remaining 1/3 of total damage.[17]

Base Damage

DNA bases have lower reduction potentials as compared to the DNA-sugar phosphate backbone, and therefore they are more vulnerable to ROS attack. The base with the lowest standard reduction potential is guanine (G) and thus it is the primary base damage target. Reaction with a ROS results in a one-electron oxidation intermediate guanine radical cation ($G^{\bullet+}$). Positive charges formed in DNA due to this process are commonly referred to as holes.[18,19] Additionally, it is assumed that any holes formed in DNA as a result of its oxidation eventually end up at guanines because of charge migration in DNA.[20-22] This has been accounted for by the predominance of guanine degradation products over those of other nucleobases. Guanine has a standard reduction potential of +1.29 V[19], which is considerably lower than for other native DNA nucleobases. Reduction potentials of DNA nucleosides are reported in Table 1, where E° values are reported at pH 7 vs. normal hydrogen electrode (NHE).

Table 1: Relative Standard Reduction Potentials for Nucleobases[19]

DNA Nucleoside	E°, V
Guanosine	1.29
Adenosine	1.42
Thymidine	1.7
Cytosine	1.6

.

Sugar Damage

In addition to base damage, ROS can also abstract hydrogen from one of the five carbon positions present in 2′-deoxyribose, resulting in a 2′-deoxyribosyl radical. Experimental data suggest that DNA damage occurs via a combination of three competing pathways: C1′, C4′, and C5′ sugar hydrogen abstraction by ROS.[23-25] Structures of all possible radicals formed by hydrogen abstraction from 2′-deoxyribose are shown in Figure 1.

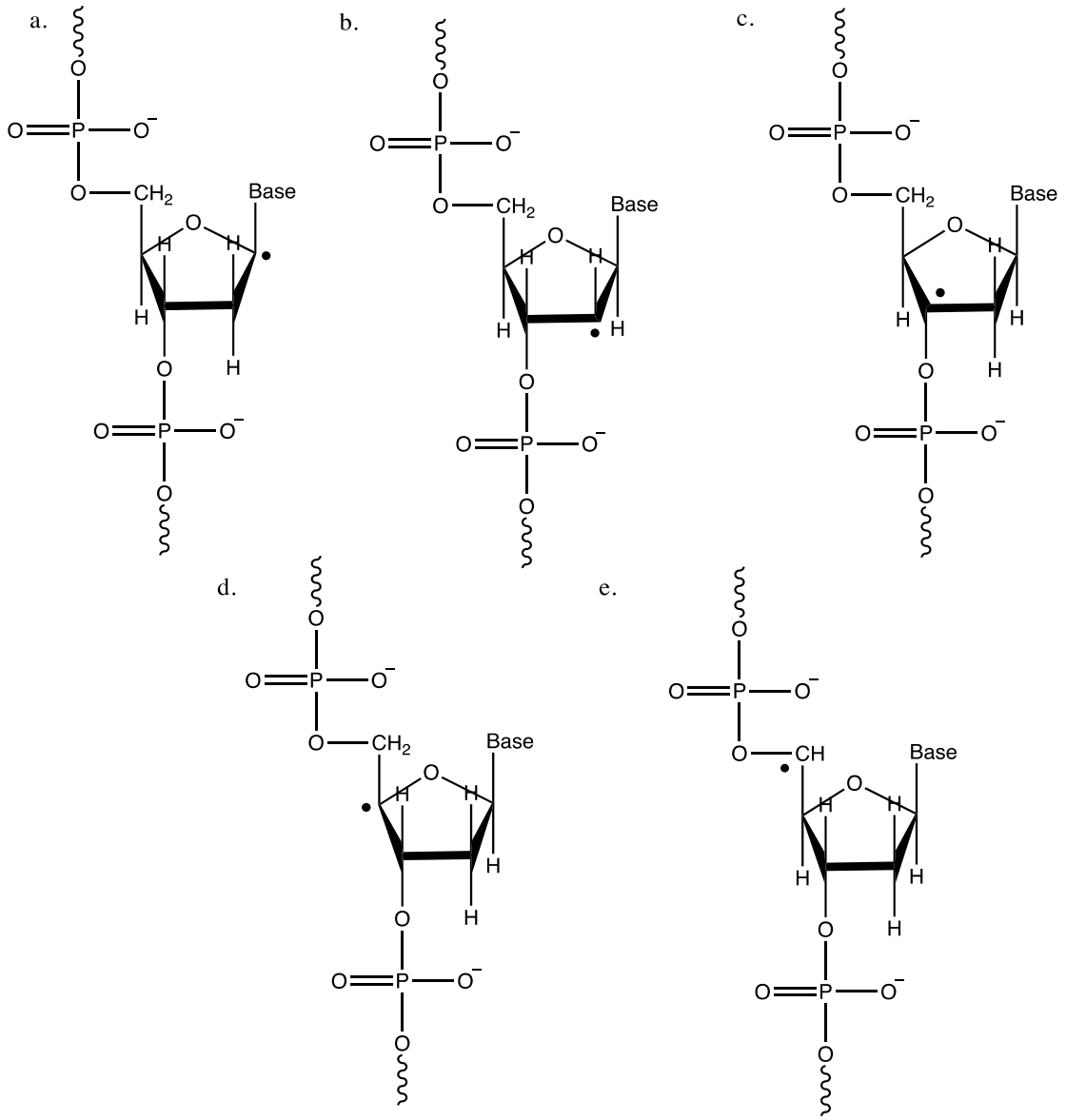

Figure 1: The structures of deoxyribosyl radicals formed via hydrogen abstraction[23]: a) C1′-radical; b) C2′-radical; c) C3′-radical; d) C4′-radical; e) C5′-radical

Mechanisms of Guanine Oxidative Damage

Guanine in DNA has been found to undergo two major pathways of oxidation, which result in a large number of intermediate and final products. However, mechanisms of their formation are not fully understood. The two pathways are via: 1) double-bond attachment with

formation of free-radical adducts, as in one possible reaction of guanine with hydroxyl radical (see Figures 2 and 3), and 2) reactions with one-electron oxidants (OEOs) (see Figure 4). As the hydroxyl radical is abundant in all living organisms, the mechanisms by which this species reacts with the guanine base have been studied more intensely than the alternative oxidation reactions.

Reaction of Guanine with Hydroxyl Radicals

The first proposed pathway involves the attack of the hydroxyl radical (•OH) on one of two guanine carbons, C4 or C8, to form a G(C4-OH)• or G(C8-OH)• adduct, respectively. The hydroxyl radical will preferentially attack the C8 carbon of the purine ring forming the intermediate G(C8-OH)• which can either be further oxidized to form 2′-deoxy-8-oxo-7,8-dihydroguanosine (8-oxo-G)[26,27] or reduced to form 2,6-diamino-4-hydroxy-5-formamidopyrimidine (FapyG)[28,29] as shown in Figure 2.

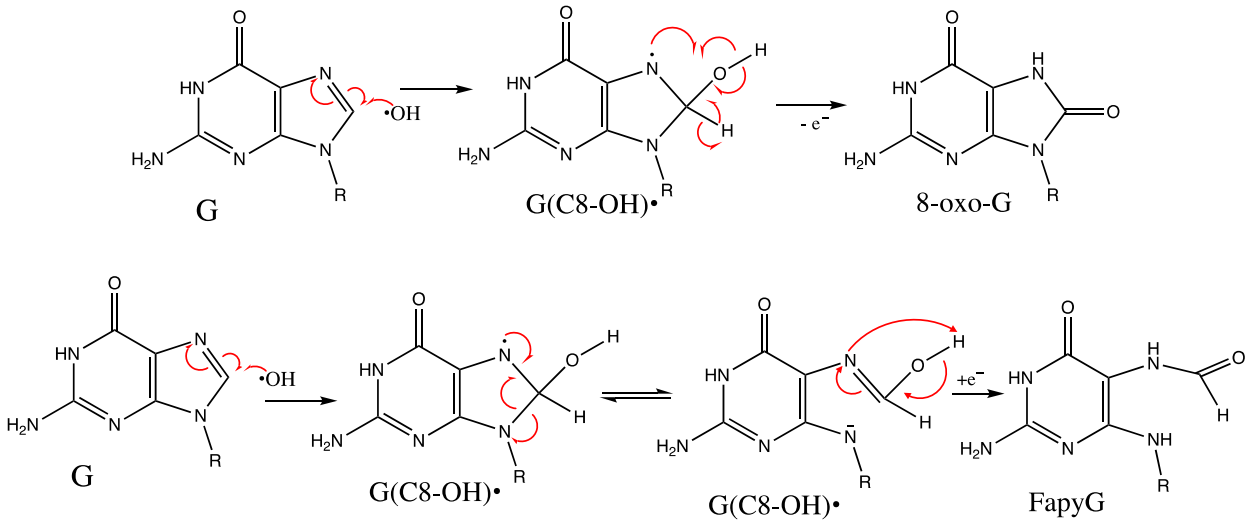

Figure 2: Mechanisms of guanine oxidation by hydroxyl radical at the C8 position[30]

If the hydroxyl radical attacks the C4 carbon in guanine, the C4-OH adduct radical, G(C4-OH)•, is formed. This neutral radical (G•), which can then undergo further oxidation reactions, is formed following a dehydration reaction.[31] According to Raoul *et al.*[31], this neutral radical can further react with molecular oxygen, although this reaction is believed to be slow with a rate constant of $\leq 10^2\ M^{-1}\ s^{-1}$.[32]

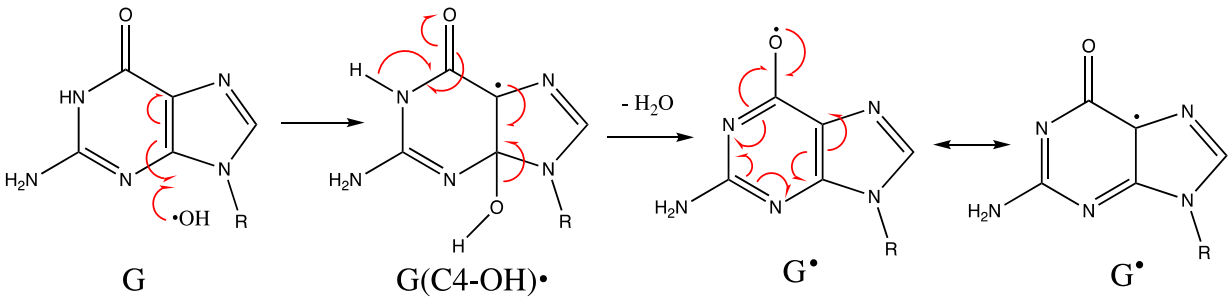

Figure 3: Mechanism of guanine oxidation by hydroxyl radical at the C4 carbon

Reaction of Guanine with One-Electron Oxidants

The second proposed pathway involves reactions of guanine with various OEOs such as carbonate radical anion ($CO_3^{\bullet-}$), selenite radical anion ($SeO_3^{\bullet-}$), sulfate radical anion ($SO_4^{\bullet-}$), or dibromide radical anion ($Br_2^{\bullet-}$). While $SO_4^{\bullet-}$ is a strong oxidant (E^o = +2.43 V) and will readily oxidize any DNA base, the carbonate, selenite, and dibromide radical anions are weaker oxidants (E^o = +1.59, +1.77, and +1.60 V, respectively) and will selectively oxidize guanines in DNA.[33,34] With a high standard reduction potential of +1.90 V at neutral or acidic pH, the hydroxyl radical is capable of acting as an OEO, although its reactivity as an OEO is observed much less often than hydrogen abstraction reactions. This is explained by the fact that reactions involving direct electron transfer to the hydroxyl radical typically occur through the formation of three-electron

bonded intermediate complexes. Such reactions are typically slow due to a high activation energy during the formation of the activated complex.[15]

In the reaction with an OEO, guanine undergoes a one-electron oxidation to form the guanine radical cation ($G^{\bullet+}$). This resulting radical cation is highly unstable and therefore undergoes further reactions. Hypothetical reactions of $G^{\bullet+}$ are summarized in Figure 4. One hypothetical pathway is the fast deprotonation of $G^{\bullet+}$ to form $G(-H)^{\bullet}$ or simply $G^{\bullet}$.[35,36] Electron spin resonance studies have shown that the unpaired electron on the radical cation is mostly localized on the N2, N3, and C8-H while the deprotonation of the $G^{\bullet+}$ occurs via dissociation of the N-H1 proton, resulting in the $G(N1\text{-}H)^{\bullet}$ radical. This neutral radical will then undergo a series of one-electron oxidation reactions resulting in a number of different products including 8-oxo-G. Alternatively, the radical cation, as it is a strong electrophile, can directly react with water to form $G(OH)^{\bullet}$ adducts whose hypothetical reactions were reported above (see Figures 2-3).[36] The reaction schemes for the one-electron oxidation reactions of guanine are summarized below in Figure 4. In neutral pH solutions consisting of free nucleosides or single-stranded DNA the deprotonation of the $G^{+\bullet}$ radical dominates, and thus 8-oxo-G is not efficiently formed. In double stranded DNA, the slightly cationic character of G-C base-pairs reduces the rate of release of the protonation and thus the 8-oxo-G lesions can be more efficiently produced.[37]

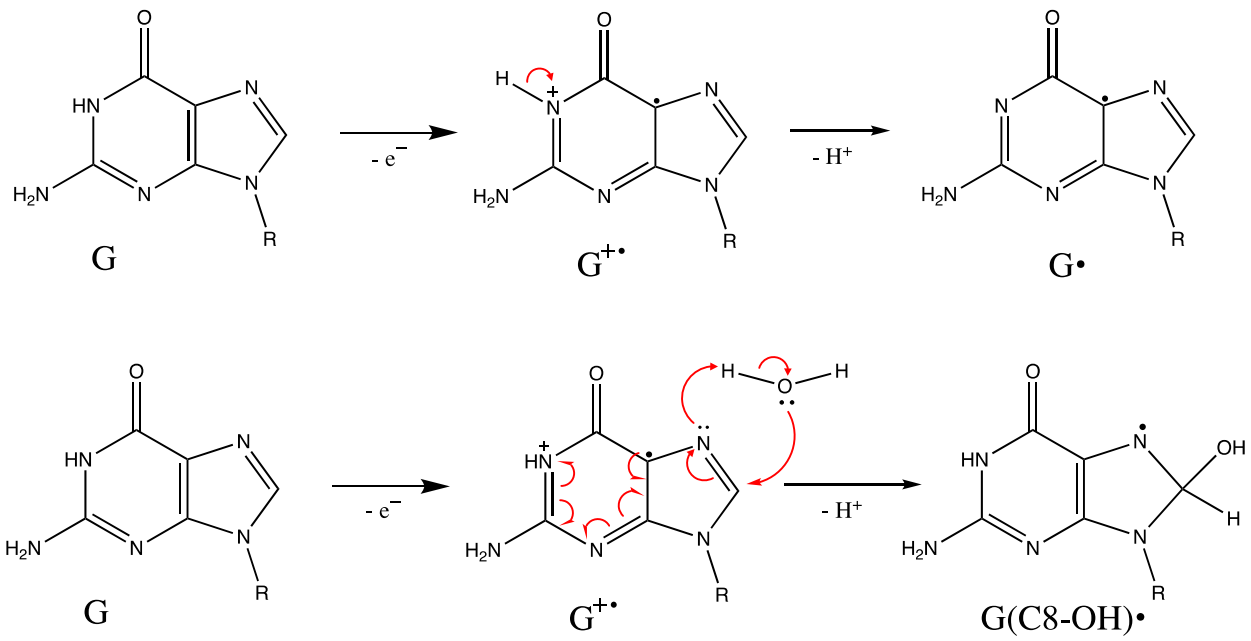

Figure 4: Two possible oxidation mechanisms of guanine oxidation by one-electron oxidants

The guanine radical cation, $G^{\bullet+}$, can also undergo additional nucleophilic reactions that give rise to DNA-protein and DNA-DNA crosslinks.[1] These crosslinks are believed to be genotoxic if left unrepaired.

8-oxo-G as a Biomarker for Oxidative Stress

8-oxo-G has been utilized in recent years as an effective biomarker for oxidative stress. Elevated levels of 8-oxo-G has been found in the lungs of people working or living in environments with high levels of asbestos fibers,[38,39] diesel exhaust particles,[40] and urban polluted areas which all caused an increase in lung cancer morbidity and cardiopulmonary mortality.[41] Because of its low reduction potential, 8-oxo-G is susceptible for further oxidation, which results in the formation of various stable products (Figure 5). All these products of 8-oxo-G oxidation are additional potential biomarkers of oxidative stress.

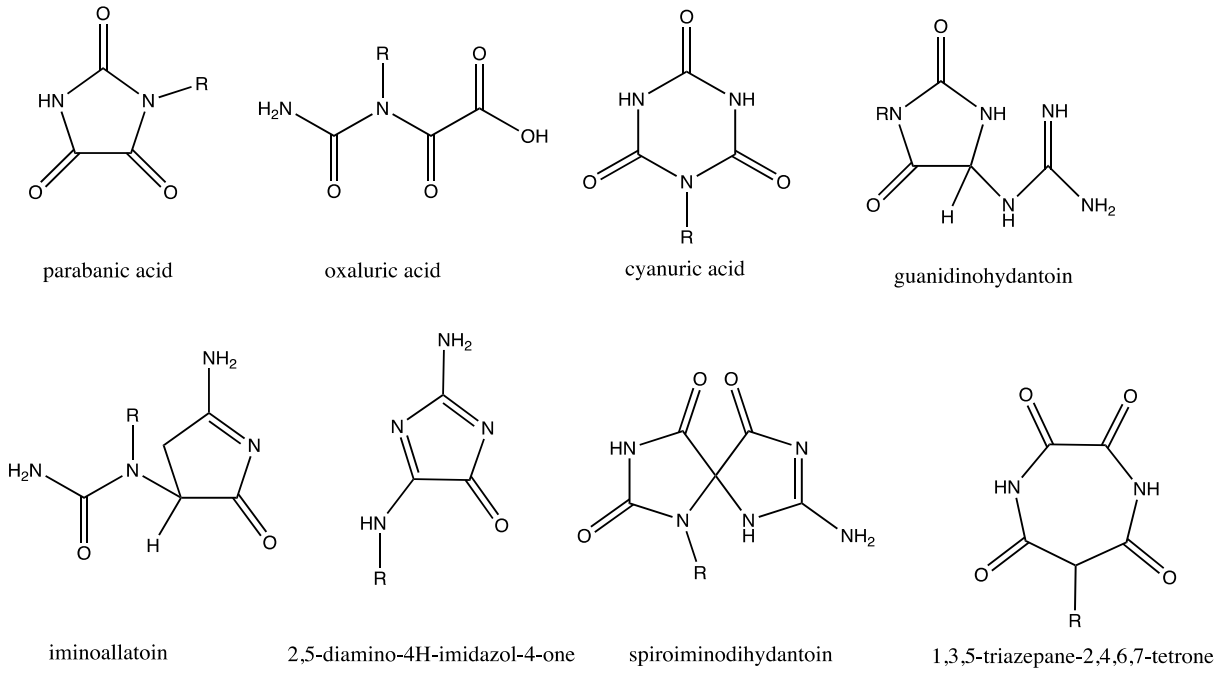

Figure 5: Chemical structures of various products of 8-oxo-G oxidation

Formation Reactions of Imidazolone

The focus of the present study is on the guanine oxidation product 2,5-diamino-4H-imidazol-4-one (imidazolone, or Iz). Iz is thought to be formed via a large number of pathways including reactions with ionizing radiation and OEOs. However, mechanisms of Iz formation remain poorly understood. Hypothetical pathways of formation of Iz described in the literature are discussed below.

Guanine Reaction with Superoxide

Misiaszek *et al.* reported the neutral guanine radical ($G^{\bullet}$) could react with another reactive species, the superoxide radical anion ($O_2^{\bullet -}$), to ultimately form stable guanine oxidation products.[42] The superoxide radical is an important biological intermediate formed from normal metabolic activity which is typically rapidly deactivated in vivo by superoxide dismutase (SOD)

into less reactive H_2O_2 and O_2.[43-45] In addition, $O_2^{\bullet-}$ can be formed from the reaction of dissolved molecular oxygen and electrons generated from ionization reactions.[46] The reported minor product of this reaction is 8-oxo-G and the major product is Iz, which subsequently hydrolyzes into 2,2,4-triamino-5(2H)-oxazolone (oxazolone, or Oz).[31] The low concentrations of 8-oxo-G indicates either a low reaction yield relative to Iz or a further oxidation of 8-oxo-G after it has been formed. The reaction scheme is shown in Figure 6.

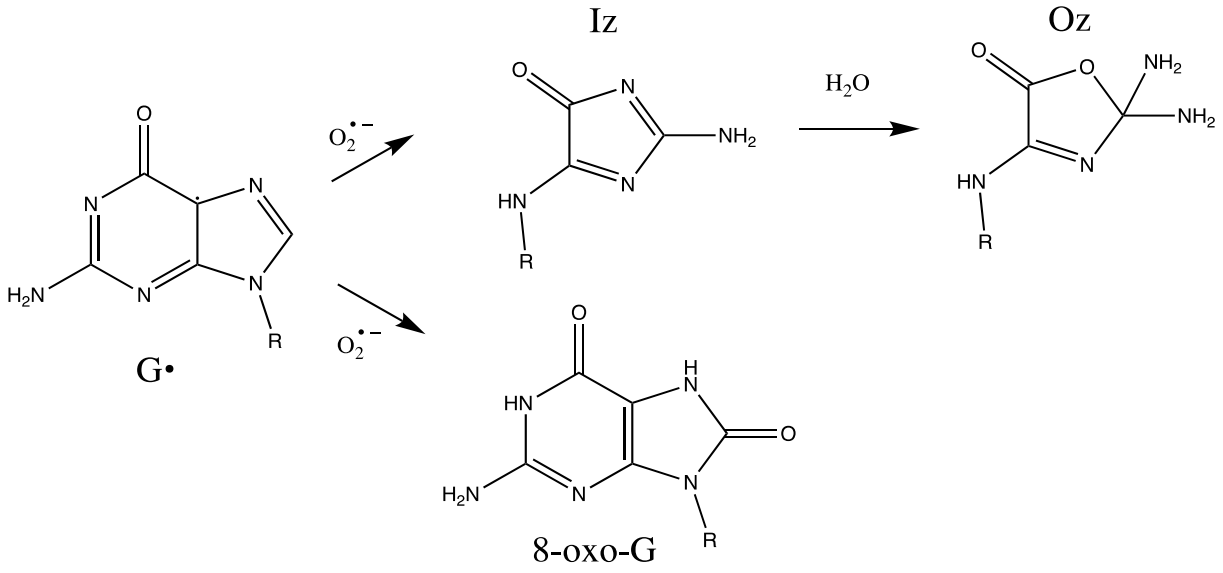

Figure 6: Reaction scheme of the oxidation of guanine radical by superoxide[42]

In this reaction, the guanine radical undergoes tautomerization into a carbon C5-centered radical. Following the addition of superoxide, a 5-hydroperoxide unstable intermediate is formed. This intermediate undergoes a series of complicated reactions and rearrangements that involves the addition of a water molecule, loss of CO_2, loss of formamide, and finally a rearrangement of the purine ring into Iz, as shown in Figure 7. Under normal conditions, the major products of the guanine radical oxidation reaction are the 8-oxo-G lesions where the superoxide radicals are not necessary.[42]

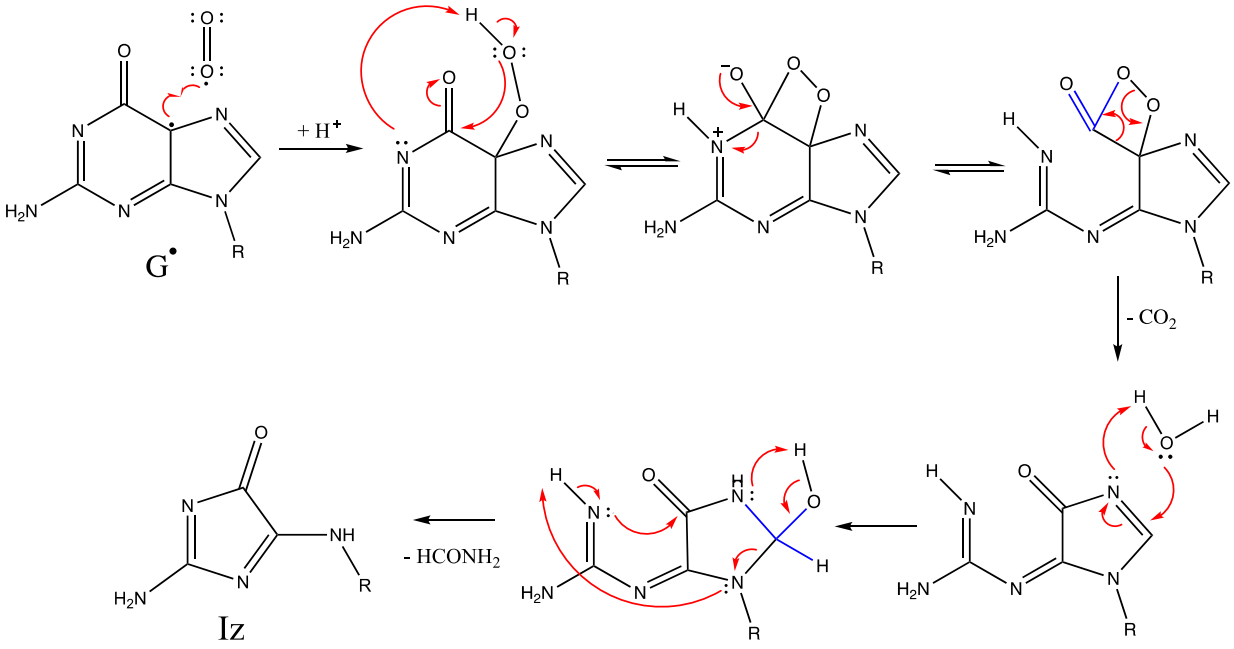

Figure 7: Mechanism of oxidation of guanine radical by superoxide which results in formation of Iz[42]

Guanine Reaction with Singlet Oxygen

Guanine in DNA can also be oxidized with singlet oxygen ($^1O_2$). $^1O_2$ can be generated either through the photodynamic effects of Type II photosensitizers[47-49] or as a side-product of myeloperoxidase reactions.[48,50] This overall 2-electron oxidation reaction is less common then other oxidation reactions for guanine because this reaction requires two individual one-electron oxidation steps with singlet oxygen. Guanine reacts with singlet oxygen to eventually form 8-hydroperoxy-dG. This hydroperoxide can then be reduced to form 8-oxo-G. Following the addition of a second singlet oxygen molecule, the intermediate 4,5-endoperoxide is formed which will rearrange into 5-dihydroperoxy-8-oxo-G. Eventually, the stable product of Oz will be formed from the hydrolysis of Iz.[51] Additionally, Iz has been reported as a minor product from the direct reaction of G with singlet oxygen.[52]

Guanine Reaction with Molecular Oxygen

According to Schmidt-Ullrich *et al*., the neutral guanine radical can react with molecular oxygen to form Iz.[12] If the hydroxyl radical attacks the C4 carbon in guanine followed by a dehydration reaction, a neutral radical (G•) is formed (Figure 3). This neutral radical will subsequently react with molecular oxygen to form Iz. Figure 8 shows the proposed mechanism of this reaction by Cadet *et al*.[53]

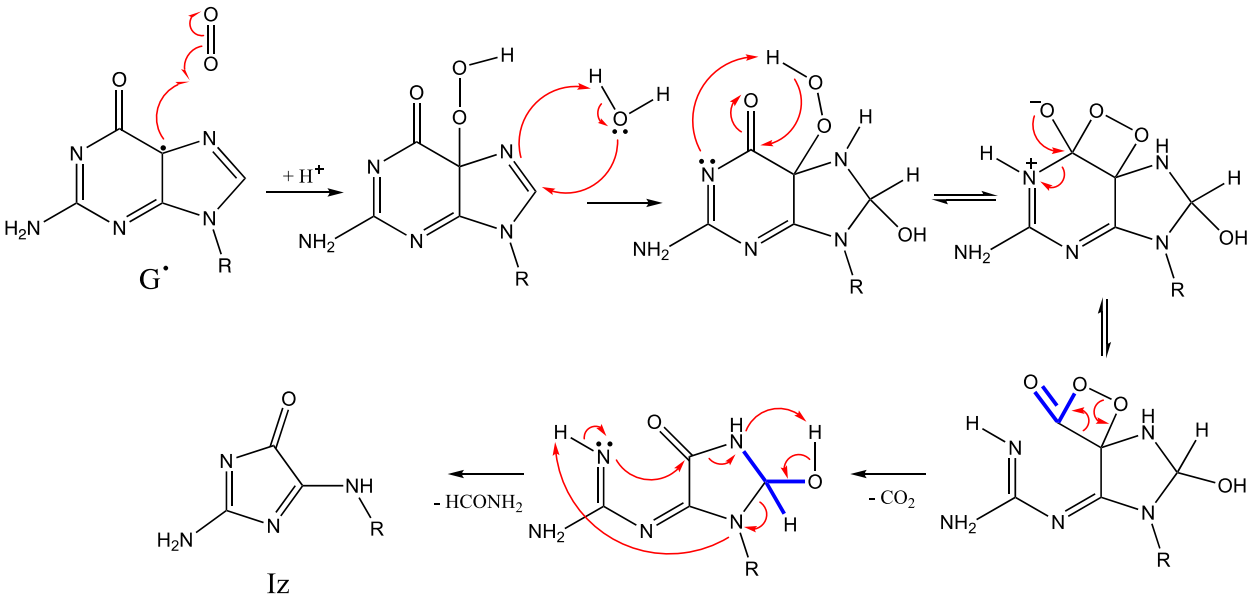

Figure 8: Mechanism of guanine radical reaction with molecular oxygen, resulting in the formation of Iz[54]

Oxidation of 8-oxo-G into Iz

Several studies have proposed that Iz is a major product of oxidation of 8-oxo-G by various oxidants including superoxide, singlet oxygen, peroxynitrite, and by photooxidation in the presence of photosensitizers.[55-58] A proposed mechanism of the oxidation of 8-oxo-G by singlet oxygen can be seen in Figure 9. Kino *et al.* reported that 8-oxo-G, an oxidation product of

G and •OH can be further oxidized into Iz via long-range hole migration. Photoirradiated samples of DNA solutions indicated that the amount of 8-oxo-G initially increased with decreased concentrations of G, then decreased with the formation of Iz. While this evidence suggests that the 8-oxo-G can be further oxidized into Iz, the mechanism still remains poorly understood.[58]

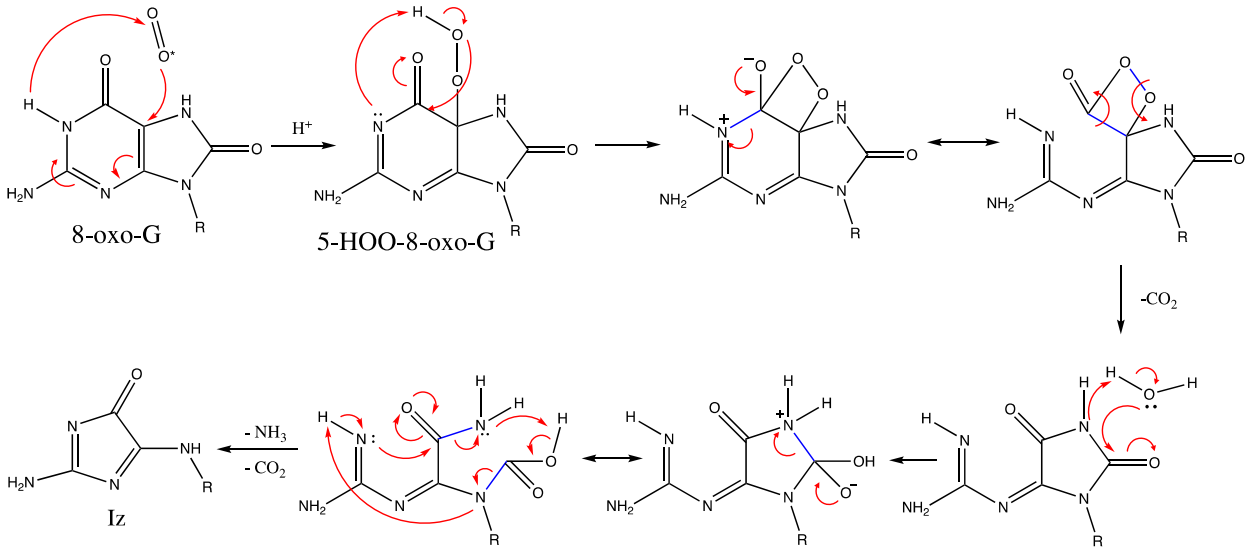

Figure 9: The proposed mechanism of the oxidation of 8-oxo-G by singlet oxygen which results in the formation of Iz[51]

Reactivity of Iz

Hydrolysis of Iz

Iz is inherently unstable; it is readily hydrolyzed to form Oz (Figure 10). Raoul *et al.* reported that in neutral aqueous solutions, Iz is hydrolyzed through the incorporation of one molecule of water into Oz with a half-life of 147 min at 37˚C.[31] This conversion of Iz into Oz has been used to quantify the amount of Iz in oxidatively damaged DNA.

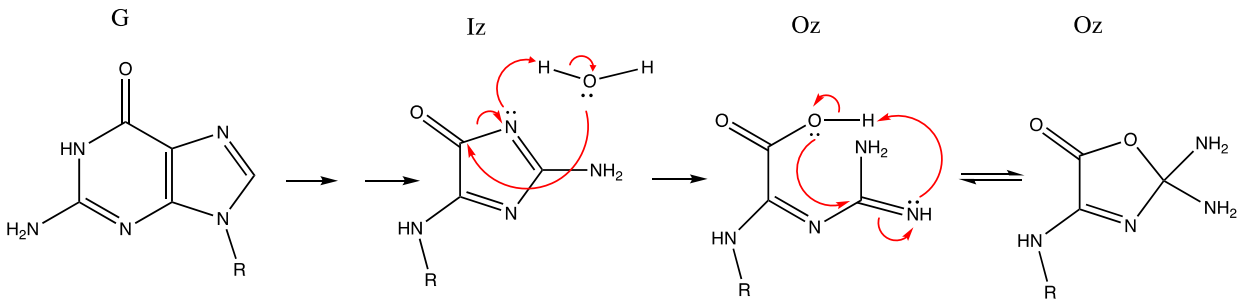

Figure 10: Mechanism for the hydrolysis of Iz into Oz[57]

While 8-oxo-G has been utilized as a biomarker for oxidative stress, it has a low reduction potential and will undergo further oxidation reactions. Because Oz is a stable end product of DNA oxidation, it could potentially be used as another biomarker for oxidative stress.[57] Matter *et al.* reported successful quantitative analysis of Oz both *in vitro* and *in vivo* by isotope dilution-capillary HPLC-ESI-MS/MS.[57]

Iz Reaction with Primary Amines

The reaction between Iz and primary amines with a general formula RNH_2 can compete with the hydrolysis of Iz. This reaction involves the nucleophilic substitution at C5 of the imidazolone ring. As a result of this reaction, a low-molecular weight free amino-derivatized Iz, (AIz) is released from DNA (Figure 11). The reaction was observed to take place with a number of amine derivatives, including methyl, ethyl, and n-propylamines, ethanolamine (EA), and γ-aminobutyric acid (GABA). In addition, this reaction can occur with polyamines or polypeptides that contain primary amino groups, such as spermine, histones, or polylysine.[59]

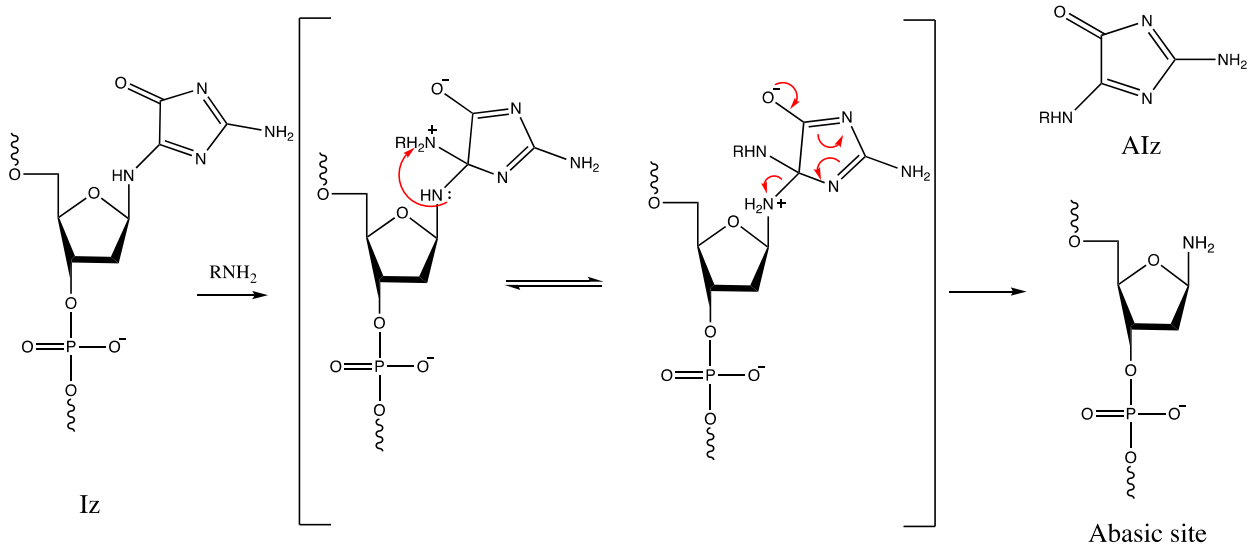

Figure 11: Reaction scheme for Iz with a generic primary amine, resulting in an abasic site and a free-amino derivatized Iz

Biological Properties of Iz

The UV-Vis spectrum for the monomeric form of Iz, 2-amino-5-[(2-deoxy-β-D-erythropentofuranosyl)-amino]-4H-imidazol-4-one or dIz, is shown below in Figure 12. The spectrum for AIz is almost identical to that of dIz and therefore was used to authenticate chromatographic peaks of AIz collected during the present research. In contrast, the spectrum for dOz is quite different, as Oz exhibits an open-ring configuration or a non-conjugated ring structure (not shown).

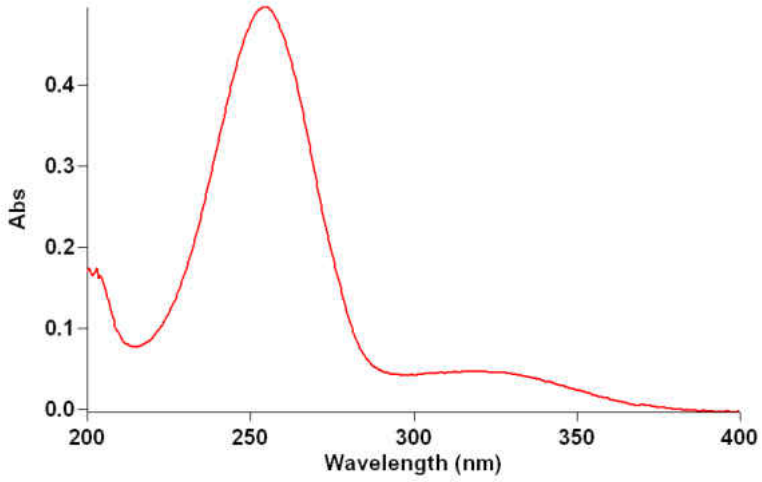

Figure 12: UV-Vis spectrum for dIz

DNA Mutations as a Result of DNA Oxidation

Damage to DNA by ROS can result in cellular death or mutagenesis.[14,15] Point mutations, such as specific base changes and frameshifts have been reported as well as large scale rearrangements of the genome. It has been reported that various guanine oxidation products are mutagenic and can lead to DNA modifications. These mutations frequently occur at important oncogenes. For example, the guanine → cytosine base transversion is frequently at codons 12 and 13 of the Ras oncogene;[60,61] however, the oxidative lesion that causes this base mutation is not known.

As the 8-oxo-G lesion mimics the thymine nucleobase, it can pair with the adenine leading to a GC →TA transversion.[62] Additionally, Sugiyama *et al.* reported that Iz can pair with a guanine molecule leading to a GC → CG base transversion.[58] The frequency of this transversion is reportedly higher during conditions of oxidative stress. Furthermore, the authors reported that guanine was the only nucleobase to be incorporated opposite both Iz and C. These

base pair mutations are summarized in Figure 13. As Iz is supposed to be a significant product formed via the pathway initiated by the one-electron oxidation of guanine[37,54], its role in *in vivo* mutagenesis might be considerably higher than previously believed and it is believed to be at least at mutagenic as 8-oxo-G.

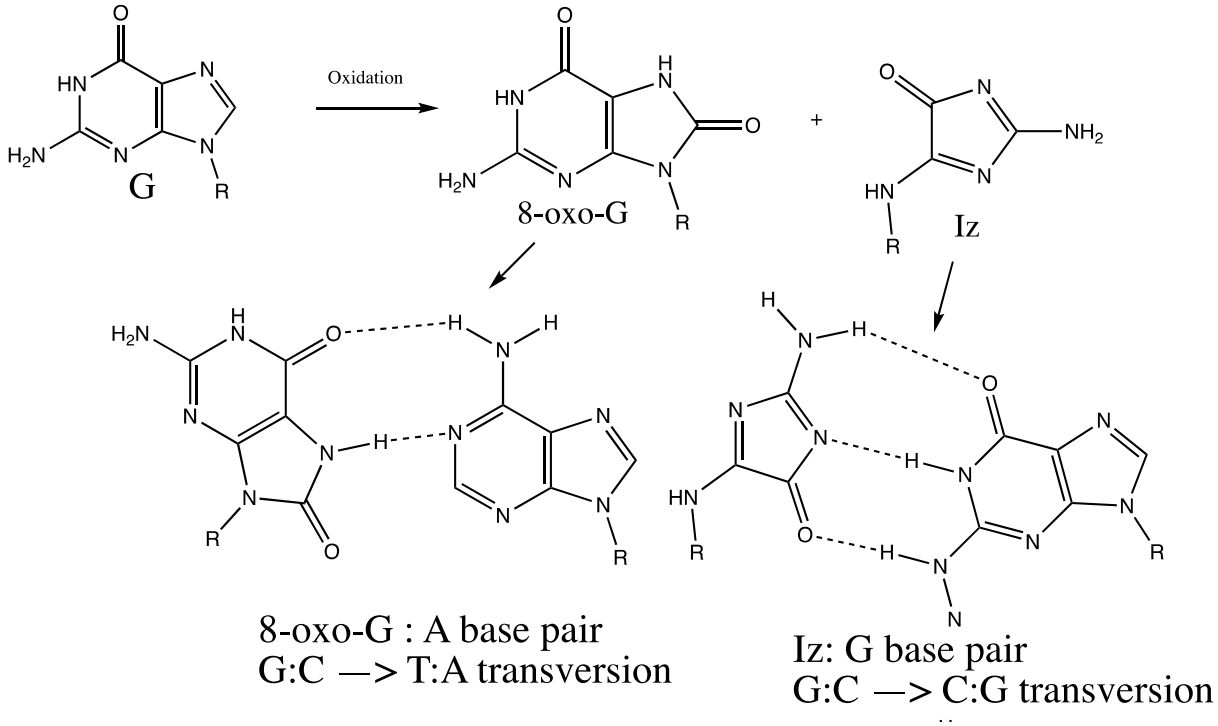

Figure 13: DNA base transversions for 8-oxo-G (GC → TA) and Iz (GC → CG)

It was proposed that Oz, like 8-oxo-G, results in G → T transversions[63], and to some extent G → C transversions.[64] It was shown that Oz-containing DNA in *E. coli* predominately produced G→ T transversions with the mispairing occurring ~10-fold more transversions than 8-oxo-G.[63] While there is experimental evidence that the Iz and Oz lesions are produced in significant quantities under biological conditions, there is still little information about these lesions in living cells. Yu *et al.* reported the yield of Oz formed in solutions of calf thymus DNA

treated with peroxynitrite as the OEO to be ~1 per 10^5 bases, approximately 20% of 8-oxo-G yield.[56] In addition, they reported that the frequencies of G→ T transversions for Oz were found to be ~95%, which is considerably higher than the frequency of similar transversions for 8-oxo-G lesions (~7%).[56] Tretyakova *et al.* reported *in vivo* data with 4-5 Oz lesions per 10^7 normal guanines (approximately 10% of 8-oxo-G lesions) in the livers of diabetic or control rats.[57] Proposed base pairing structures of Oz are shown below in Figure 14.

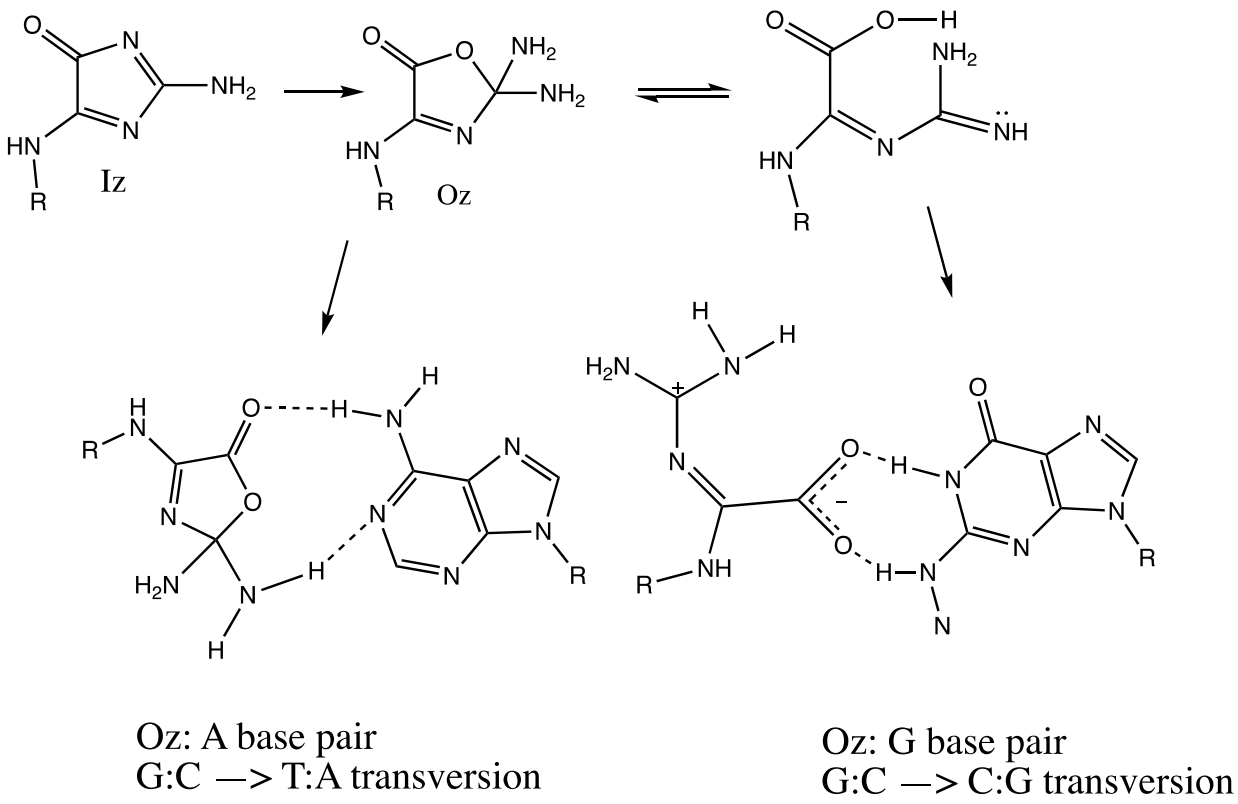

Figure 14: Proposed structures for Oz mutagenic base pairings: G:C → T:A[63] and G:C → C:G[65]

Quantitative Analysis of DNA Damage Products using HPLC

Several methods of quantification of DNA damage products have been developed including HPLC analysis with photodetection or electrochemical detection,[66] enzyme-linked immunosorbent assay (ELISA),[67] GS-MS,[68] and HPLC-MS.[69] Although electrochemical detection is very sensitive, it lacks specificity and requires intense sample preparation. The ELISA method is simple and sensitive, but lacks the selectivity required for determining products. For example, an ELISA study cannot distinguish between 8-oxo-dG and 8-oxo-dGMP, and therefore the accuracy of ELISA has been questioned.[70] GC-MS has excellent sensitivity and selectivity but requires intense sample preparation, making it impractical for large sample testing.

Quantification of Sugar-Damage Products

The Roginskaya research group has elaborated upon an HPLC-based method of quantification of low-molecular-weight products (LMP) released as a result of DNA damage. Initially, the focus was on quantification of LMP released during oxidative damage to DNA 2′-deoxyribose ring (sugar). Oxidized DNA sugar lesions tend to undergo fragmentation of the 2′-deoxyribose ring during heat and/or catalytic treatment. This fragmentation produces a strand break, a free DNA base, and a distinctive LMP product. HPLC-based quantification of the DNA sugar damage at the C4′ position is based on the reaction of oxidized DNA with primary amines in neutral or slightly acidic solutions that results in N-substituted 5-methylene-Δ^3-pyrrolin-2-ones (Lac).[71-74] The proposed mechanism of Lac formation under these conditions is shown in Figure 15.

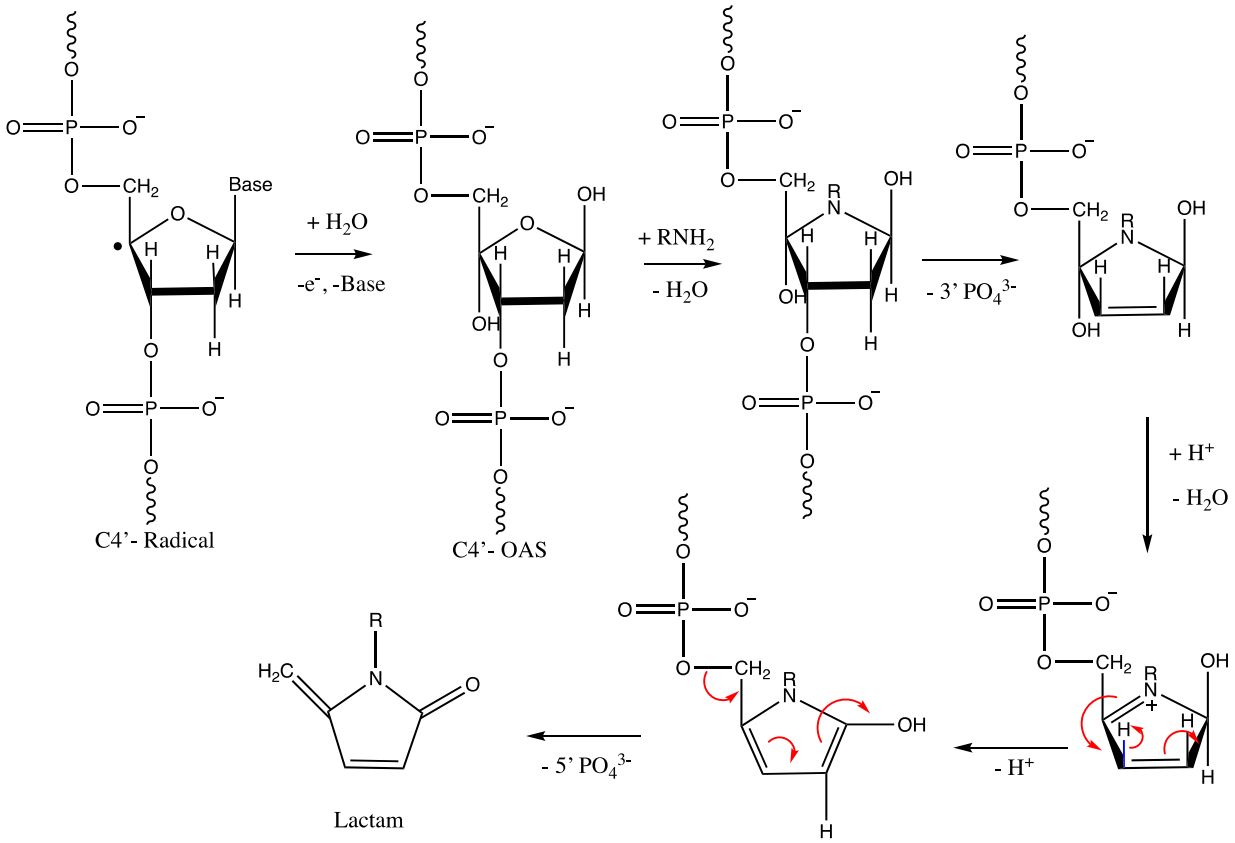

Figure 15: Reaction of C4′-oxidized abasic site with primary amines, which results in the formation of Lac

DNA deoxyribose oxidative damage at the C1′ results in the formation of 5-methylene-2-furanone (5-MF). Irradiation of DNA results in an oxidized abasic site, and release of 5-MF from irradiated DNA was achieved through heat treatment at 90°C in the presence of polyamines and divalent metal cations. Oxidation through the C1′ pathway, and subsequent formation of 5-MF, are believed to contribute significantly to total overall sugar damage (up to ~72%).[24] Deoxyribose oxidative damage to the C5′ results in 5′-aldehydes which are known to release furfural (Fur). Like the C1′ pathway, this release is catalyzed by Lewis acids like polyamines.[25]

The majority of free radical damage to the sugar-phosphate moiety results in the destabilization of the glycosidic bond and subsequent FBR. Therefore, the amount of FBR measured in an irradiated DNA system could serve as an internal benchmark for the total damage inflicted to the sugar-phosphate backbone.[72]

Quantification of 8-oxo-G

Since its discovery, 8-oxo-G has been employed as an effective biomarker for oxidative stress. Several methods of quantitative analysis have been utilized including urine analysis[75,76] as well as HPLC-based techniques.[75-78] HPLC with electrochemical detection has been identified as a sensitive and reliable tool. Derrick Ampadu-Boateng in his MS thesis research in the Roginskaya research group utilized an HPLC-based method of 8-oxo-G quantification with spectrophotometrical detection.[79] In this method, DNA was completely hydrolyzed by boiling in concentrated formic acid which resulted in a nearly quantitative release of all nucleobases, including modified bases (such as 8-oxo-G), which can then be analyzed by HPLC.[79]

Quantification of Iz

Iz is inherently unstable as it readily hydrolyzes to form Oz[31] (see Figure 9), making understanding its mechanisms of formation and its quantitative analysis even more difficult. The premise that the reaction of Iz with primary amines can successfully compete with the hydrolysis of Iz into Oz has allowed for the quantification of Iz through HPLC analysis.

Roginskaya *et al*. first reported a LMP released upon treatment of oxidatively damaged DNA with primary amines in neutral or slightly acidic solutions at moderate temperatures

(<70°C).[72] The retention times of the products were dependent on the structure of the amine and the UV-Vis spectrum was similar to that of dIz (Figure 12).

This product was later identified as 2-amino-5-alkylamino-4H-imidazol-4-one (AIz), a derivative of Iz. A hypothetical mechanism of its formation is shown in Figure 16. The DNA lesion initially produced upon release of AIz is a 1-amino substituted deoxyribose residue which is further hydrolyzed to form an abasic site. Reactions with a number of primary amines revealed the presence of AIz among the products of DNA damage by hydroxyl radicals as well as various OEOs. Unlike Iz, the C-N glycosidic bond in Oz is stable towards hydrolysis at neutral pH and does not contribute to the production of AP sites.[80]

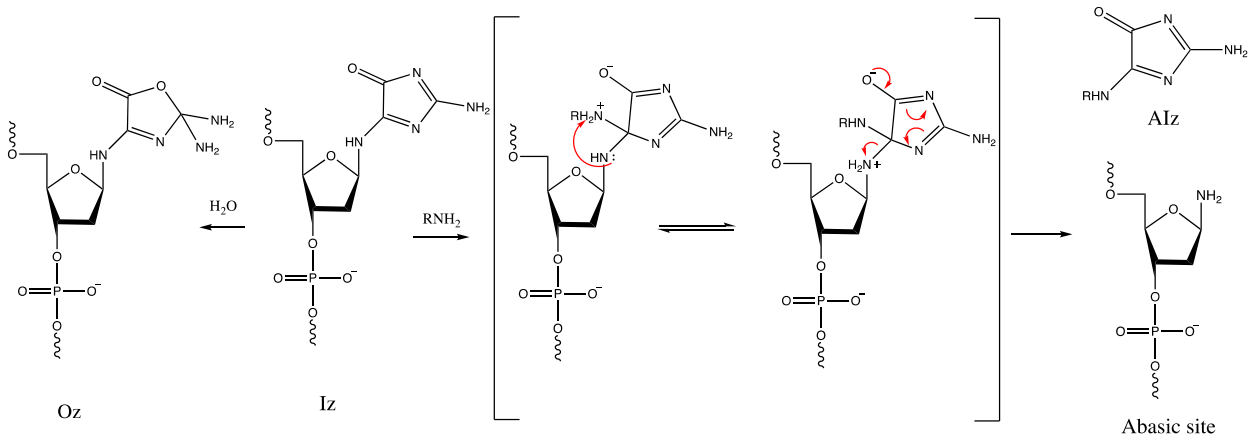

Figure 16: The competing reactions of Iz: hydrolysis into Oz and reaction with primary amines to form AIz.

Biogenic and Model OEOs Used in the Present Study

Various OEOs were utilized throughout the present research to compare the production of DNA oxidation damage products, specifically Iz. Each was selected based on four main criteria:

1. High standard reduction potentials of these radical anions indicating their strong capability of oxidizing guanine in DNA (i.e. larger than +1.29 V)

2. Radiolysis of aqueous solutions generates hydroxyl radicals and solvated electrons with high yields. Ideally, a desired OEO should be a product of reactions with participation of both the hydroxyl radical, and a solvated electron and a precursor to a given OEO, which will ensure maximal conversion of these reactive species into the desired product and minimal impact of undesired side reactions such as attack of $^{\bullet}OH$ on DNA.

3. Minimal contributions of other side reactions, which can obscure the results.

4. Presence of conventional method(s) to generate a given OEO.

Reduction potentials of OEOs used in the present study are shown below in Table 2.

Table 2: Standard Reduction Potentials of Various OEOs[15]

Couple	**E°/V**
$SO_4^{\bullet-}/SO_4^{2-}$	+2.47
$^{\bullet}OH/ H^+, H_2O$	+1.90
$SeO_3^{\bullet-}/ SeO_3^{2-}$	+1.77
$Br_2^{\bullet-}/ 2Br^-$	+1.60
$N_3^{\bullet}/N_3^-$	+1.30

Hydroxyl Radical

The hydroxyl radical ($^{\bullet}OH$) is a versatile and reactive ROS studied in the present research. It is one of the most abundant ROS found in living organisms and it is continuously

formed via the Haber-Weiss reaction, or from the reaction of ferric ions and the hydroxyl anion, without any additional redox agents.[81]

Hydroxyl radicals can also be generated via radiolysis of water through ionization or excitation of water. (The symbol γ represents ionizing radiation).

$$H_2O + \gamma \rightarrow H_2O^{\bullet +} + e^- \text{ (ionization)} \quad (1.1)$$

$$H_2O \rightarrow H_2O^* \text{(excitation)} \quad (1.2)$$

The ionized or excited water molecule then undergoes further reactions to produce the hydroxyl radical:

$$H_2O^{\bullet +} + H_2O \rightarrow H_3O^+ + {}^{\bullet}OH \quad (1.3)$$

$$H_2O^* \rightarrow H^{\bullet} + {}^{\bullet}OH \quad (1.4)$$

Three major reactions of ˙OH have been identified. These are: addition to double bonds, hydrogen abstraction, and electron transfer.[15] The hydroxyl radical will react readily with carbon-carbon double bonds at close to diffusion-controlled rates, but it is regioselective due to its electrophilic nature. There is a high driving force for H-abstraction in saturated hydrocarbons, where the bond-dissociation energy between the carbon and hydrogen is much weaker than the HO-H bond bond-dissociation energy.[15] The hydroxyl radical has a high standard reduction potential of +2.73 V in basic solutions and +1.90 V in acidic or neutral solutions. In spite of such a high standard reduction potential, electron transfer reactions with the hydroxyl radical occur less often than the double-bond addition and hydrogen-abstraction reactions, likely due to the fact that direct electron transfer to ˙OH proceeds via unstable intermediate complexes and hence cannot kinetically compete with the double-bond addition and hydrogen-abstraction reactions.[15]

Dibromide Radical Anion

Hydroxyl radicals may react with halide or pseudohalide ions at close to diffusion-controlled rates, thereby forming a three-electron-bonded adduct radical. These adducts may decompose into $^{\bullet}OH$ and the halide radical which can complex with another halide, forming a dihalogen radical anion (such as $Br_2^{\bullet-}$).[15] This is the case for the dibromide radical anion. Because the initial reaction is very fast, and the formation constant of $Br_2^{\bullet-}$ is large, hydroxyl radicals produced during radiolysis of water in the presence of bromide are nearly quantitatively converted into $Br_2^{\bullet-}$. The reactions, as well as their respective rate constants or equilibrium constants, are summarized below.[15,82]

$$Br^- + {}^{\bullet}OH \rightarrow BrOH^{\bullet-} \ (k = 1.1x10^{10}\ M^{-1}s^{-1}) \quad (1.5)$$

$$BrOH^{\bullet-} \rightarrow Br^{\bullet} + OH^- \ (k = 4.2x10^{6}\ M^{-1}s^{-1}) \quad (1.6)$$

$$Br^{\bullet} + Br^- \rightleftharpoons Br_2^{\bullet-} \ (K = 3.9x10^{5}) \quad (1.7)$$

The dibromide radical anion, with its standard reduction potential of +1.60 V is capable of selectivly oxidizing both purine nucleobases, guanine and adenine.

Sulfate Radical Anion

The sulfate radical anion ($SO_4^{\bullet-}$) can be formed from persulfate, $S_2O_8^{2-}$ either photolytically, or through reaction with e_{aq}^- or $H^{\bullet}$.[46,83]

$$S_2O_8^{2-} + h\nu \rightarrow 2SO_4^{\bullet-} \quad (1.9)$$

$$S_2O_8^{2-} + e_{aq}^- \rightarrow SO_4^{\bullet-} + SO_4^{2-} \ (k = 1.2x10^{10}\ M^{-1}s^{-1}) \quad (1.10)$$

$$S_2O_8^{2-} + {}^{\bullet}H \rightarrow SO_4^{\bullet-} + HSO_4^- \ (k=1.4x10^{7}\ M^{-1}s^{-1}) \quad (1.11)$$

Sulfate radical anions are the strongest oxidant shown in Table 2 (E^o = +2.47 V) and thus react non-selectively with all DNA bases, similar to the hydroxyl radical. As the sulfate radical anion is electrophilic in nature, it will preferentially add to the electron-rich position of a substrate. In addition, the sulfate radical anion can abstract hydrogen from the deoxyribose with the C4' pathway of abstraction dominating over the C1' and C5' pathways. H-abstraction occurs less often with the sulfate radical than with the hydroxyl radical, although the explanation for this still remains unclear.[59]

Selenite Radical Anion

The selenite radical anion ($SeO_3^{\bullet-}$) can be produced radiolytically upon reduction by e_{aq}^- of the selenate anion or oxidation by $^{\bullet}OH$ or the selenite anion:[84]

$$SeO_4^{2-} + e_{aq}^- \rightarrow SeO_3^{\bullet-} \quad (k = 1.4 \times 10^9\ M^{-1}s^{-1}) \tag{1.12}$$

$$SeO_3^{2-} + {}^{\bullet}OH \rightarrow SeO_3^{\bullet-} + OH^- \quad (k = 3.5 \times 10^9\ M^{-1}s^{-1}) \tag{1.13}$$

The selenite radical anion can also be produced by oxidation of the hydroselenite ion with $^{\bullet}OH$.[84]

$$HSeO_3^- + {}^{\bullet}OH \rightarrow SeO_3^{\bullet-} + H_2O \quad (k = 1.6 \times 10^8\ M^{-1}s^{-1}) \tag{1.14}$$

With a relatively high redox potential of +1.77 V, the $SeO_3^{\bullet-}$ is expected to react with nucleobases less selectively than $Br_2^{\bullet-}$.

Azide Radical

The azide radical ($N_3^{\bullet}$) can be produced in the reaction of the hydroxyl radical with the azide anion.[85]

$$N_3^- + {}^{\bullet}OH \rightarrow OH^- + N_3^{\bullet} \quad (k = 1.25 \times 10^{10}\ M^{-1}s^{-1}) \tag{1.15}$$

With a reduction potential only slightly higher than guanine (+1.30 V vs. +1.29 V), it has a boundary potential to oxidize G in DNA, but it is difficult to predict whether it is really capable of this oxidation.

Biologically Relevant OEOs

While the current research mostly focuses on Iz formation in model systems, there are biologically relevant OEOs located or formed in close proximity to DNA in the cell nucleus, including the carbonate radical anions and transition metal cations, first of all, Fe^{3+} and Cu^{2+} ions. These species are capable of oxidizing guanine.

The carbonate radical anion ($CO_3^{\bullet-}$) is an important ROS that is produced *in vivo* by the one-electron oxidation of CO_2 or bicarbonate, a major component of an organism's physiological buffer. With a reduction potential of $CO_3^{\bullet-}/CO_3^{2-}$ = 1.59 V, the carbonate radical anion will selectively oxidize guanine, although it is believed to be a slow hydrogen-abstractor as well.[86] Although $CO_3^{\bullet-}$ is an abundant biologenic ROS, the present research did not focus on the oxidation of guanine by $CO_3^{\bullet-}$. In the present study, ROS were produced by X-ray radiolysis of aqueous solutions and Josh Moore demonstrated in his MS thesis that $CO_3^{\bullet-}$ are not efficiently formed by this method as the rate constant between bicarbonate and hydroxyl radicals is slow (k = 1.0 x 10^7 $M^{-1}s^{-1}$) (Reaction 1.16).[23] Carbonate radical anions are much more efficiently formed through photolysis methods.

$$HCO_3^- + {}^{\bullet}OH \rightarrow H_2O + CO_3^{\bullet-} \quad (k = 1.0 \times 10^7\ M^{-1}s^{-1}) \qquad (1.16)$$

$CO_3^{\bullet-}$ oxidizes guanine with a slow rate constant of 1.5-3.0 x 10^7 $M^{-1}s^{-1}$.[87] The oxidation of guanine by carbonate radical anions leads to the formation of sprioiminodihydantion (Sp), guanidinohydantion (Gh) (see Figure 5 for structures). The Sp lesions are considered the terminal

products of G and 8-oxo-G oxidation by the carbonate radical anion. In addition, Shafirovich *et al.* reported that the oxidation of the single guanine yields intrastrand cross-linked oxidation products.[88]

Fe^{2+} has the capacity to reduce molecular oxygen to superoxide radical (Reaction 1.17), which can then react with DNA.[5]

$$Fe^{2+} + O_2 \rightarrow Fe^{3+} + O_2^{\bullet -} \quad (1.17)$$

In addition, *in vitro* experiments confirmed the production of hydroxyl radicals via the Fenton Reaction (Reaction 1.18).[5]

$$Fe^{2+} + H_2O_2 \rightarrow Fe^{3+} + {}^{\bullet}OH + OH^{-} \quad (1.18)$$

It has been established that oxidative damage to DNA is enhanced by iron and copper cations. In the absence of transition metals, such as iron and copper, DNA is relatively non-reactive with oxidants such as H_2O_2.[38] The products of reactions between DNA, iron, and oxidants are not fully known but include strand breaks, modified bases, DNA-protein cross-links, and modified bases.[89,90]

The cupric ion (Cu^{2+}) can be reduced to cuprous ion (Cu^{+}) which is capable of catalyzing the formation of reactive hydroxyl radicals via the Fenton Reaction (Reaction 1.19)

$$Cu^{+} + H_2O_2 \rightarrow Cu^{2+} + {}^{\bullet}OH + OH^{-} \quad (1.19)$$

Studies have also confirmed that copper is capable of inducing DNA strand breaks and oxidation of bases via oxygen free radicals.[91]

Specific Aims

The overall aim of the current research was to test the hypothesis that DNA-bound imidazolone (Iz), a product of four-electron oxidation of guanine in DNA, is formed in significant quantities as a result of oxidizing of guanine by various one-electron oxidants (OEOs) and to get an insight into the mechanisms of its formation. The first goal of the current research was to optimize the reaction conditions to study the kinetics of Iz accumulation in reactions of native polymerized DNA in aqueous solutions with the following OEOs: hydroxyl radicals ($^{\bullet}OH$), dibromide radical cation ($Br_2^{\bullet-}$), sulfate radical anion ($SO_4^{\bullet-}$), selenite radical anion ($SeO_3^{\bullet-}$), and azide radical ($N_3^{\bullet}$)

Using experimental conditions optimized in Goal 1, the kinetics of Iz formation by the OEOs mentioned in Goal 1 have been studied. The relative yields of Iz and other characteristic LMPs of DNA damage have been compared for each OEO.

Secondly, experiments have been performed to test: i) if the formation of Iz is dependent on the presence of the superoxide radical anion or molecular oxygen and ii) the hypothesis that 8-oxo-G is not a major precursor of Iz.

CHAPTER 2

EXPERIMENTAL METHODS

Instrumentation, Glassware, and Other Materials

Instrumentation

A Prominence High Performance Liquid Chromatograph (from Shimadzu) equipped with an autosampler, degasser, column oven, and a photodiode array (PDA) detector was used as the major instrument for product separation and analysis. The HPLC was equipped with an analytical column from Phenomenex Gemini^{TM} (C18, reversed phase, 250 mm x 4.6 mm, 5μm). A Cary 100 Bio UV-Visible Spectrophotometer (from Agilent) was used to determine concentration of samples, sample analysis, and as a check for complete DNA precipitation. A Phillips X-ray tube with a tungsten anode, courtesy of Dr. David Close (Department of Physics and Astronomy, East Tennessee State University) was used as the source of radiation. Other instrumentation used in the research included a water bath, oven, vortex mixer, microcentrifuge, spin-vacuum system, and laboratory electronic balance (all from Fisher Scientific).

Glassware and Other Materials

Glassware and materials such as beakers, volumetric flasks, graduated cylinders, Pasteur pipettes, glass vials, graduated pipettes, pipette tips, graduated mixed plastic centrifuge tubes 0.5 mL/1.5 mL, centrifuge tubes 15 mL/50 mL, and magnetic stirrers used extensively throughout the experiments were purchased from Fisher Scientific. HPLC inserts (200 μL) from Fisher Scientific

were used to reduce the volume of solution required for HPLC analysis. Quartz cuvettes (50 µL) were used for spectrophotometric measurements.

Reagents

Deoxyribonucleic Acid

Highly polymerized salmon testes DNA sodium salt was purchased from Sigma-Aldrich Chemical Company.

Other Reagents

Reagents used in this study were purchased from Sigma-Aldrich or Fisher Scientific. Sodium bromide was used to produce $Br_2^{\bullet -}$ by radiolysis. Potassium persulfate was used to generate $SO_4^{\bullet -}$ by radiolysis and as an electron scavenger in dibromide systems. Sodium selenate or sodium hydroselenite were used to generate $SeO_3^{\bullet -}$ by radiolysis. Sodium azide was used to generate $N_3^{\bullet}$. Ethanolamine (EA) and sodium acetate were used in the reaction for quantification of Iz. Absolute ethanol and protamine sulfate were used to precipitate DNA. 1-methyl cytosine (1MeC) was used as an internal standard to determine concentration of products generated from the oxidation of DNA. Tricholoroacetate (TCA) was utilized as an electron scavenger to test the dependence of AIz formation on superoxide.

HPLC Solvents

HPLC-grade acetonitrile (from VWR), HPLC-grade water (from Fisher), and ammonium acetate (ACS grade from Fisher) were used for preparation of HPLC solvents. 4 M stock solution of ammonium acetate was prepared by dissolving 154 g of ammonium acetate in 500 mL HPLC grade water. From this stock solution, 40 mM ammonium acetate was prepared for the HPLC aqueous mobile phase and stored at 4˚C. The HPLC organic mobile phase, 80% v/v acetonitrile/water, was prepared by mixing 4 volumes of pure HPLC grade acetonitrile with 1 volume HPLC grade water.

Buffers and Solutions

HPLC-grade water was used for preparation of all stock solutions. 1 M stock solutions of potassium dibasic phosphate K_2HPO_4 and potassium monobasic phosphate KH_2PO_4 (both from Sigma) were mixed in a 1:1 ratio to make a 1 M phosphate buffer, pH 6.9. This was diluted to 10 mM phosphate buffer, pH 6.9 to mimic physiological conditions in the DNA sample solutions.

Preparation of DNA Solutions. 10 mM DNA stock solution was prepared by dissolving 36 mg salmon testes DNA salt (average MW per nucleotide = 360 g/mol) in 10 mL of 10 mM phosphate buffer, pH 6.9. The solution was stored at 4˚C overnight and then the solution was homogenized by gentle stirring. The stock solution was stored at 4˚C.

Other Stock Solutions. 2 M Ethanolamine (EA) used in the reaction for quantification of Iz. 1 M sodium acetate was added to the stock of EA to maintain pH close to neutral. A saturated solution of protamine sulfate from salmon testes was used for the precipitation of DNA. 1 M solution of NaBr was prepared by dissolving 2.573 g NaBr in 25 mL distilled water.

1 M solution of NaN_3 was prepared by dissolving 0.650 g NaN_3 in 10 mL distilled water. 1 M solution of Na_2SeO_4 was prepared by dissolving 1.889 g Na_2SeO_4 in 10 mL distilled water. 2 M solution of $NaHSeO_3$ was prepared by dissolving 3.02 g $NaHSeO_3$ in 10 mL distilled water. 0.1 M solution of $K_2S_2O_8$ was prepared by dissolving 0.2703 g $K_2S_2O_8$ in 10 mL distilled water. This solution was stored at 4ºC. When needed, it was brought to room temperature and stirred to dissolve the crystals. 50 mM solution of 1MeC was produced by dissolving 2.503 g 1-methyl cytosine in 10 mL distilled water. 2 M solution of TCA was prepared by diluting a 6 M TCA solution with distilled water.

Gases

Argon gas (100% purity) and molecular oxygen gas (USP) provided by Airgas were used for sample purging.

Methods of Generation of OEOs

Generation of OEOs by X-Irradiation of Solutions

Preparation of Reaction Solutions. In a typical experiment, a master solution containing appropriate amounts of 10 mM salmon testes DNA (ST DNA) in 10 mM phosphate buffer, pH 6.9 and stock solutions of additives were made as described in Table 3.

Table 3: DNA and OEO Solution Concentrations

Stock Solutions	OEO	Formation reactions	Final Concentrations of Additives
	$^{\bullet}OH$	$H_2O + \gamma \rightarrow H_2O^{\bullet+} + e^-$ $H_2O^{\bullet+} + H_2O \rightarrow H_3O^+ + {}^{\bullet}OH$	-
1 M NaBr	$Br_2^{\bullet-}$	$Br^- + {}^{\bullet}OH \rightarrow BrOH^{\bullet-}$ $BrOH^{\bullet-} \rightarrow Br^{\bullet} + OH^-$ $Br^{\bullet} + Br^- \leftrightarrow Br_2^{\bullet-}$	100 mM NaBr
1 M NaBr 0.1 $K_2S_2O_8$	$Br_2^{\bullet-}$		100 mM NaBr 10 mM $K_2S_2O_8$
1 M Na_2SeO_4	$SeO_3^{\bullet-}$	$SeO_4^{2-} + e_{aq}^- \rightarrow SeO_3^{\bullet-}$	100 mM Na_2SeO_4
2 M $NaHSeO_3$	$SeO_3^{\bullet-}$	$HSeO_3^- + {}^{\bullet}OH \rightarrow SeO_3^{\bullet-} + H_2O$	100 mM $NaHSeO_3$
0.1 M $K_2S_2O_8$	$SO_4^{\bullet-}$	$S_2O_8^{2-} + e_{aq}^- \rightarrow SO_4^{\bullet-} + SO_4^{2-}$	10 mM $K_2S_2O_8$
1 M NaN_3	$N_3^{\bullet}$	$N_3^- + {}^{\bullet}OH \rightarrow OH^- + N_3^{\bullet}$	100 mM NaN_3

X-Irradiation of Reaction Solution. 210 μL aliquots of the master solution were placed into glass vials. The samples were irradiated at room temperature from the bottom with X-ray from a Philips tube with a tungsten anode with doses from ~ 0.1 kGy to ~ 4 kGy (10 s to 6 min), with each experiment containing a non-irradiated control sample. An X-ray tube with tungsten anode operated at 55 kV is characterized by a continuous emission spectrum with the onset at about 10 keV, a maximum around 30 keV, and a sharp cutoff at 55 keV, which corresponds to the maximum energy of the electrons striking the target. The tube was run at 20 mM which produced a dose of 10.9 Gy/s, as previously determined by Fricke dosimetry.[23]

Post-Irradiation Sample Treatments. After irradiation, typically 190 μL of each solution was transferred to a 1.5 mL plastic tube and 10 μL (5% by volume) of 2 M EA in 1 M sodium acetate was added (final concentrations of EA were 0.1 M). The solutions were heated for 30 min

at 45˚C to complete the reaction of Iz with EA, thus converting DNA-bound Iz into a key LMP amino-imidazolone (AIz). After heating, the tubes were cooled on ice for 1 min and then centrifuged to collect the condensate. 30 μL (15% by volume) of saturated protamine sulfate was added to the side of each tube and then vortexed immediately for approximately 30 s. As a result, DNA precipitate was formed. The samples were placed on ice for 15 min to ensure more complete DNA precipitation and then centrifuged for 2 min. 150 μL of the supernatant was collected into HPLC vials fitted with 200 μL HPLC inserts. The samples were analyzed by HPLC with an injection volume of 100 μL.

Superoxide Dependence Experiments

The dependence of superoxide was experimentally tested by adding persulfate (for $Br_2^{\bullet-}$ systems) or TCA (for $^{\bullet}OH$ systems). These species act as electron scavengers, thus suppressing the formation of superoxide which is formed from the reaction of molecular oxygen with solvated electrons. For $Br_2^{\bullet-}$ systems, a master solution containing ~9 mM ST DNA, 100 mM NaBr, and 10 mM $K_2S_2O_8$ was made from 10 mM stock solution of ST DNA in 10 mM phosphate buffer, pH 6.9, 1 M stock solution of NaBr, and 0.1 M stock solution $K_2S_2O_8$. For $^{\bullet}OH$ systems, a master solution containing ~9 mM ST DNA and 20 mM TCA was made from 10 mM stock solution of ST DNA in 10 mM phosphate buffer, pH 6.9, and 2 M TCA. 210 μL aliquot samples were then treated as previously described.

Oxygen Dependence Experiments

A master solution was prepared containing 9 mM ST DNA and either 100 mM NaBr (final concentration), 100 mM NaBr and 10 mM $K_2S_2O_8$ (final concentrations), or no additives (to generate hydroxyl radicals) using 10 mM stock solution of ST DNA in 10 mM phosphate buffer, pH 6.9, 1 M stock solution of NaBr, and 0.1 M stock solution $K_2S_2O_8$. 250 μL aliquots were placed into vials with slightly open screw caps and bubbled either for ~20 min to saturate with argon gas or ~10 min to saturate with oxygen gas. Argon and oxygen saturated samples were treated as previously described.

Generation of Pre-Oxidized DNA

A master solution containing 9 mM ST DNA and 100 mM NaBr (final concentrations) was prepared from 10 mM stock solution of ST DNA in 10 mM phosphate buffer, pH 6.9 and 1 M stock solution of NaBr. Half of the solution (1-1.5 mL) was X-irradiated at ~3 kGy in a 10 mL glass beaker covered with aluminum foil to generate pre-oxidized DNA (Ox-DNA). As shown in Figure 17, the dose of 3 kGy is located in a plateau region of the dose-dependence curve for 8-oxo-G formation.

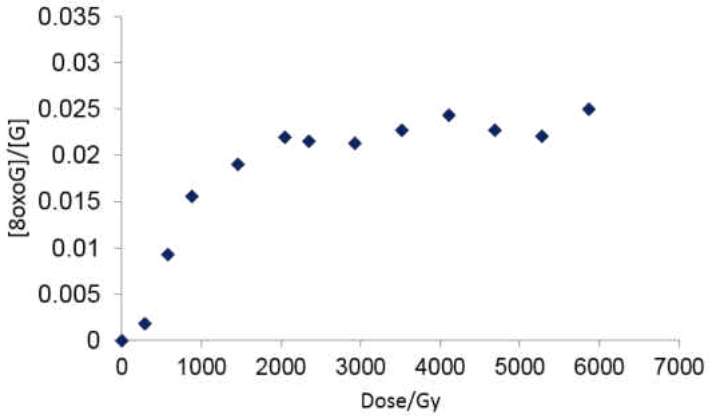

Figure 17: Yields of 8-oxo-G as a function of dose for 10 mM concentration of salmon testes DNA (in nucleotides). DNA solutions were irradiated in the presence of 100 mM NaBr[79]

200 µL aliquots of irradiated (Ox-DNA) or non-irradiated control (Ctrl-DNA) solutions were placed into 1.5 mL plastic centrifuge tubes. Absolute ethanol (EtOH) was added to each sample in a 30:70 v/v ratio of DNA: EtOH and vortexed immediately to precipitate DNA. Samples were kept on ice for 15 min for complete precipitation and then centrifuged for 5 min. Supernatants were removed and the precipitates were washed twice with 500 µL 70% aqueous ethanol. Supernatants were removed and then spin-dried until precipitates were dry. DNA solutions were reconstituted by adding appropriate amounts of 10 mM phosphate buffer, pH 6.9 and 100 mM NaBr (final concentration), if used. Ctrl-DNA and Ox-DNA samples were treated as previously described with varying doses of X-irradiation, followed by treatment with EA, and then saturated protamine sulfate. 115 µL of the supernatant was collected into HPLC vials fitted with 200 µL HPLC inserts. The samples were analyzed by HPLC with an injection volume of 100 µL.

HPLC Analysis

For all HPLC analysis, a two-solvent system was used: 40 mM aqueous ammonium acetate buffer was designated as solvent A, and 80% v/v aqueous acetonitrile was designated as solvent B. The column was equilibrated for a minimum of 30 min with 100% solvent A, followed by a conditioning run (no sample) injection. The flow rate was 1 mL/min, the column temperature was maintained at 30°C, and samples in the auto-sampler tray were kept at 4°C. Optical measurements were performed by a two-lamp photodiode array (PDA), consisting of a deuterium lamp for the UV wavelength range, and a tungsten filament lamp for visible wavelengths.

Linear acetonitrile (solvent B) gradients were applied to elute the products from 0% to 20% over 15 min, which corresponds to a linear increase of acetonitrile from 0% to 16%. Then the concentration of acetonitrile was increased to 40% for 2 min to wash the column. After 20 min from the beginning of the run, PDA detection was ceased, and the system was returned to 100% solvent A and equilibrated for 10 min until the next injection (Figure 18).

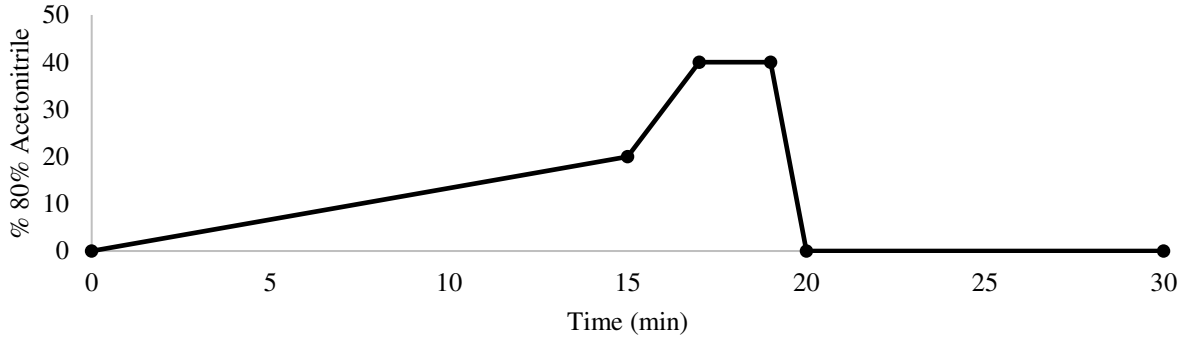

Figure 18: HPLC solvent analysis linear gradient of acetonitrile solvent for a typical sample analysis

Quantification of HPLC Chromatograms

Products were identified based on comparisons of retention times with authentic samples and UV spectra at 254 nm. 1-methyl cytosine (1MeC) was utilized as an internal standard for the quantification of low-molecular products (LMPs) during the initial stages of current work. Using the known concentration of 1MeC in each reaction solution, the concentration of respective products, [X], can be calculated using Equation 2.1 derived from the Beer-Lambert law. Products included both those from guanine oxidation (AIz) and sugar damage (free bases: guanine (G), adenine (A), cytosine (C), thymine (T), as well as lactam (Lac)).

$$\frac{A_x}{A_{1MeC}} = \frac{\varepsilon_X l[X]}{\varepsilon_{1MeC} l[MeC]} = \frac{\varepsilon_X[X]}{\varepsilon_{1MeC}[MeC]} \tag{2.1}$$

A_X is the area under the assigned chromatographic peak of product X, A_{1MeC} is the area under the chromatographic peak of 1MeC, ε_X is the molar extinction coefficient of product X, and ε_{1MeC} is the extinction coefficient for 1MeC. Equation 2.1 can be rearranged into Equation 2.2, which can be easily used to calculate the concentration of any product.

$$[X] = [1MeC]\frac{A_X}{A_{1MeC}}\frac{\varepsilon_{1MeC}}{\varepsilon_X} \tag{2.2}$$

The extinction coefficients for AIz, Lac, and 1MeC were previously experimentally determined by the Roginskaya research group in 40 mM ammonium acetate, pH 6.9. These extinction coefficients are summarized in Table 4.

Table 4: Extinction Coefficients for DNA Damage Products

Product	**Molar extinction coefficient (ε) at 254 nm, $M^{-1}cm^{-1}$**
AIz	15,000
Lactam	8,700
1MeC	4,300
Adenine (A)	11,990
Guanine (G)	9,280
Thymine (T)	6,690
Cytosine (C)	5,070

1MeC gave unreliable and inconsistent data for many experiments when used as in internal standard and for this reason it was not used for all experiments. Instead, areas of the peaks were calibrated using known concentrations of 1MeC and then a recalculation coefficient 'k' was used to convert peak areas into concentrations. Four samples of 4.67 μM 1MeC were analyzed via HPLC and the average area under the 1MeC peaks at 254 nm was measured to be 1.23×10^5. By using the average area for 1MeC, the known extinction coefficient for 1MeC, as well as respective coefficients for various products, a recalculation coefficient 'k' was calculated for each product using Equation 2.2. Recalculation coefficients are shown in Table 5.

Table 5: Recalculation Coefficient 'k' For Each Product

Product	k
C	3.22×10^{-5}
AIz	1.09×10^{-5}
G	1.76×10^{-5}
T	2.44×10^{-5}
A	1.36×10^{-5}
Lac	1.88×10^{-5}

Using the recalculated extinction coefficient, the concentration of each product was calculated using Equation 2.3.

$$[X] = Area_X * k_X \tag{2.3}$$

Concentrations of major products for each OEO (in μM) were plotted against dose (in kGy). The linear portions of the dose response plots were analyzed using linear regression for each product and were used to determine respective radiation chemical yields (in nmol/J) using the fact that:

$$\text{kGy} = \frac{\text{kJ of radiation energy}}{\text{kg of matter}} \tag{2.4}$$

and the assumption that the density of each solution is equivalent to the density of water (1 g/mL = 1 kg/L). Therefore, as shown in Equation 2.5, the slope of the plot is equivalent to radiation chemical yields of products (in nmol/J)

$$Slope = \frac{\mu M}{kGy} = \frac{\mu mol}{L}\frac{kg}{J}\frac{1}{1000} = \frac{nmol}{J} \tag{2.5}$$

CHAPTER 3

RESULTS AND DISCUSSION

The Effect of the Nature of the Oxidant on the Production of Iz

Hydroxyl radicals, $^{\bullet}OH$, and solvated electrons, e_{aq}^{-}, are efficiently generated via the indirect effect during radiolysis of water with the radiation chemical yields of 265 nmol/J.[15] $^{\bullet}OH$ and e_{aq}^{-} are reported to react with DNA with similar second-order rate constants of 2.5 x 10^{8} $M^{-1}s^{-1}$ and 1.4 x 10^{8} $M^{-1}s^{-1}$, respectively.[15] The solvated electron also reacts with oxygen in the solution to form superoxide with a close to diffusion controlled rate constant of $1.9x10^{10}$ $M^{-1}s^{-1}$ [92] OEOs studied in the present work ($Br_2^{\bullet-}$, $SeO_3^{\bullet-}$, $SO_4^{\bullet-}$, and $N_3^{\bullet}$) were produced by X-irradiation of aqueous solutions of ST DNA in the presence of corresponding anions (Br^{-}, SeO_4^{2-} or $HSeO_3^{-}$, $S_2O_8^{2-}$, and N_3^{-}). The assumption of all the experiments described in this section is that since these anions react with $^{\bullet}OH$ or e_{aq}^{-} significantly faster than $^{\bullet}OH$ or e_{aq}^{-} react with DNA, these species, when present in significant concentrations in the solution (e.g. 100 mM), will successfully compete with DNA for the hydroxyl radicals or solvated electrons and will successfully scavenge $^{\bullet}OH$ or e_{aq}^{-}. As a result of the reactions of these anions with $^{\bullet}OH$ or e_{aq}^{-}, the above-mentioned OEOs can be, at least theoretically, formed with high yields and selectivity.

Reaction solutions containing 9 mM DNA in 10 mM phosphate buffer, pH 6.9 and typically 100 mM of additives containing anions of OEOs were prepared following protocols described in Chapter 2. These reaction conditions roughly mimic physiological conditions, with nearly physiological pH and ~0.2 mM of dissolved oxygen in air-saturated solutions at room temperature. The solutions were X-irradiated at a 10.9 Gy/s dose rate for doses ranging from 0 to

~4 kGy. Following irradiation, samples were heated with EA to convert DNA-bound Iz into a key LMP amino-imidazolone (AIz), followed by addition of saturated protamine sulfate to precipitate DNA. Solution supernatants were analyzed by reverse phase HPLC to quantify the yield of each respective product. Each chromatogram is labeled with the 4 DNA nucleobases (C, G, T, and A), 1MeC (when used), AIz, and C4´-sugar damage product lactam (Lac).

Chromatographic peaks were analyzed as discussed in Chapter 2. Replicate experiments (duplicate or triplicate) using the same conditions were performed and average concentrations for each of the aforementioned LMPs were calculated. For each experiment, yields of AIz, Lac, and total FBR (free base release) which is a sum of yields of all four nucleobases released from DNA were plotted as a function of radiation dose and the data were compared for different OEOs as discussed below.

Hydroxyl Radical

The hydroxyl radical, (•OH), is a highly reactive species; in the absence of scavengers it reacts non-selectively with DNA with both the nucleobases and at the deoxyribose moiety. While •OH will preferentially react through H-abstraction of the deoxyribose, resulting in FBR and Lac, it is believed that the hydroxyl radical also reacts with the double bonds in guanine to form the G(OH)• adducts, which then produce a neutral G• radical, a precursor it Iz. A representative chromatogram for this system, indicating all oxidative damage products, is shown below in Figure 19. Dose response curves for each LMP are shown below in Figure 20 and radiation chemical yields are shown in Table 6.

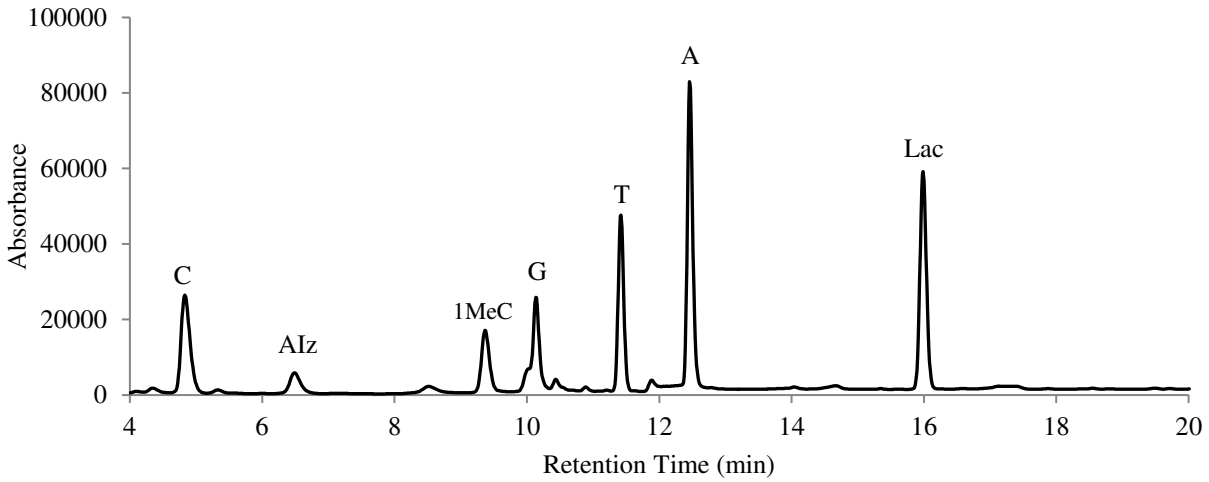

Figure 19: Representative chromatogram showing peaks for LMPs of DNA damage by hydroxyl radicals produced by X-irradiation of 9 mM DNA solution in 10 mM phosphate buffer, pH 6.9 at 0.69 kGy. 1MeC was added into the solution as an internal standard.

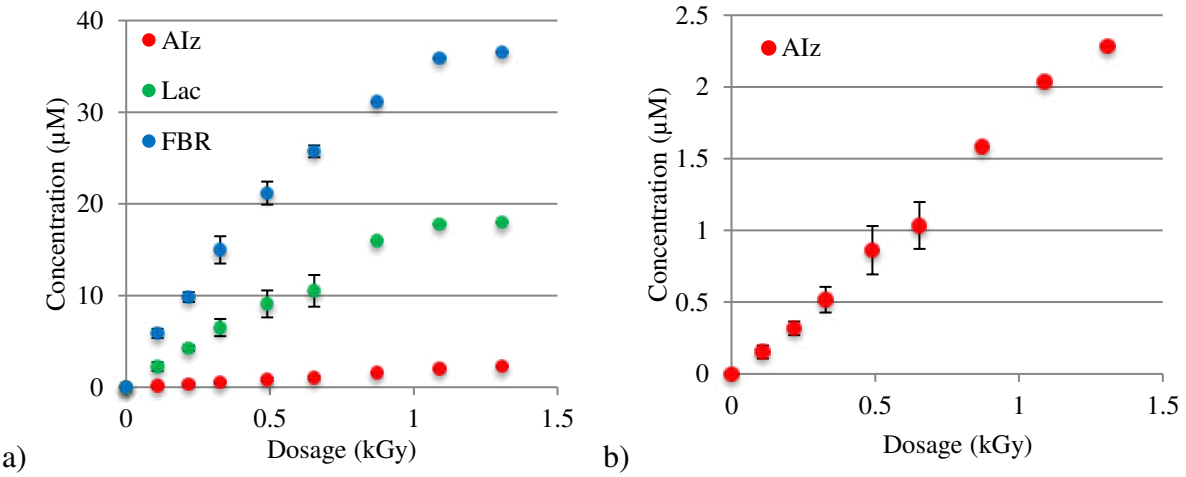

Figure 20: Dose dependence of the yields of a) major LMPs and b) AIz alone as a result DNA oxidation by •OH. Reaction conditions are the same as indicated in the previous figure

As it may be seen from the dose response curve in Figure 20b, AIz accumulates linearly during practically all ranges of the radiation doses used, while dose response curves of Lac and FBR plateau off at higher doses as seen in Figure 20a. Relative contribution of AIz to the overall damage of DNA by $^{\bullet}OH$ is low, only ~ 4%, (Table 6), indicating that $^{\bullet}OH$ does in fact react primarily though H-abstraction rather than with guanine. Our method of post-irradiation treatment of the samples with EA has been optimized for the quantitative analysis of Iz based on the yields of AIz. These conditions are not optimal for quantification of characteristic LMPs of 2-deoxyribose damage by $^{\bullet}OH$, *i.e.* FBR and Lac. Nevertheless, radiation chemical yields of FBR and Lac in the present experiment (44.4 and 19.1 nmol/J, respectively, see Table 6) approach those described in an earlier work of Roginskaya research group (51.0 and 18.1 nmol/J, respectively).[72]

Dibromide Radical Anion

$Br_2^{\bullet-}$ produced in 100 mM solution of NaBr. Unlike $^{\bullet}OH$ or $SO_4^{\bullet-}$, $Br_2^{\bullet-}$ is a very inefficient hydrogen abstractor[15] and hence no production of FBR or Lac is expected in its reaction with DNA provided that $^{\bullet}OH$ undergo 100% conversion into $Br_2^{\bullet-}$ via Reactions 1.5-1.7. However, as a representative chromatogram in Figure 21 shows, while AIz is the major product in this system, free base release and production of Lac also occur. Dose response curves (Figure 22) show that all products of DNA damage by $Br_2^{\bullet-}$ accumulate linearly up to doses of ~ 4 kGy, which is quite a high dose for aqueous solutions of DNA.

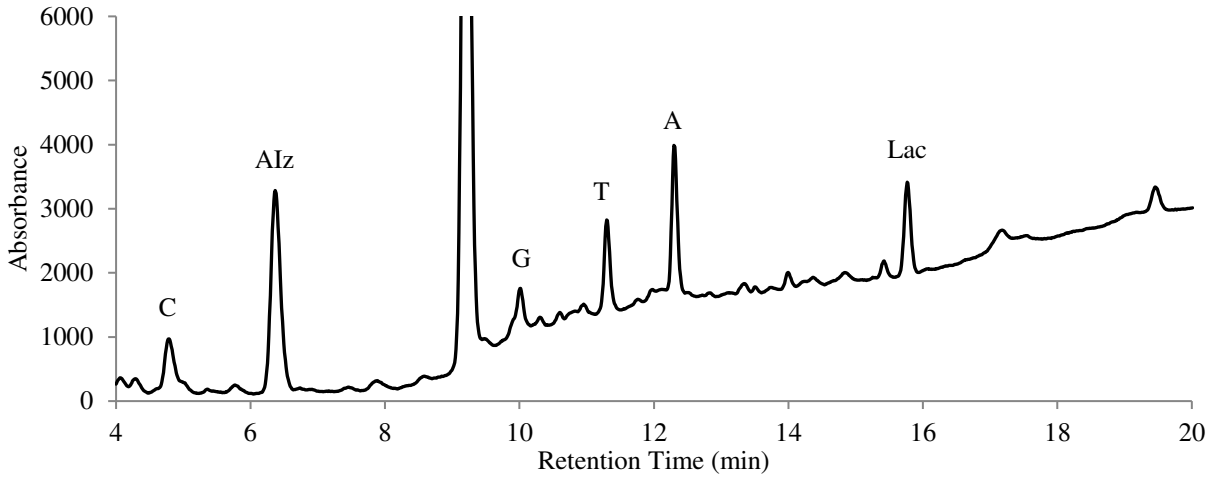

Figure 21: Representative chromatogram showing peaks for LMPs of DNA damage by $Br_2^{\bullet-}$. All conditions are the same as described in the legend for Figure 19 except the reaction solutions also contained 100 mM NaBr

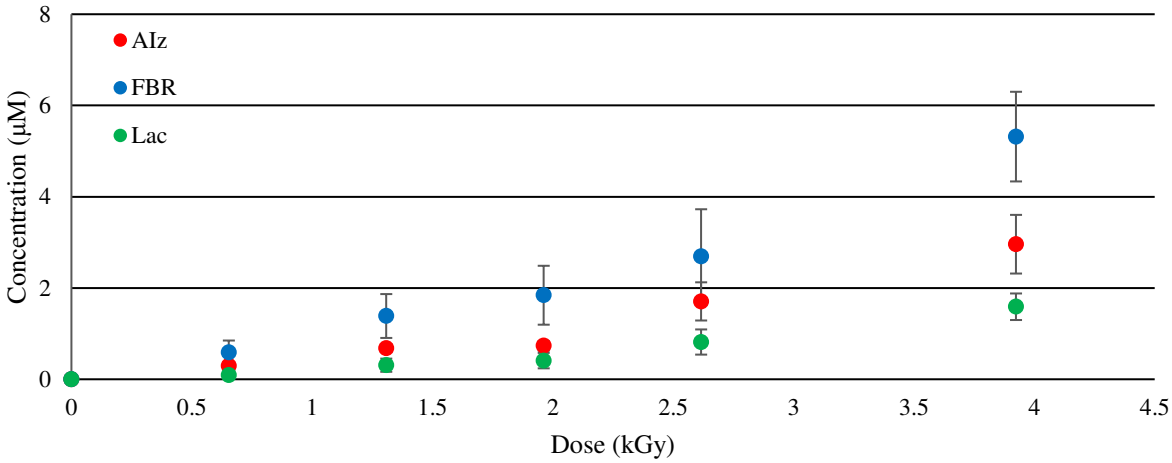

Figure 22: Dose dependence of the yields of major LMPs and as a result DNA oxidation by $Br_2^{\bullet-}$ Reaction conditions are the same as indicated in the previous figure

There are two possible explanations why free base release and production of Lac occur in this system: 1) due to the presence of residual amounts of hydroxyl radicals because of an incomplete conversion of $^{\bullet}OH$ into $Br_2^{\bullet-}$ or 2) because of the presence of superoxide ($O_2^{\bullet-}$)

produced via the reaction of solvated electrons (e_{aq}^-) with molecular oxygen. While superoxide itself reacts with DNA slowly, with $k < 1 \times 10^{-6}$ M^{-1} s^{-1},[93] it might participate in recombination reactions with DNA peroxyl radicals, which, in turn, are the products of reactions of carbon-centered radicals at deoxyribose or nucleobases moieties. Since superoxide is produced in large amounts during radiolysis in oxygenated solutions and is a long-lived ROS, the role of such reactions might be significant. However, little is known about the role of superoxide in processes of DNA oxidative damage.[15]

While it is difficult to selectively scavenge hydroxyl radicals without scavenging other reactive species to test the first hypothesis, the second hypothesis was tested by using a superoxide-free system.

$Br_2^{\bullet-}$ produced in 100 mM solution of NaBr and 10 mM $K_2S_2O_8$. Solvated electrons (e_{aq}^-) are responsible for the production of superoxide in X-irradiated solutions via Reaction 3.1.[92]

$$O_2 + e_{aq}^- \rightarrow O_2^{\bullet-} \quad (k = 1.9 \times 10^{10}\ M^{-1}\ s^{-1} \text{ in } H_2O) \qquad (3.1)$$

As oxygen may be required for the production of Iz, the only way to generate a superoxide-free system is to remove the electrons. $S_2O_8^{2-}$ will scavenge essentially all electrons via Reaction 1.10 which has a diffusion-controlled reaction rate constant, while bromide will react with $^{\bullet}OH$ to produce $Br_2^{\bullet-}$, as before. In addition, the sulfate radical anion will also produce $Br_2^{\bullet-}$ by oxidizing Br^- (Reaction 3.2) which yields $Br_2^{\bullet-}$ (Reaction 1.7). So, in this system the expected yield of $Br_2^{\bullet-}$ is doubled as compared to the solution containing only Br^-.[94]

$$SO_4^{\bullet-} + Br^- \rightarrow Br^{\bullet} + SO_4^{2-} \quad (k = 3.5 \times 10^9\ M^{-1}\ s^{-1}) \qquad (3.2)$$

As seen in the representative chromatogram shown below in Figure 23, the major product is AIz and almost no sugar damage products were observed (other than small amounts of adenine and even less of thymine). This indicates that in this system $Br_2^{\bullet-}$ is essentially the only reactive species responsible for the DNA damage detected.

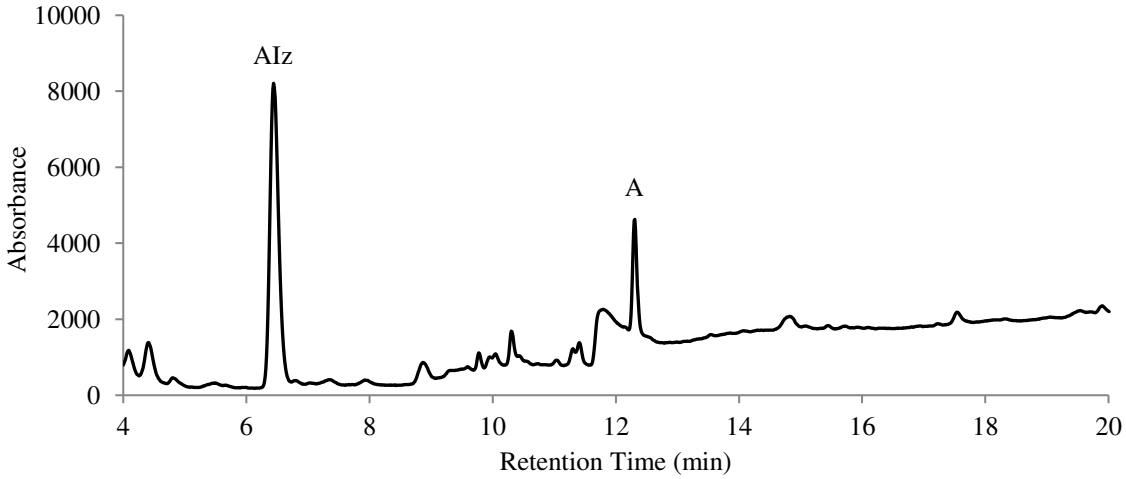

Figure 23: Representative chromatogram showing peaks for LMPs of DNA damage by $Br_2^{\bullet-}$. All conditions are the same as described in the legend for Figure 19 except the reaction solutions also contained 100 mM NaBr and 10 mM $K_2S_2O_8$

These experiments produced impressive results. The radiation chemical yield for Iz was the highest obtained for any reaction (3.54 nmol/J as obtained from the slope of the linear regression line for the experimental data points after the lag period) and, in addition, almost no sugar damage products were observed (~0.5 nmol/J), resulting in a relative yield of AIz/FBR ~ 696%. Dose response curves for each LMP are shown below in Figure 24.

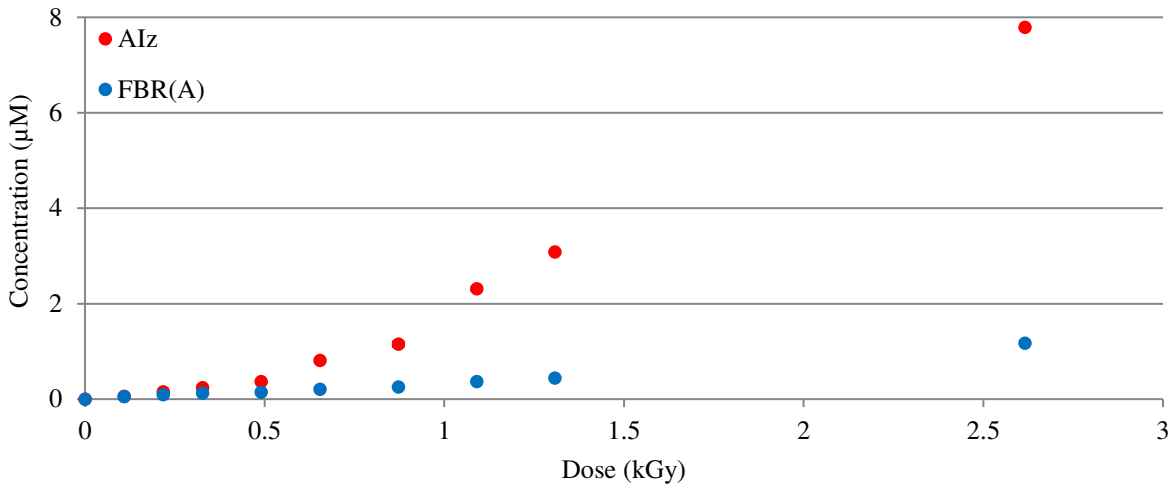

Figure 24: Dose dependence of the yields of major LMPs and as a result DNA oxidation by $Br_2^{\bullet-}$. Reaction conditions are the same as indicated in the previous figure

The dose dependence curve for Iz in Figure 24 shows a pronounced lag period, indicating that Iz formation occurs via a sequential reaction A → B → Iz, where B is an unknown intermediate product or products, and A is unknown precursor, which most likely in this system is $G^{\bullet+}$. The presence of a lag period in accumulation of Iz indicates that the reaction rate constant for the first step, k_1, is not much lower than the reaction rate constant for the second step, k_2.[95] This is in contrast to the Br^- alone system, which produces a much more linear dose dependence curve for AIz. Comparison of the data obtained for two systems, Br^- alone and a mixture of Br^- and $S_2O_8^{2-}$ indicates that the latter system provides a cleaner method of generation of $Br_2^{\bullet-}$ by X-ray radiolysis of aqueous solutions because the effects of undesired free radicals ($^{\bullet}OH$ and $O_2^{\bullet-}$) have been minimized.

Selenite Radical Anion

Two alternative methods were used for the generation of the selenite radical anion,

$SeO_3^{\bullet-}$, 1) radiolysis of selenate (SeO_4^{2-}) solution and 2) radiolysis of the hydroselenite ($HSeO_3^-$) solution.

Selenite Radical Anion via SeO_4^{2-}. The reaction of selenite formation via the selenate anion does not use hydroxyl radicals (Reaction 1.12), thus the resulting DNA solution contains both $SeO_3^{\bullet-}$ and $^{\bullet}OH$. Therefore, products obtained in this system can be expected to be a cumulative result of DNA oxidation of the two OEOs: selenite radical anion and hydroxyl radicals. A representative chromatogram for this system, indicating all oxidative damage products, is shown below in Figure 25.

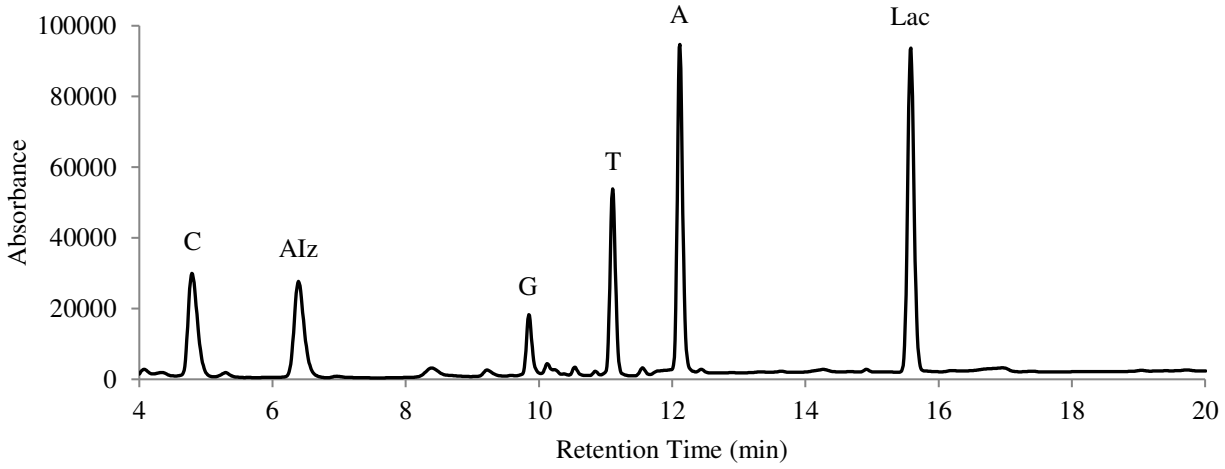

Figure 25: Representative chromatogram showing peaks for LMPs of DNA damage by $SeO_3^{\bullet-}$. All conditions are the same as described in the legend for Figure 19 except the reaction solutions also contained 100 mM Na_2SeO_4

As expected, this system generated high yields of AIz (4.66 nmol/J), which is believed to be a combination of oxidation of guanine by $SeO_3^{\bullet-}$ and $^{\bullet}OH$. While hydrogen-abstracting

properties of $SeO_3^{\bullet-}$ are not described in the literature, comparison with a similar radical anion, $SO_3^{\bullet-}$, which abstracts hydrogen from ethanol with a reaction rate constant of lower than 2 x 10^3 $M^{-1}s^{-1}$ [96], allows one to assume that the selenite radical anion species is also a much less effective hydrogen abstractor than $^{\bullet}OH$. Therefore, the sugar damage products (FBR and Lac) are expected to be mostly the result of hydrogen abstraction from deoxyribose moiety by the hydroxyl radicals. However, the yields of FBR and Lac are lower than that of $^{\bullet}OH$ alone indicating that the parent selenate anion may act as a weak scavenger of $^{\bullet}OH$ ($k = 4.2x10^5$ $M^{-1}s^{-1}$).[97] Dose response curves for each LMP are shown below in Figure 26.

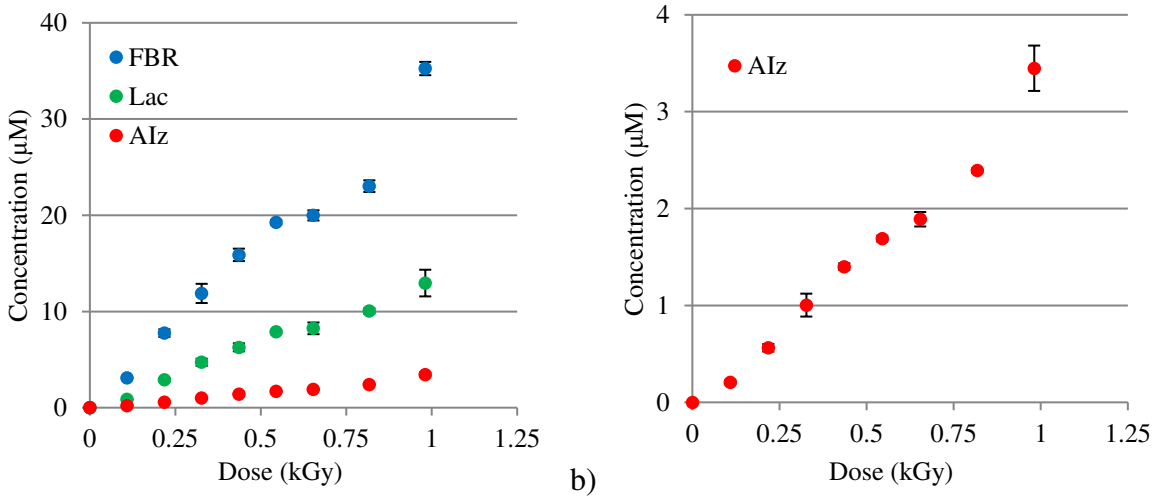

Figure 26: Dose dependence of the yields of a) major LMPs and b) AIz alone and as a result DNA oxidation by $SeO_3^{\bullet-}$ (generated from SeO_4^{2-}). Reaction conditions are the same as indicated in the previous figure

Because the yields of products by hydroxyl radicals are known, the yield of AIz by selenite radical anions alone can be estimated by the difference in the yields of AIz in the systems generating upon radiolysis of both hydroxyl radicals and selenite radical anions and of

hydroxyl radicals only (see Table 6). This approach gives a value of radiation chemical yield production of AIz by selenite radical anions alone of ~2.9 nmol/J.

Selenite Radical Anion via $HSeO_3^-$. The approach of generation of selenite radical anions from hydroselenite anions, $HSeO_3^-$, was theoretically promising as the hydroselenite anions participate in two reactions: 1) the reaction with solvated electrons to convert the hydroselenite anions into poorly reactive selenium oxide radical anions, and 2) the reaction with hydroxyl radicals to produce the selenite radical anions (Reactions 3.5-3.6), therefore both solvated electrons and hydroxyl radicals are removed in this system.[98]

$$HSeO_3^- + e_{aq}^- \rightarrow SeO_2^{\bullet -} + OH^- \quad (k = 1.7 \times 10^9\ M^{-1}s^{-1}) \tag{3.5}$$

$$HSeO_3^- + {}^{\bullet}OH \rightarrow SeO_3^{\bullet -} + H_2O \quad (k \approx 3 \times 10^8\ M^{-1}s^{-1}) \tag{3.6}$$

A representative chromatogram for this system indicating all oxidative damage products is shown below in Figure 27.

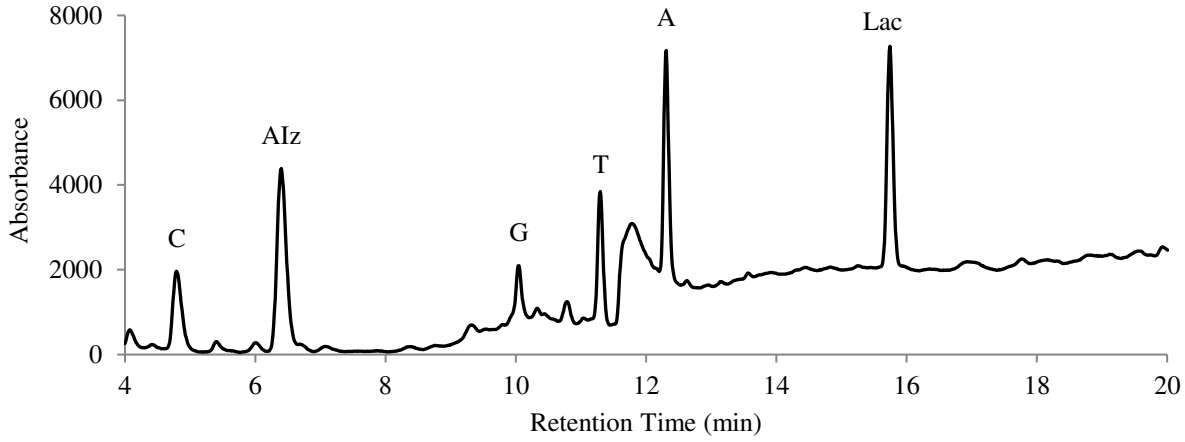

Figure 27: Representative chromatogram showing peaks for LMPs of DNA damage by $SeO_3^{\bullet-}$. All conditions are the same as described in the legend for Figure 19 except the reaction solutions also contained 100 mM $NaHSeO_3$

As shown below in the dose response curves for LMP, $SeO_3^{\bullet-}$ is more selective to production of AIz than $^{\bullet}OH$, as the radiation chemical yield of AIz was ~0.98 nmol/J, with an AIz/FBR of 34.5%. However, the presence of Lac and FBR in large relative amounts indicates that most likely not all hydroxyl radicals are scavenged by the hydroselenite anion.

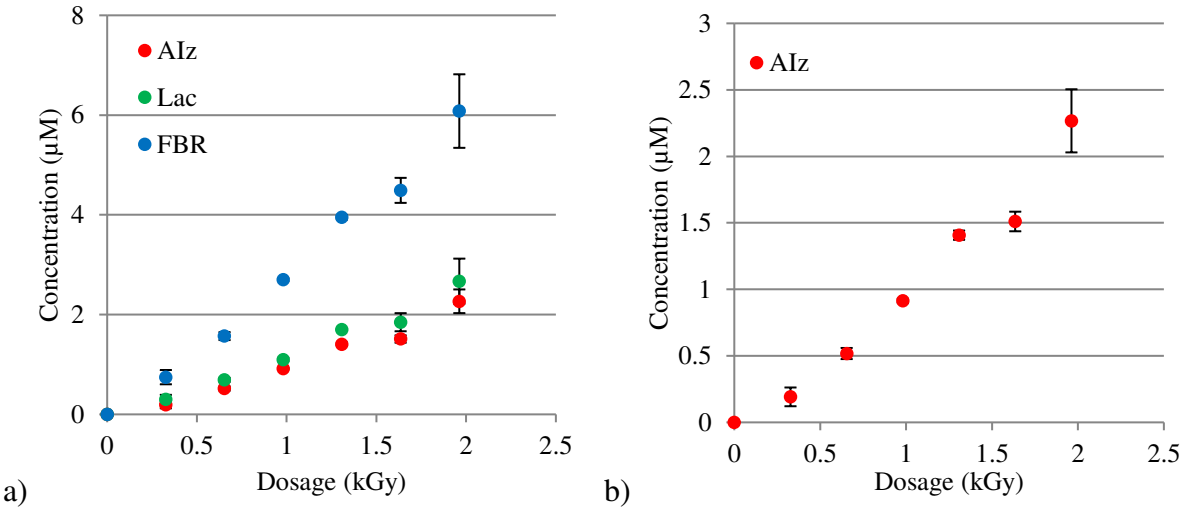

Figure 28: Dose dependence of the yields of a) all major LMPs and b) AIz alone as a result DNA oxidation by $SeO_3^{\bullet-}$ (generated from $HSeO_3^-$). Reaction conditions are the same as indicated in the previous figure

Thus, the approach of using $HSeO_3^-$ to generate $SeO_3^{\bullet-}$ appears unsuccessful because the reaction between hydroxyl radicals and hydroselenite is too slow ($k \approx 3 \times 10^8$ $M^{-1}s^{-1}$) to successfully compete with the reaction of hydroxyl radicals with guanines in DNA ($k \approx 8 \times 10^9$ $M^{-1}s^{-1}$), so the conversion of hydroxyl radicals into selenite radical anions is incomplete. An attempt to push the reaction of hydroselenite with hydroxyl radical was made by increasing the concentration of hydroselenite from 100 mM to 200 mM, however this resulted in the actual decrease in yield of AIz. This indicates that in this system the observed release of AIz is due primarily from the oxidation of guanine by the hydroxyl radicals left in solution, rather than by the selenite radical anions. Figure 29 below shows the dose response curve for AIz production for solutions containing 100 mM and 200 mM $HSeO_3^-$.

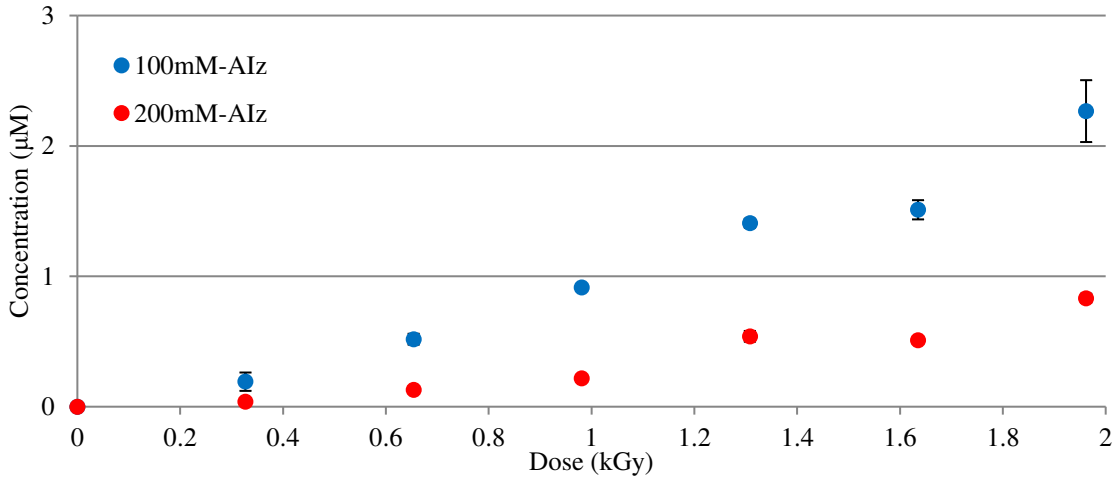

Figure 29: Dose dependence of the yields of AIz and as a result DNA oxidation by $SeO_3^{\bullet-}$ (generated from $HSeO_3^-$) from 100 mM or 200 mM $HSeO_3^-$. Reaction conditions are the same as indicated in the previous figure

Sulfate Radical Anion

The sulfate radical anion, $SO_4^{\bullet-}$, has a high reduction potential of +2.43 V and is capable of oxidizing all four nucleobases. As shown in Roginskaya's research group recent publication, sulfate radical anions are also fairly efficient hydrogen abstractors.[59] Radiolysis of aqueous solution of 10 mM persulfate anions produces both sulfate radical anions (through the solvated electron channel) and hydroxyl radicals as seen in Reactions 1.9-1.11. Persulfate anions are relatively inefficient scavengers of hydroxyl radical, $k = 1.2 \times 10^7\ M^{-1}s^{-1}$.[92] As of yet, there is no reliable method to produce sulfate radical anions only (for example, the formate anion, widely used as a hydroxyl radical scavenger[15] will not only scavenge hydroxyl radicals but sulfate radical anions as well). Therefore, production of AIz is a result of oxidation of guanine by both hydroxyl radicals and sulfate radical anions. A representative chromatogram for this system, indicating all oxidative damage products, is shown below in Figure 30.

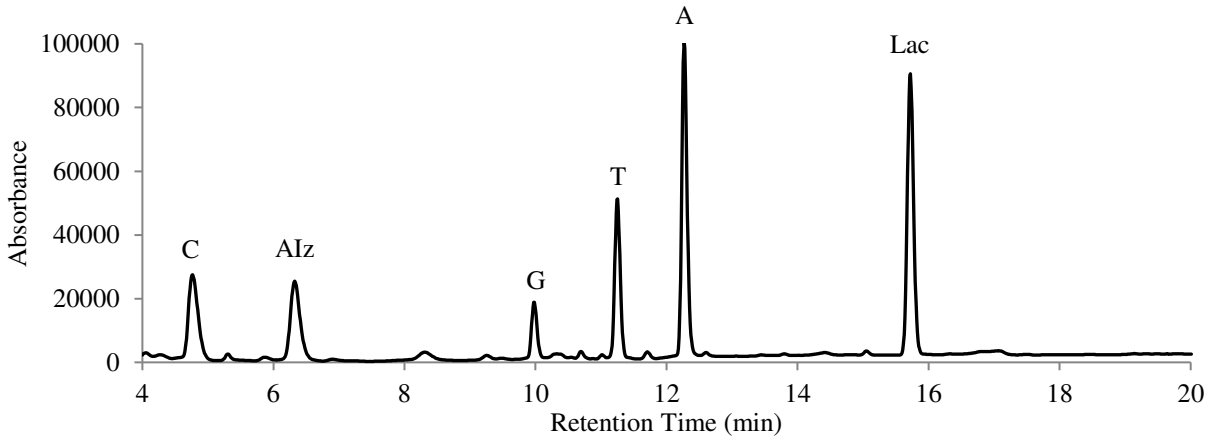

Figure 30: Representative chromatogram showing peaks for LMPs of DNA damage by $SO_4^{\bullet-}$ (and $^{\bullet}OH$). All conditions are the same as described in the legend for Figure 19 except the reaction solutions also contained 100 mM $K_2S_2O_8$

The yields of LMPs are supposed to be a cumulative result of DNA damage by both hydroxyl radicals and sulfate radical anions. Dose response curves for each LMP are shown below in Figure 31.

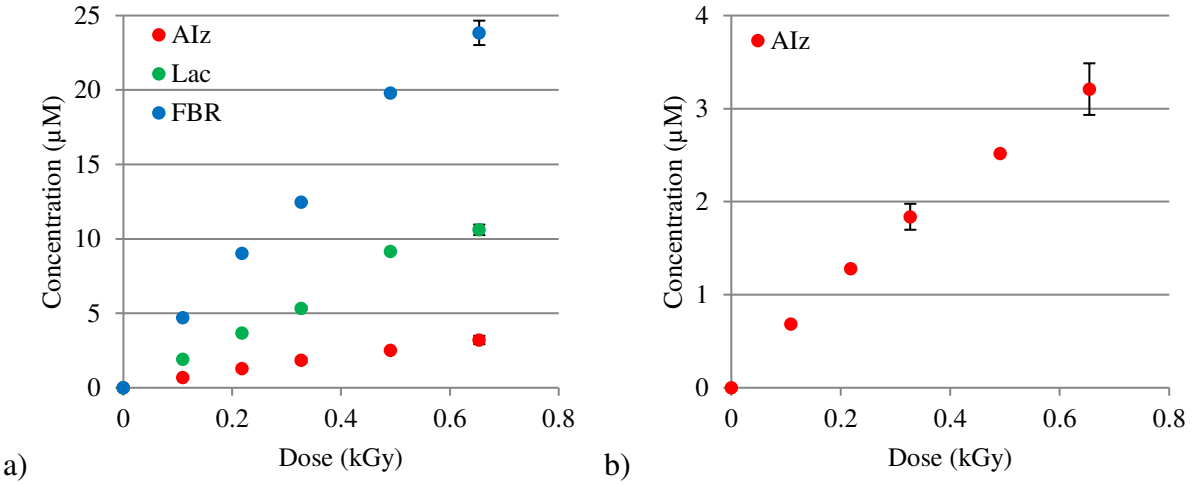

Figure 31: Dose dependence of the yields of a) major LMPs and b) AIz alone and as a result DNA oxidation by $SO_4^{\bullet-}$ (and $^{\bullet}OH$). Reaction conditions are the same as indicated in the previous figure

Because the yields of products by hydroxyl radicals are known, and the contribution of the reaction between persulfate and hydroxyl radicals is low, the yield of AIz by sulfate radical anions alone can be estimated by the difference in the yields of AIz in the systems generating upon radiolysis of both hydroxyl radicals and persulfate radical anions and of hydroxyl radicals only (see Table 6). This approach gives a value of radiation chemical yield production of AIz by sulfate radical anions alone of ~3.3 nmol/J.

Azide Radical

As expected, the azide radical, $N_3^{\bullet}$, does not produce measurable yields of AIz, as shown below in the representative chromatogram (Figure 32).

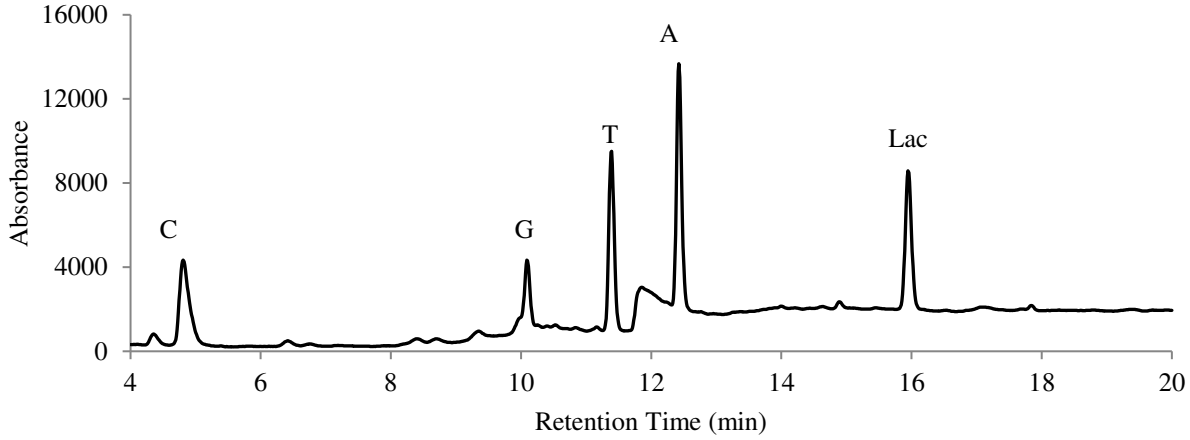

Figure 32: Representative chromatogram showing peaks for LMPs of DNA damage by $N_3^{\bullet}$. All conditions are the same as described in the legend for Figure 19 except the reaction solutions also contained 100 mM NaN_3

Because the azide radical has a reduction potential only slightly higher than that of guanine (+1.30 V vs. +1.29 V), it is likely not capable of effectively oxidizing the guanine to form AIz. The mechanism of formation of residual amounts of FBR and Lac in this system is not clear. Most likely, it is the result of action of hydroxyl radicals remaining in the solution due to their incomplete scavenging by the azide anion. Dose response curves for the residual sugar damage products, FBR and Lac, are shown below in Figure 33. The results found in Figure 33 are from a singular pilot experiment and no error bars are associated with the data.

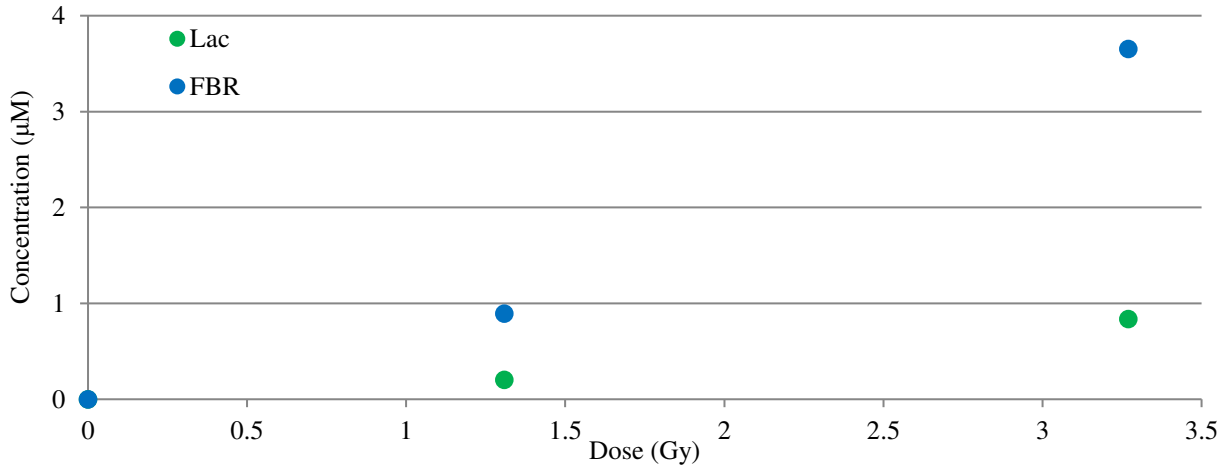

Figure 33: Dose dependence of the yields of FBR and Lac as a result DNA oxidation by $N_3^{\bullet}$. Reaction conditions are the same as indicated in the previous figure

Representative chromatograms for all solutions under these experimental conditions, with samples X-rayed at the dose of 0.69 kGy are shown in Figure 34, which allows for a more accurate comparison of absolute yields of AIz.

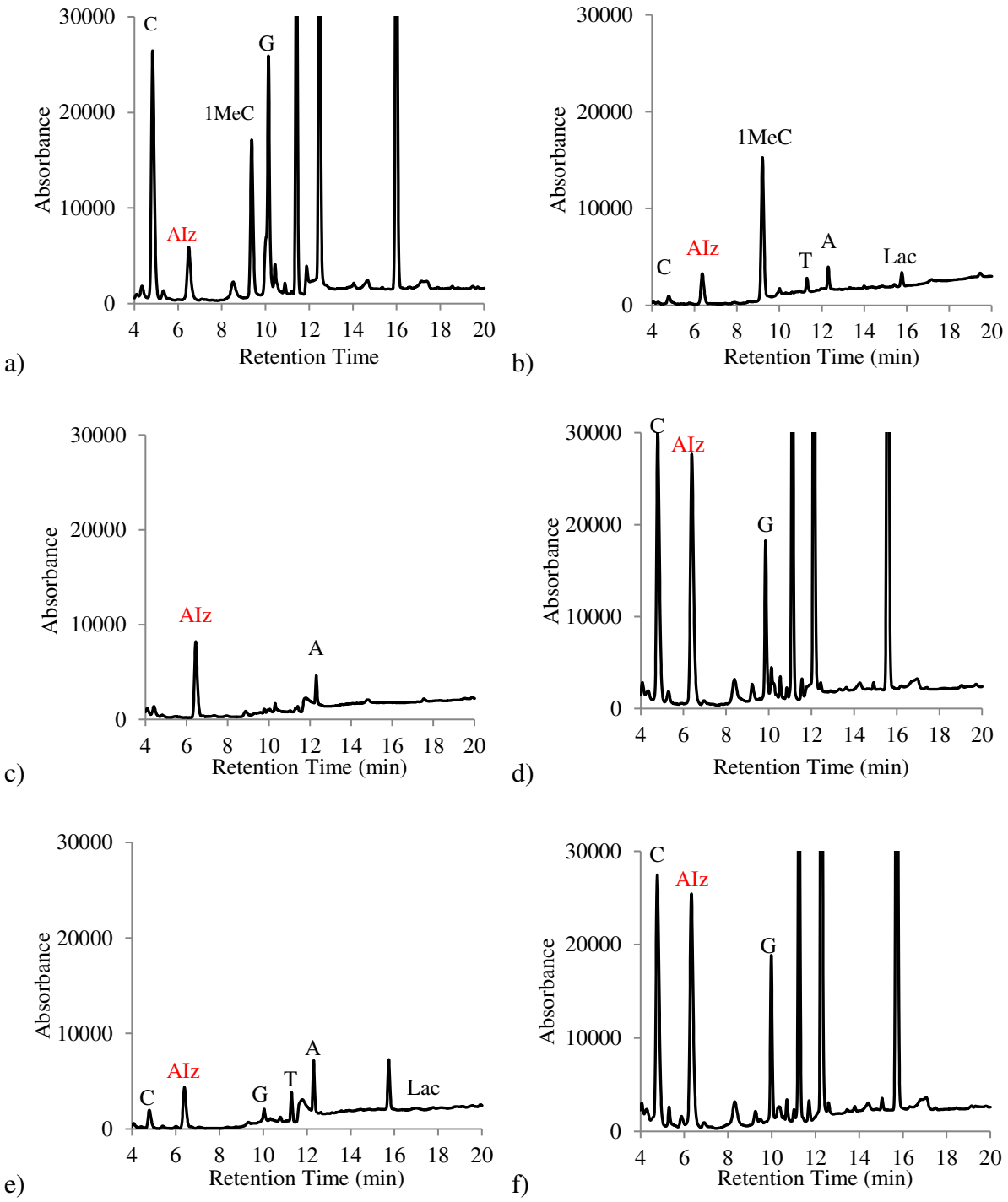

Figure 34: Representative chromatograms for each OEO, X-irradiated at a dose of 0.69 kGy: a) $^{\bullet}OH$ b) $Br_2^{\bullet-}$ c) $Br_2^{\bullet-}$ ($Br^- + S_2O_8^{2-}$) d) $SeO_3^{\bullet-}$ via SeO_4^{2-} e) $SeO_3^{\bullet-}$ via $HSeO_3^-$ f) $SO_4^{\bullet-}$

Radiation chemical yields (in nmol/J) were calculated from the slopes of the linear regression as described in Chapter 2. The value of the slope for FBR is normalized to 100% and the relative yield for each damage product is expressed as the ratio of slope values of the product and the total FBR. The yields of each damage product were normalized to yield of FBR because, as previously mentioned in Chapter 1, the total yield of FBR is an excellent internal benchmark of the total damage inflicted to the sugar-phosphate backbone. A representative graph for solutions with •OH as the oxidant is shown in Figure 35.

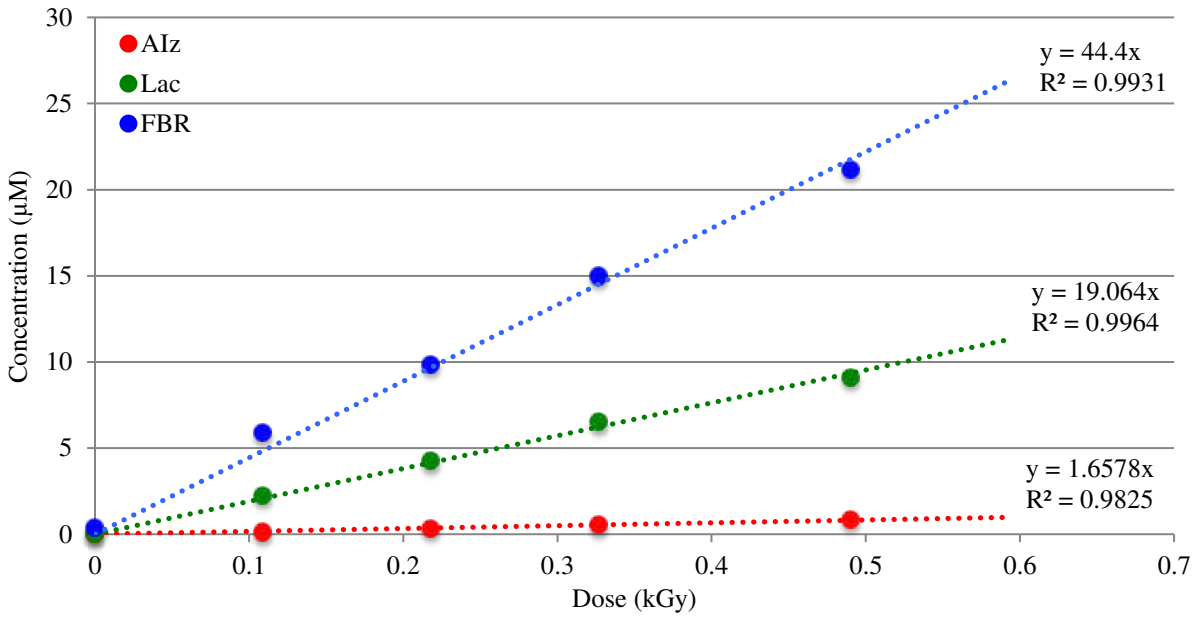

Figure 35: Radiation chemical yields (in nmol/J) of major DNA oxidation damage products for solutions with •OH as the oxidant determined from linear regression analysis of dose dependence curves at low doses

The radiation chemical yields and relative yields for each damage product are summarized in Table 6.

Table 6: Radiation Chemical Yields and Relative Percentage Yields for DNA Damage Products

OEO	Iz (nmol/J)	Relative Percentage Yield of Iz	Lac (nmol/J)	Relative Percentage Yield of Lac	FBR (nmol/J)
$^{\bullet}OH$	1.78	4.01%	19.1	42.9%	44.4
$Br_2^{\bullet-}$ (Br^- only)	0.620	56.5%	0.362	29.2%	1.24
$Br_2^{\bullet-}$ ($Br^- + S_2O_8^{2-}$)	3.54[b)]	696%	0	0%	0.509[b)]
$SeO_3^{\bullet-}$ (via SeO_4^{2-})	4.66 2.88 ($SeO_3^{\bullet-}$ only)[a)]	14.2%	14.7	44.8%	32.8
$SeO_3^{\bullet-}$ (via $HSeO_3^-$)	0.978	34.5%	1.20	42.4%	2.83
$SO_4^{\bullet-}$	5.12 3.34 ($SO_4^{\bullet-}$ only)[a)]	12.8%	18.2	45.5%	40.0
$N_3^{\bullet}$	0	0%	0.261	22.9%	1.14

[a)] Calculated by subtracting the radiation chemical yield of AIz in the reaction of DNA with $^{\bullet}OH$.

[b)] Estimated based on the slope of the linear part of the regression line to experimental points obtained after the lag period.

As expected, the OEOs which oxidize guanine selectively ($Br_2^{\bullet-}$ and $SeO_3^{\bullet-}$) resulted in the largest relative yields of AIz. $Br_2^{\bullet-}$ is selective towards the production of Iz with AIz/FBR ~ 7.0 in the X-rayed $Br^-/S_2O_8^{2-}$ solutions. The data in the X-rayed $Br^-/S_2O_8^{2-}$ solutions seemed to produce a cleaner system of producing AIz, *i.e.* one where the contribution of undesirable free radicals, such as hydroxyl radicals and superoxide, is minimized. This is indicated by the lack of sugar damage products, FBR and Lac, the very large AIz relative percentage yield (~696%), as

well as the largest absolute yield for any single OEO (~3.54 nmol/J). Br^- solutions still produced a reasonably large relative yield of AIz, but the results are obscured due to the presence of other oxidants that can also produce AIz. The approach of generation of $SeO_3^{\bullet-}$ by radiolysis of solutions containing $HSeO_3^-$ turned out to be unsuccessful because a slow reaction between $HSeO_3^-$ and $^{\bullet}OH$ results in an incomplete scavenging of $^{\bullet}OH$. The majority of AIz produced in this system is assumed to be a result of DNA oxidation by $^{\bullet}OH$.

Radiolysis of solutions containing selenate or persulfate anions apparently produces a mixture of OEOs ($SeO_3^{\bullet-}$ together with $^{\bullet}OH$ and $SO_4^{\bullet-}$ together with $^{\bullet}OH$, respectively) therefore the contribution of individual OEOs is unclear. Despite having the largest absolute yields of AIz, the relative yield of AIz for both of these systems was much smaller than that of the $Br_2^{\bullet-}$ systems, indicating that at the DNA is oxidized non-selectively. While hydroxyl radicals have a large reduction potential and are very reactive, they have very low selectivity towards the production of Iz, with an AIz/FBR~ 0.037. They primarily react through H-abstraction from the deoxyribose, as visualized by free base release and production of Lac. $N_3^{\bullet}$ produces essentially no AIz, most likely due to not having a high enough reduction potential to successively oxidize guanine (+1.29 V).

The Effect of Superoxide on Production of Iz

Shafirovich *et al.* reported that Iz is produced by the reaction of the guanine radical with superoxide.[34] However, there has been accumulating evidence based on data from the Roginskaya research group's experiments that superoxide is not necessarily required for the production of Iz in DNA. The hypothesis is that the formation of Iz in DNA can be preceded by the reaction of guanine radical or guanine radical cation with molecular oxygen.

As shown in Reaction 3.1, solvated electrons (e_{aq}^-) are responsible for the production of superoxide in X-irradiated solutions. As oxygen may be required for the production of Iz, the only option to prevent the production of superoxide is to remove the electrons from the reaction system. By adding electron scavengers such as persulfate or trichloroacetate (TCA) to the reaction solution, the production of superoxide is suppressed. DNA can also react with solvated electrons (Reaction 3.7), but relatively slowly as compared with the reactions of solvated electrons with molecular oxygen and scavengers such as persulfate of TCA which have diffusion-controlled reactions rate constants.[99]

$$DNA + e_{aq}^- \rightarrow products \quad (k = 1.0 \times 10^8\ M^{-1}s^{-1} \text{ in } H_2O, \text{ pH } 6.5) \qquad (3.7)$$

Persulfate

The results of the experiments in X-rayed solutions of 100 mM NaBr and 10 mM $K_2S_2O_8$ have been earlier described in this chapter (see Figures 23-24). Although it was expected that the yields of AIz would be doubled for solutions containing persulfate, as the $Br_2^{\bullet-}$ is formed from two separate channels, the absolute yields of AIz for solutions containing Br^- with persulfate (~3.5 nmol/J) were significantly higher than for the Br^- alone system (~0.70 nmol/J). This indicates the superoxide may actually suppress the formation of Iz through some unknown mechanism. Overall, the data support the hypothesis that superoxide is not required for the formation of Iz in systems containing $Br_2^{\bullet-}$ as the OEO, as when superoxide formation is suppressed through the addition of persulfate, AIz is still produced in significant quantities.

Trichloroacetate

For systems containing •OH as the oxidizing species, trichloroacetate (TCA) was selected as an electron scavenger. TCA, through dissociative electron capture, is an efficient scavenger of electrons (Reaction 3.8).[100]

$$CCl_3COO^- + e_{aq}^- \rightarrow {}^\bullet CCl_2COO^- + Cl^- \quad (k = 8.5 \times 10^9\ M^{-1}\ s^{-1}\ \text{in}\ H_2O) \tag{3.8}$$

The resulting free radical rapidly reacts with oxygen to form a peroxyl radical anion (Reaction 3.9), which is believed to be poorly reactive under ambient conditions and does not participate in further transformations:

$$^\bullet CCl_2COO^- + O_2 \rightarrow {}^\bullet OOCCl_2COO^- \quad (k \sim 1.0 \times 10^{10}\ M^{-1}s^{-1}) \tag{3.9}$$

When using a concentration of 20 mM of TCA, the ratio of rates for Reaction 3.8 to 3.1 (the formation of superoxide) is approximately 45, assuming the concentration of dissolved oxygen in air-saturated solutions is ~0.2 mM. Therefore, the production of superoxide is practically suppressed in solutions containing 20 mM TCA. In addition, TCA, at least at these concentrations, does not efficiently scavenge •OH since its reaction constant is estimated as lower that $6 \times 10^7\ M^{-1}\ s^{-1}$ in H_2O at pH 6.2.[101] Therefore, we can assume the formation of Iz in these systems is a result of the reaction of oxidative damage to DNA by •OH. Dose response curves for LMP produced in solutions with and without TCA are shown below in Figure 36:

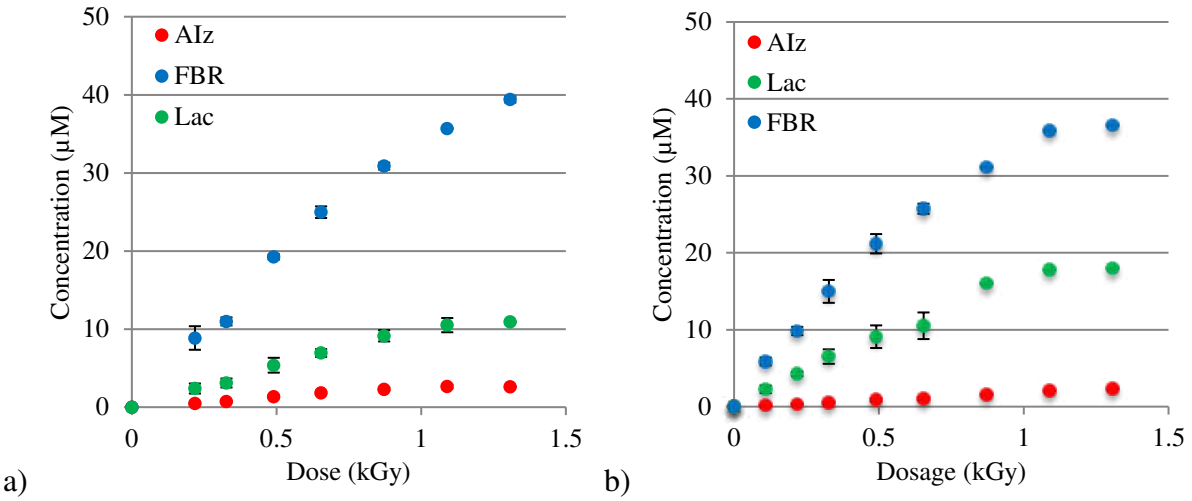

Figure 36: Dose dependence of major DNA oxidation products for DNA solutions containing a) DNA with 20 mM TCA and b) DNA only

Linear regression analysis of AIz formation produced radiation chemical yields for DNA solutions of ~1.8 nmol/J and DNA solutions with TCA of ~2.5 nmol/J. The slight increase in the yield if AIz in superoxide-free systems indicates the possibility that superoxide suppresses the formation of AIz. Dose response curves for AIz formation are shown below in Figure 37.

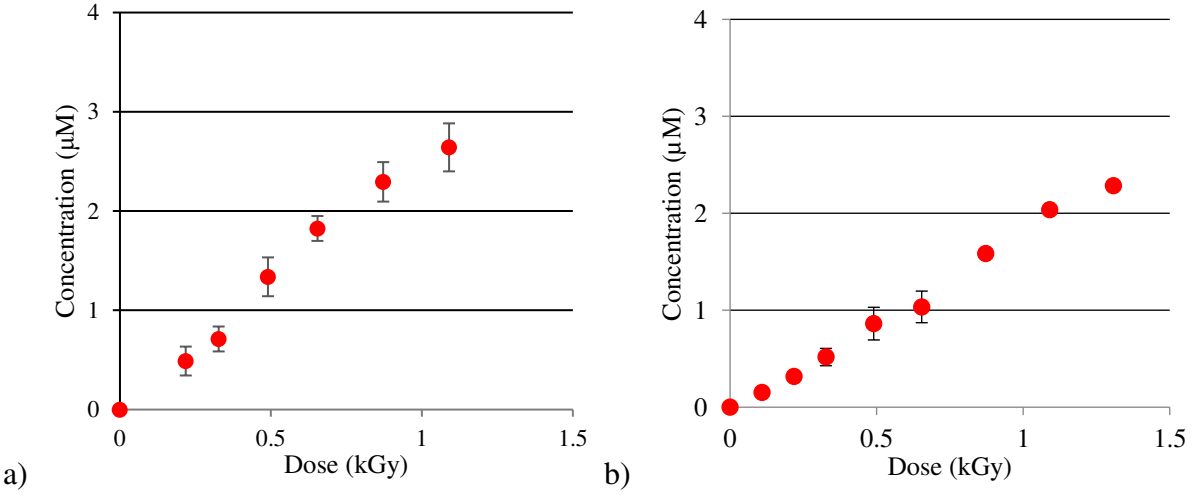

Figure 37: Dose dependence for AIz production for DNA solutions containing a) DNA with 20 mM TCA and b) DNA only

Based on the data collected from the previous experiments, it can be concluded that in superoxide-free systems, AIz is still efficiently produced, therefore AIz formation is not dependent on the presence of $O_2^{\bullet-}$. Both systems showed an increase in the yield if AIz in superoxide-free systems indicating the possibility that superoxide suppresses the formation of Iz, although the mechanism by which this would occur still remains unclear.

The Effect of Oxygen on the Production of Iz

It is well known that many reactions of oxidative damage to DNA are sensitive to gassing conditions and that many are absolutely dependent on the presence of molecular oxygen.[15] It is believed that the formation of Iz from its precursors is oxygen-dependent. Therefore, studying the effect of molecular oxygen on the production of Iz by various OEOs could shed light on the mechanisms of formation for Iz. In addition to the conditions of naturally aerated solutions (air-saturated solutions, with the concentration of dissolved oxygen of ~0.2 mM at room temperature) routinely used, two more gassing conditions were tested: oxygenated solutions (saturated with oxygen gas, with concentration of dissolved oxygen of ~1 mM) and deoxygenated solutions (purged with argon gas).

Experiments on the effect of oxygen have been performed to confirm whether the presence of oxygen affects the process of Iz formation. These experiments were performed for the systems generating $^{\bullet}OH$ or $Br_2^{\bullet-}$ as the OEO. 10 mM of salmon testes DNA in 10 mM phosphate buffer, pH 6.9 either with 100 mM NaBr with or without 10 mM $K_2S_2O_8$, for $Br_2^{\bullet-}$, or without any additives for $^{\bullet}OH$. In addition, 'Oxygenated' samples were saturated with O_2 gas for ~10 min and 'Deoxygenated' samples were saturated with argon gas for ~20 min. Immediately following saturation, samples were X-rayed and then treated as previously described.

•OH with and without Oxygen

The yields of all products of DNA damage by hydroxyl radicals were drastically decreased in deoxygenated solutions and the production of Iz was practically completely suppressed (Figure 38). Therefore, as expected, formation of Iz in DNA by hydroxyl radicals is absolutely dependent on oxygen, which is also the case for 8-oxo-G.[79] Representative chromatograms (Figure 38) and dose dependence curves (Figure 39) are shown below.

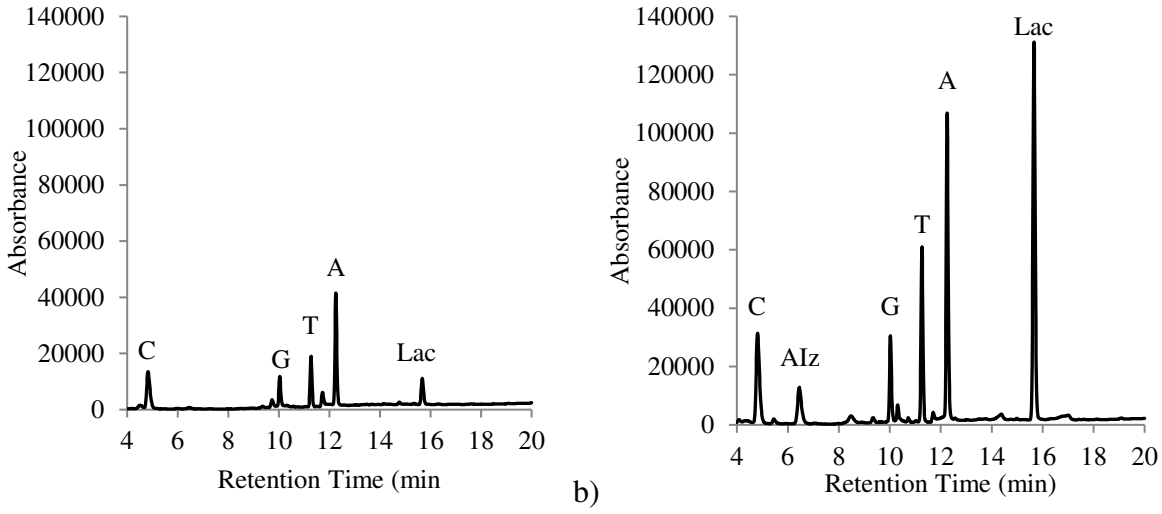

Figure 38: Representative chromatogram showing peaks for LMPs of DNA damage by •OH for solutions saturated with a) argon and b) oxygen. All conditions are the same as described in the legend for Figure 19

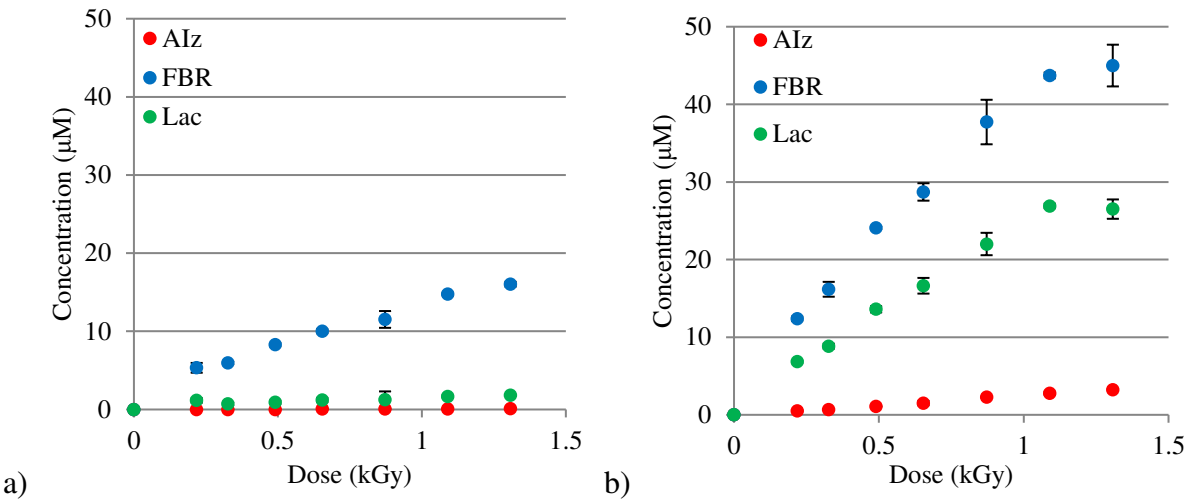

Figure 39: Dose dependence of major DNA oxidation products for DNA saturated with a) argon and b) oxygen

Figure 40 focuses on the dose dependence curves for AIz for solutions under each of the gassing conditions. Clearly the mechanism by which Iz is produced from hydroxyl radicals is dependent on oxygen, as the yield of AIz is suppressed when oxygen is removed and increased when solutions are saturated in oxygen.

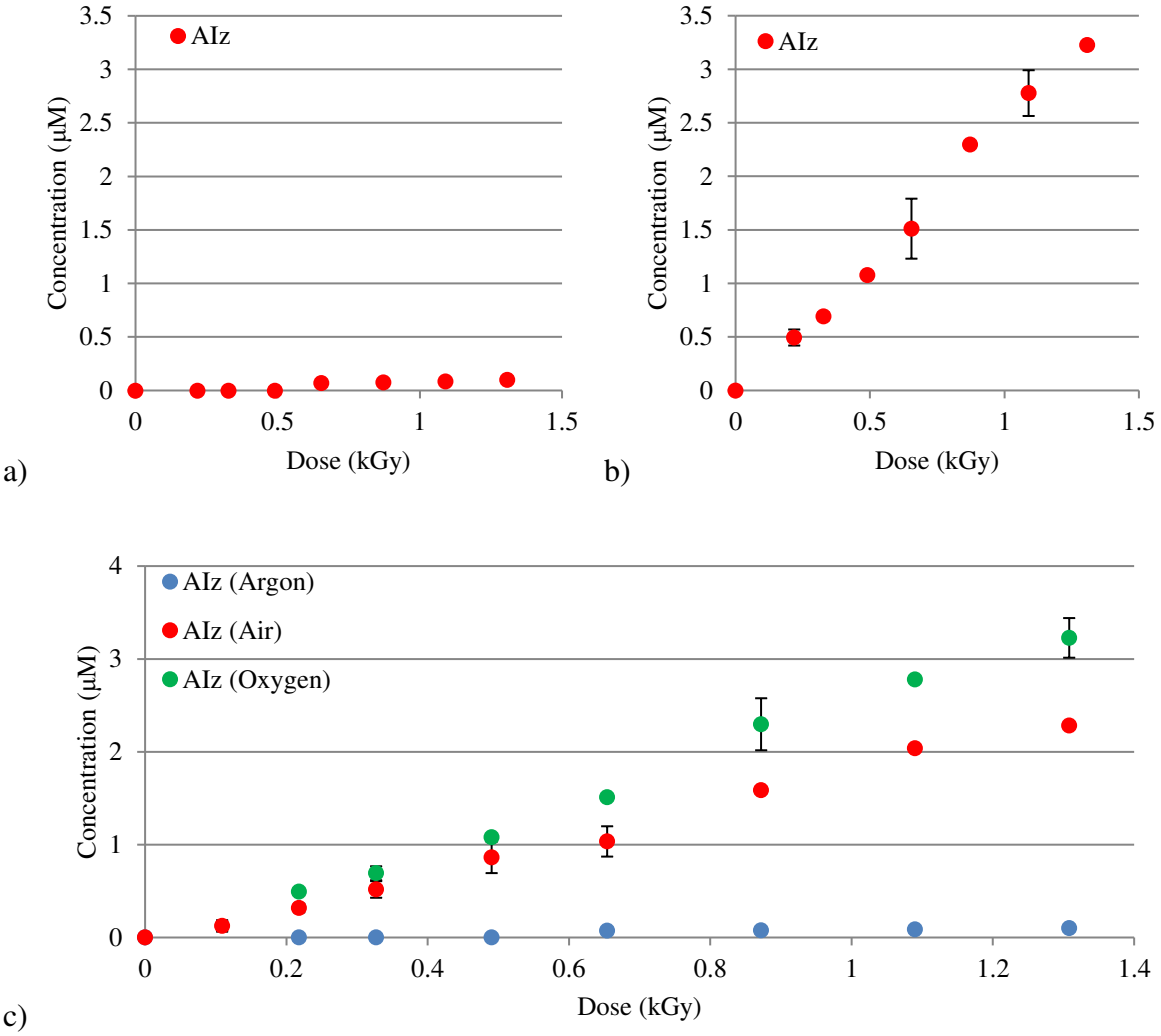

Figure 40: Dose dependence of AIz formation by hydroxyl radicals for DNA solution saturated with a) argon, b) oxygen or c) all tested gassing conditions

<u>$Br_2^{\bullet-}$ with and without Oxygen</u>

While one might hypothesize that production of Iz via the reaction of dibromide radical anions with DNA is also oxygen-dependent, our experimental data showed this is not necessarily true. The absence of oxygen did not completely suppress AIz formation as it was the case for the hydroxyl radicals (Figures 38-40) and it appears the mechanism by which Iz is formed is different for NaBr DNA solutions containing persulfate.

$Br_2^{\bullet-}$ produced in 100 mM solution of NaBr. As previously discussed, DNA solutions containing only NaBr produce AIz as well as products of sugar damage (FBR and Lac). It was proposed that these products are a result of oxidation from superoxide. As shown below in representative chromatograms (Figure 41) and dose response curves (Figure 42), DNA solutions which have been deoxygenated produce more FBR and Lac than those which have been saturated with oxygen, indicating that the mechanism of sugar damage is suppressed in the presence of oxygen. In contrast, the yields of AIz increase in the presence of oxygen, indicating they mechanism by which AIz is formed through this system may be oxygen-dependent.

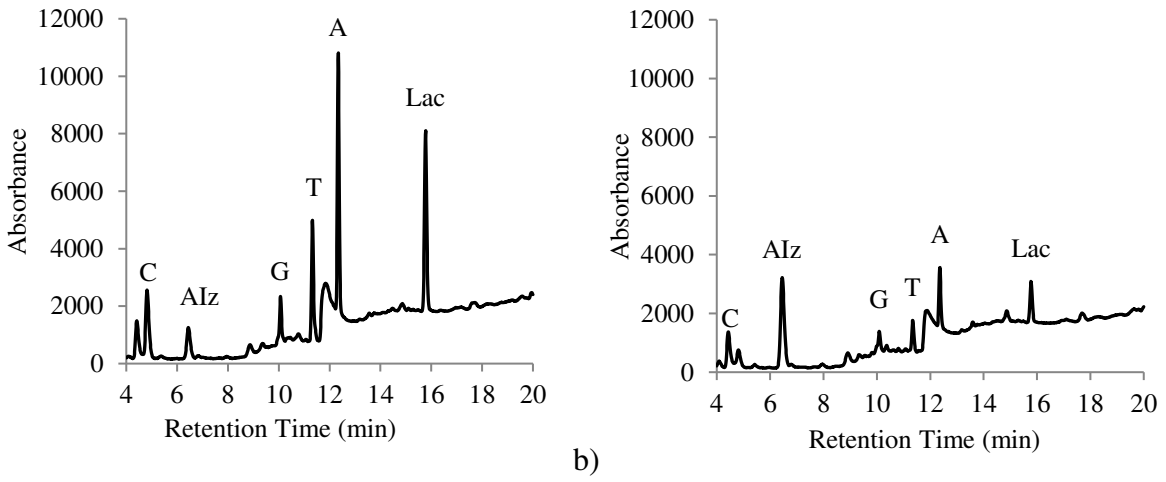

Figure 41: Representative chromatogram showing DNA damage products for DNA solutions X-irradiated in the presence of 100 mM NaBr, saturated with a) argon and b) oxygen; dose 0.69 kGy

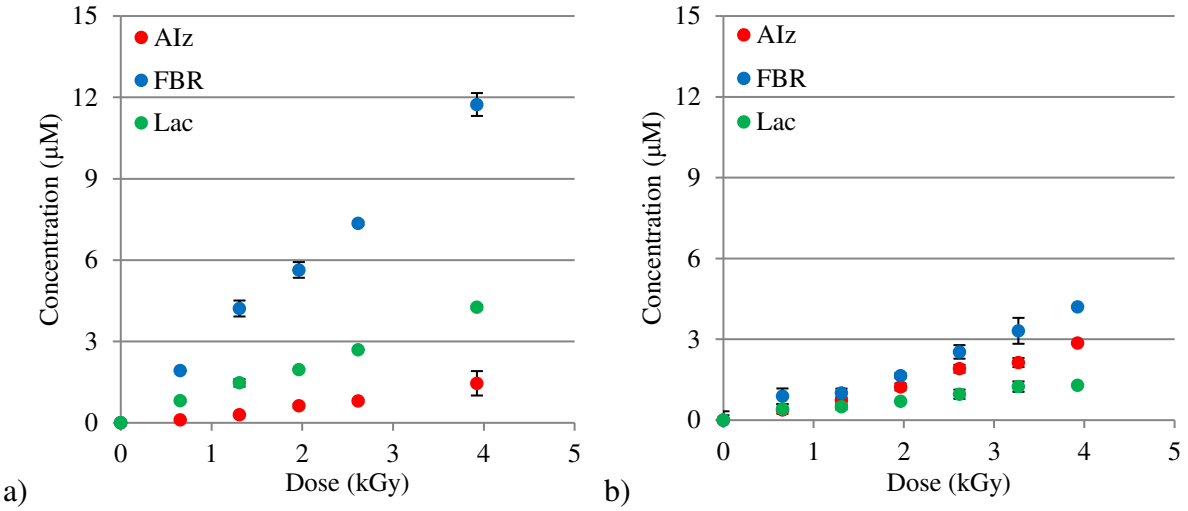

Figure 42: Dose dependence curve for DNA damage product formation for DNA solutions X-irradiated in the presence of 100 mM NaBr that have been saturated with a) argon or b) oxygen

As shown below in Figure 43, the relative yields of AIz decrease when DNA solutions are saturated with argon (~0.3 nmol/J) as compared with those under normal air (~0.62 nmol/J) or saturated with oxygen (~0.67 nmol/J). In contrast, we see a suppression in the yields of FBR and Lac in oxygenated samples. One possible explanation is that in oxygenated samples, molecular oxygen can compete with hydroxyl radicals for solvated electrons, producing additional superoxide, which reacts with DNA much more slowly (Reaction 3.1). In this scenario, the hydroxyl radical is free to react with Br^-, eventually resulting in the formation of additional $Br_2^{\bullet-}$, which explains the slight increase in the yield of AIz. In deoxygenated solutions, the hydroxyl radical reacts with solvated electrons more quickly than Br^-, resulting in less formation of $Br_2^{\bullet-}$, and consequently AIz. However, the radiation chemical yields of AIz under air-saturated (~0.62 nmol/J) and oxygen saturated (~0.67 nmol/J) solutions are very similar, especially when considering the standard deviation of the solutions, so it is also possible that

oxygen-saturated solutions and air-saturated solutions produce approximately the same yield of AIz.

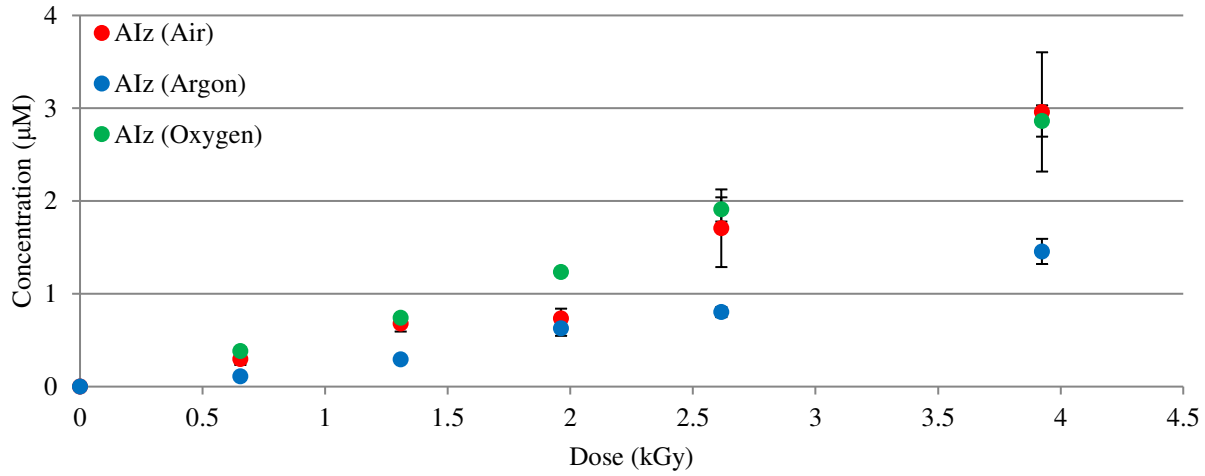

Figure 43: Dose dependence curve for AIz formation for DNA solutions X-irradiated in the presence of 100 mM NaBr that have been saturated with argon, oxygen, or air

$Br_2^{\bullet-}$ produced in 100 mM solution of NaBr and 10 mM $K_2S_2O_8$. In the persulfate/dibromide system, the yield of AIz approximately doubles in deoxygenated solutions as compared to oxygenated solutions as seen below in the system's representative chromatograms (Figure 44). One possible explanation is the competition of molecular oxygen with persulfate anions for solvated electrons, which compromises the solvated electron channel of production of dibromide radical anions. However, both molecular oxygen and persulfate anion react with solvated electrons at nearly diffusion-controlled rates, while the concentration of dissolved oxygen even in oxygenated solutions is ~1 mM, which is 10 times lower than the concentration of persulfate (10 mM). Therefore, the ratio of rates for the reaction of persulfate

with solvated electrons and molecular oxygen with solvated electrons is approximately 10, which means most likely molecular oxygen cannot compete efficiently for the solvated electrons.

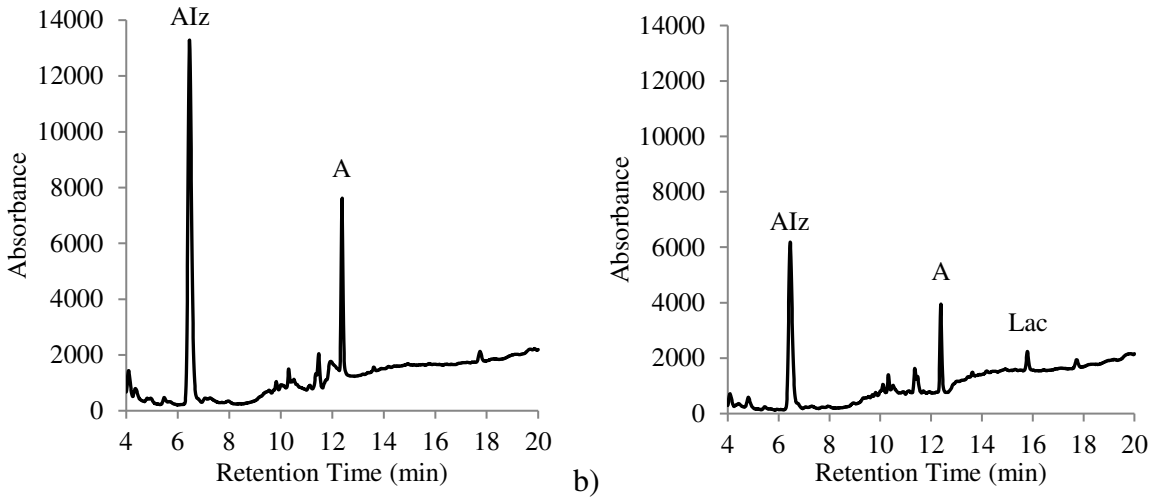

Figure 44: Representative chromatogram showing DNA damage products for DNA solutions X-irradiated in the presence of 100 mM NaBr and 10 mM $K_2S_2O_2$, saturated with a) argon and b) oxygen; dose 0.69 kGy

Surprisingly, deoxygenated samples produced significantly more FBR (~1.41 nmol/J) than samples under air (~0.505 nmol/J) or saturated with oxygen (~0.914 nmol/J). Dose dependence curves for each system are shown below in Figure 45.

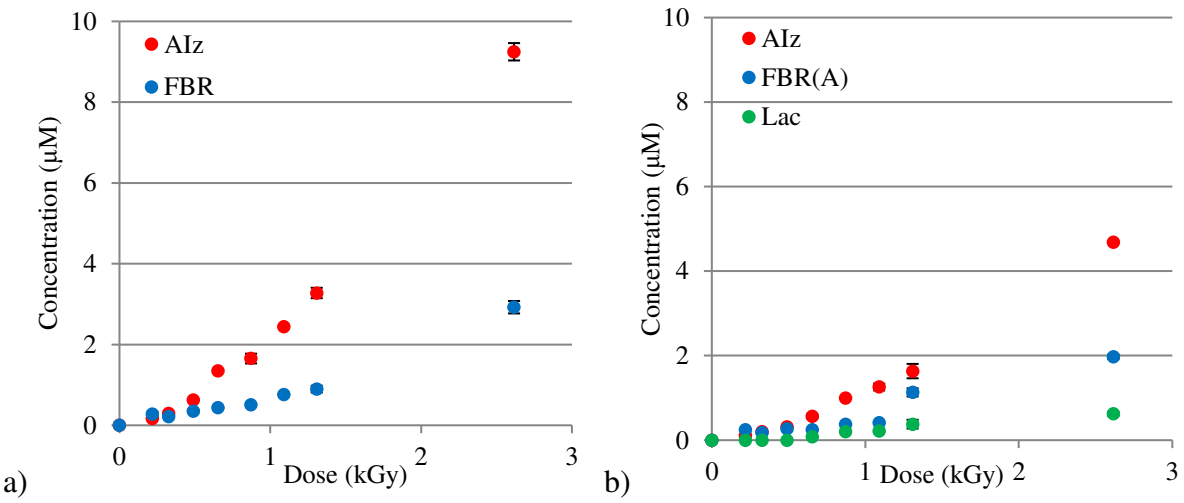

Figure 45: Dose dependence curve for DNA damage product formation for DNA solutions 100 mM NaBr and 10 mM $K_2S_2O_8$, saturated in a) argon and b) oxygen

The sugar damage product Lac, also began formation at higher doses in oxygen-saturated solutions, indicating the mechanism by which Lac is formed in the persulfate/dibromide system is oxygen dependent. In the persulfate/dibromide system, the yield of AIz increases in deoxygenated solutions (~4.4 nmol/J) as compared to air-saturated solutions (~3.5 nmol/J) and oxygenated solutions AIz (~2.1 nmol/J), where AIz formation appears to be suppressed. Because the formation of AIz was suppressed in solutions saturated with oxygen, it is possible there is a competing reaction, although the mechanism of formation of Iz in dibromide systems still remains unclear. Dose response curve for each gassing condition is shown below in Figure 46.

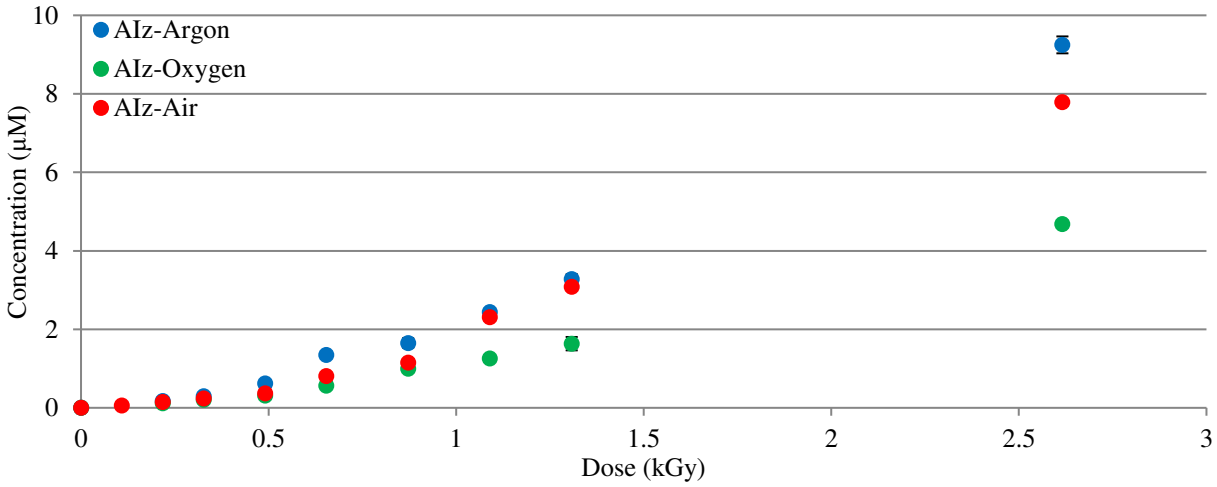

Figure 46: Dose dependence curve for AIz formation for DNA solutions X-irradiated in the presence of 100 mM NaBr and 10 mM $K_2S_2O_8$, saturated with argon, oxygen, or air

It must also be stated that the formation of 8-oxo-G (a proposed precursor to Iz) by dibromide radical anions was also suppressed in oxygenated solutions as compared to deoxygenated DNA solutions.[79] This provides evidence for the hypothesis that guanine is first oxidized into 8-oxo-G, which then is further oxidized into Iz.

The Effect of Pre-Oxidized DNA on the Production of Iz

Several studies have proposed Iz to be one of the major products of further oxidation of 8-oxo-G by various oxidants including superoxide, singlet oxygen, peroxynitrite, and by DNA photooxidation in the presence of photosensitizers.[55-58] Kino and Sugiyama provided experimental evidence that Iz is produced from 8-oxo-G by photooxdiation of double-stranded oligonucleotides containing 8-oxo-G lesions linked to anthraquinone as a photosensitizer.[58] Despite this evidence, mechanistic aspects of this pathway remain unknown.

However, experimental data of the Roginskaya research group indicate that 8-oxo-G is not necessarily a major precursor of Iz. Iz accumulates linearly during DNA oxidation by the majority of OEOs employed in this study except for the dibromide radical anions produced in the absence superoxide. In the meantime, as Derrick Ampadu-Boateng showed in his Masters thesis research, the kinetic curve of 8-oxo-G accumulation by all OEOs he studied has a sigmoid shape, with fast accumulation of 8-oxo-G during the initial period of its formation and a steady-state period during later times.[79] As shown in Roginskaya *et al.'s* recent publications, 8-oxo-G is a dominant product generated in ST DNA by sulfate and carbonate radical anions, with the relative ratio of [8-oxo-G]: [FBR] = 6.8 for $SO_4^{\bullet-}$ [59] and [8-oxo-G]: [FBR] ~ 2 x 10^3 for $CO_3^{\bullet-}$.[102] Thus, one can assume formation of 8-oxo-G in high concentration during the initial period of the oxidation reaction, which, in turn, increases the rate of formation of further products.

In order to test the hypothesis that 8-oxo-G is **not** a major precursor to AIz, DNA was pre-oxidized to first form DNA containing 8-oxo-G ("Ox-DNA"). Solutions containing DNA and 10 mM NaBr were X-rayed for 3 kGy. The choice of the X-ray dose was based on its location in the middle of the plateau in the dose-response curve of 8-oxo-G by dibromide radical anions so reproducible results can be expected at this dose.[79] This Ox-DNA can then be treated along with control ('Ctrl-DNA') to compare the amount of AIz, FBR, and Lac produced. Both pre-oxidized and control samples of ST DNA were treated with 100 mM NaBr (to produce $Br_2^{\bullet-}$) or without (to produce $^{\bullet}OH$).

The kinetic curves of formation of AIz can provide information on mechanism of formation of AIz when considering two different possible scenarios:

(i) Iz is formed predominately from 8-oxo-G. In this mechanism, $G^{\bullet+}$ or $G^{\bullet}$ are converted to the intermediate 8-oxo-G which then can generate many different products, including Iz.

In this scenario, a dose-dependence curve of formation of AIz from pre-oxidized DNA is expected to have a linear shape, as shown below in Figure 47a. Non-zero initial concentrations of AIz can be expected because of the presence of pre-formed Iz as an immediate precursor to AIz as well as pre-formed 8-oxo-G as a precursor to Iz.

(ii) 8-oxo-G does not play a significant role as Iz precursor. In this mechanism, Iz is formed from another precursor, which, in turn, is an intermediate product of oxidation of guanine. Then a dose-dependence curve of formation of AIz from pre-oxidized DNA is expected to have a lag period as shown in Figure 47b. Non-zero initial concentrations of AIz are still expected because of the presence of pre-formed Iz as an immediate precursor to AIz plus possibly the presence of a yet unknown precursor accumulated during the pre-oxidation step.

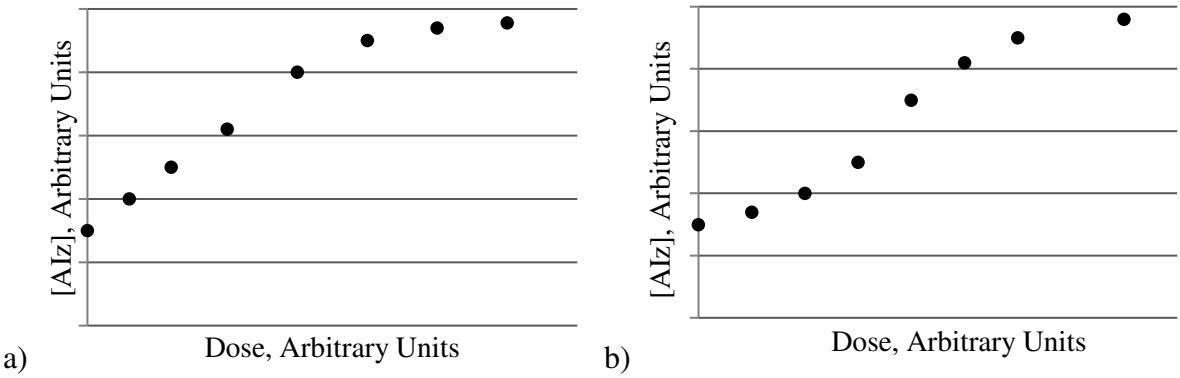

Figure 47: Theoretical kinetic curves for the mechanisms of a) 8-oxo-G is a precursor to Iz and b) 8-oxo-G is not a precursor to Iz

Pre-oxidized DNA X-irradiated in the presence of 100 mM NaBr

Pre-oxidized and control samples of ST DNA were X-irradiated in the presence of 100 mM NaBr (to produce $Br_2^{\bullet-}$). The dose response curves for AIz production for both sets of samples are shown below in Figure 48.

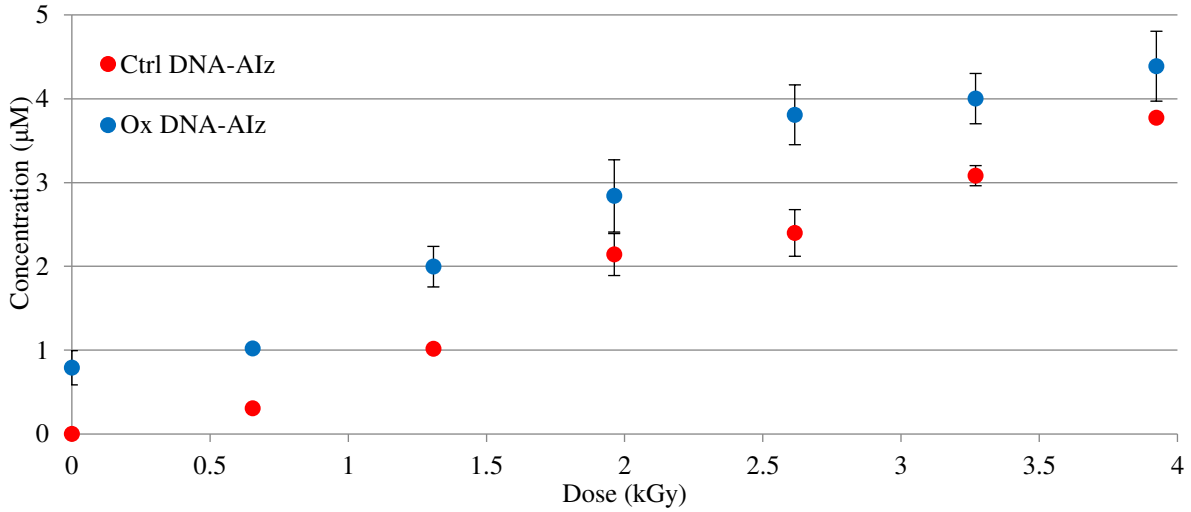

Figure 48: Dose dependence curve for AIz formation for control (Ctrl-DNA) and pre-oxidized (Ox-DNA) DNA solutions X-irradiated in the presence of 100 mM NaBr

As expected, the Ox-DNA samples show a non-zero initial concentration of AIz at a dose of 0 kGy due to the accumulation of Iz lesions during the production of the pre-oxidized DNA, which is then released during heat treatment with EA. Both kinetic curves of AIz production in the Ox-DNA and Ctrl-DNA samples have pronounced lag periods. Furthermore, the shapes of both kinetic curves are very similar to each other and to the S-shaped curve described in hypothesis ii (8-oxo-G is NOT a precursor to Iz). This indicates that AIz is likely formed from the same mechanisms in both control and pre-oxidized DNA.

Pre-oxidized DNA Treated without NaBr

Pre-oxidized and control samples of ST DNA were X-irradiated without NaBr (to produce $^{\bullet}OH$). The dose response curves for AIz production for both sets of samples are shown below in Figure 49. Again, as in the case with the reaction of pre-oxidized and control DNA with $Br_2^{\bullet-}$, both dose dependence curves for the Ox-DNA and Ctrl-DNA samples have similar shapes and show a lag period. As expected, initial concentration of AIz in Ox-DNA samples for this series of experiments is about the same as for the series with $Br_2^{\bullet-}$.

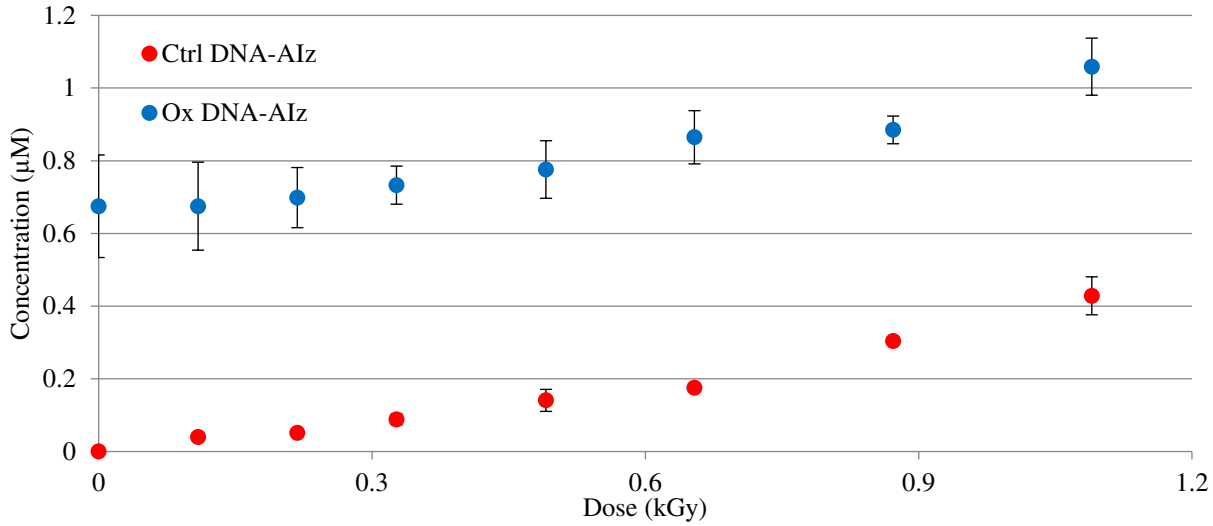

Figure 49: Dose dependence curve for AIz formation for control (Ctrl-DNA) and pre-oxidized (Ox-DNA) DNA solutions X-irradiated in the absence of NaBr

The kinetic curves for AIz formation of Ox-DNA solutions containing $^{\bullet}OH$ have a less pronounced S-shaped curve when compared to solutions containing $Br_2^{\bullet-}$. Since significantly lower doses are required for formation of AIz by the hydroxyl radicals than by the dibromide radical anions, kinetic curves in the case of $^{\bullet}OH$ do not reach the plateau state. It has already been proposed that Iz is formed via a different mechanism by $^{\bullet}OH$ and $Br_2^{\bullet-}$. Nonetheless, they

both appear to be the result of a sequential reaction A → B → C, where A is guanine, C is Iz, and B is an unknown intermediate. One likely mechanism of Iz formation for the $^{\bullet}OH$ system involves the reaction of the guanine radical with molecular oxygen, which seems reasonable, as the mechanism of Iz formation in the $^{\bullet}OH$ system is absolutely oxygen-dependent. The mechanism of Iz formation in the $Br_2^{\bullet-}$ system (and in the case of other OEOs) remains unknown and requires further investigation.

CHAPTER 4

CONCLUSIONS

Damage to the DNA molecule due to oxidative stress has been a major area of study over the last several decades. The focus of previous research has been primarily directed towards the reactions of DNA with hydroxyl radicals, as they are the most reactive and biologically relevant ROS. However, recent studies of DNA oxidation have indicated that reactions of OEOs with guanine produce significant amounts of oxidative damage products, thus shifting the focus to these reactions and away from hydroxyl radicals. While 8-oxo-G has primarily been studied as an oxidative damage product of guanine and used widely as a biomarker for oxidative stress, there is accumulating evidence that other products of guanine oxidation are also formed in significant quantities. In particular, Iz, a product of $4e^-$ oxidation of guanine in DNA, has been named as one such product. Iz, as well as its hydrolysis product Oz, have the potential to serve as biomarkers of oxidative stress. As 8-oxo-G, Iz, and Oz, are mutagenic, it is important to further understand the mechanism of their formation to predict their potential biological impacts. From the experimental data described in Chapter 3, the following conclusions regarding mechanisms of formation of Iz have been made:

1. Iz is produced in significant quantities in DNA as a result of guanine oxidation and the efficiency of its formation correlates with the reduction potential and selectivity of a given OEO. OEOs studied in the present research include $^{\bullet}OH$ (+1.90 V), $SO_4^{\bullet-}$ (+2.47 V), $SeO_3^{\bullet-}$ (+1.77 V), $Br_2^{\bullet-}$ (+1.60 V), and $N_3^{\bullet}$ (+1.30 V). While hydroxyl radicals have a

large reduction potential and are very reactive, they have very low selectivity towards the production of Iz, with an AIz/FBR~ 0.037. They primarily react through H-abstraction from 2-deoxyribose, as visualized by free base release and production of Lac after treatment with EA. $Br_2^{\bullet-}$ is selective towards the production of Iz with AIz/FBR ~ 7.0 in the X-rayed $Br^-/S_2O_8^{2-}$ solutions. The data in the X-rayed $Br^-/S_2O_8^{2-}$ solutions seem more reliable than in the X-rayed Br^- solutions since in this system the contribution of undesirable free radicals, such as hydroxyl radicals and superoxide, is minimized. Radiolysis of solutions containing selenate or persulfate anions produces a mixture of OEOs ($SeO_3^{\bullet-}$ together with $^{\bullet}OH$ and $SO_4^{\bullet-}$ together with $^{\bullet}OH$, respectively) and therefore the contribution of individual OEOs is unclear. In theory, because the contribution of $^{\bullet}OH$ alone to the yield of AIz is known, the contribution due to the OEO could be estimated using the difference in the radiation chemical yields of OEOs and $^{\bullet}OH$ alone. However, this approach does not account for possible side reactions between OEOs and therefore is only used as an approximation. The approach of generation of $SeO_3^{\bullet-}$ by radiolysis of solutions containing $HSeO_3^-$ turned out to be unsuccessful because a reaction between $HSeO_3^-$ and $^{\bullet}OH$ which results in the formation of $SeO_3^{\bullet-}$ is too slow and results in an incomplete scavenging of $^{\bullet}OH$. $N_3^{\bullet}$ produces essentially no AIz, most likely due to not having a high enough reduction potential to successively oxidize guanine (+1.29 V).

2. Experimental data suggest that formation of Iz is not dependent on superoxide. The formation of superoxide was suppressed through the addition of electron scavengers such as persulfate (for the $Br_2^{\bullet-}$ system) or TCA (for the $^{\bullet}OH$ system), both of which react with the solvated electrons faster than dissolved oxygen present in air-saturated solutions. The absolute yields of AIz for solutions containing Br^- with persulfate (~3.5 nmol/J) were

significantly higher than for the Br^- alone system (~0.70 nmol/J), indicating that superoxide may actually suppress the formation of Iz. Similarly, absolute yields of AIz solutions containing TCA (~2.5 nmol/J) were higher than DNA solutions without TCA (~1.8 nmol/J), although we see a smaller increase when compared to the $Br_2^{\bullet-}$ system. Based on the data collected in this study, it can be concluded that in superoxide-free systems, AIz is still efficiently produced, and therefore Iz formation is not dependent on the presence of $O_2^{\bullet-}$.

3. Experiments were conducted to test whether the formation of Iz is dependent on oxygen for $Br_2^{\bullet-}$ and $^{\bullet}OH$ systems. DNA solutions were saturated with argon gas to purge the solutions from oxygen or saturated with oxygen gas, and then compared to air-saturated solutions (concentration of dissolved oxygen is ~ 0.2 mM at room temperature). As expected, data showed that the hydroxyl radical system is absolutely oxygen dependent as yields of all products drastically decreased in deoxygenated solutions and the production of AIz was practically completely suppressed. The oxygen dependence of the $Br_2^{\bullet-}$ system was reliant on whether or not persulfate was added to the Br^-. Although the formation of Iz was not completely suppressed in solutions containing only Br^-, like in $^{\bullet}OH$ solutions, the relative yields of AIz did decrease when DNA solutions are saturated with argon (~0.3 nmol/J) as compared with those under normal air (~0.62 nmol/J) or saturated with oxygen (~0.67 nmol/J). However, the presence of sugar damage products (FBR and Lac) indicates that a second oxidizing species is present in these solutions which could also be affected by gassing conditions. By comparison, in the persulfate/dibromide system, the yield of AIz increased in deoxygenated solutions (~4.4 nmol/J) as compared to air-saturated solutions (~3.5 nmol/J) and oxygenated solutions

AIz (~2.1 nmol/J), where AIz formation appears to be suppressed. Suppression of AIz formation in solutions saturated with oxygen in this system points to the occurrence of a competing reaction with participation of molecular oxygen, although the mechanism of formation of Iz in dibromide systems still remains unclear. These data strongly support the hypothesis that Iz is formed via different mechanisms when using $Br_2^{\bullet-}$ or $^{\bullet}OH$, where production of Iz by $Br_2^{\bullet-}$ is most likely not dependent on the presence of oxygen (and is possibly even suppressed by its presence), but is absolutely dependent on oxygen when produced by $^{\bullet}OH$-mediated DNA oxidation.

4. A hypothesis that 8-oxo-G, a well-known biomarker of oxidative stress, does not play a significant role as a precursor to Iz has been experimentally tested. "Pre-oxidized" DNA, or Ox-DNA was generated by X-ray radiolysis of DNA solutions containing 100 mM NaBr, which produced ~2.5% 8-oxo-G and ~0.5% Iz in place of guanine, as estimated in our earlier studies. Ox-DNA samples and non-irradiated Ctrl-DNA samples were subjected to further radiolysis in order to compare the kinetics of Iz formation from Ox-DNA and Ctrl-DNA. The two kinetic scenarios: i) 8-oxo-G IS a precursor, and ii) 8-oxo-G is NOT a precursor theoretically correspond to two distinctively different dose dependence curves of Iz formation. Both assume that Iz is a product of a sequential reaction A → B → Iz, where B is an unknown intermediate product, and A is unknown precursor, which can be $G^{\bullet+}$ or $G^{\bullet}$, or one of their products. The first hypothesis, where 8-oxo-G plays the role of B, would produce a sigmoid-shape curve (or linear if saturation is not attained) and the second hypothesis, where some unknown precursor different from 8-oxo-G plays the role of B would produce an S-shaped curve (or a parabola-shaped if saturation is not attained). Experimental data dose response curves for both $Br_2^{\bullet-}$ and $^{\bullet}OH$

systems show S-shaped dose-dependence curves which indicates that mostly likely 8-oxo-G is NOT a major precursor to Iz.

5. One of the possible hypotheses on the mechanism of Iz formation is that it occurs via the pathway initiated by oxidation of the guanine radical by molecular oxygen. This hypothesis seems reasonable at least for the mechanism of formation of Iz in the reaction of DNA with hydroxyl radicals, which is absolutely oxygen-dependent. However, formation of Iz by $Br_2^{\bullet-}$ in the absence of molecular oxygen and, moreover, negative influence on the oxygen presence on the yield of Iz, indicate, that there might be alternative mechanisms of Iz formation. Different shapes of dose response curves for $^{\bullet}OH$ and $Br_2^{\bullet-}$ support the hypothesis that Iz is formed in these systems via different mechanisms.

To summarize, Iz is formed in significant quantities by the reaction of guanine with various OEOs and the mechanism of formation of Iz is appears to be different, at least in the $Br_2^{\bullet-}$ and $^{\bullet}OH$ systems. The mechanism does not appear to be dependent on the presence of superoxide but is dependent on the presence of molecular oxygen, at least in the hydroxyl radical system. One possible mechanism of Iz formation involves the oxidation of guanine by molecular oxygen. The following future works have been proposed which will continue the investigation into these mechanisms:

1. The approach of generation of a number of OEOs by radiolysis of aqueous solutions of DNA in the presence of additives was often complicated by undesirable side reactions as in the case of sulfate radical anions. As it has been experimentally shown by the

Roginskaya research group, photochemical generation of such OEOs as carbonate radical anions[102] and sulfate radical anions[59] provides a cleaner method of production of these reactive species.

2. The dependence of oxygen (though saturation with argon or oxygen gas) on the yield of Iz will be studied more extensively using more OEOs in order to better understand the mechanism of Iz formation.
3. Experiments aimed at detection of intermediate precursors to Iz will be conducted using monomeric Iz (dIz) produced from 2-deoxyguanosine (dG).[80] This method allows for direct quantitative HPLC analysis of Iz itself and its precursors since all these derivatives of dG are low-molecular-weight products as opposed to their analogs in highly polymerized DNA. Intermediate products will be isolated by using a semi-preparative HPLC column and characterized by using LC-MS.

REFERENCES

1. Toyokuni, K; Yodoi, J; Hiai, H. *FEBS Lett.* **1995**, *358,*1-3.
2. Shirley, O; Work, L. *Antioxidants.* **2014**, *3,*472-501.
3. Aoshiba, F; Tsuji, T; Nagai, A. *Eur Respir J.* **2012**, *39,*1368-1376.
4. Gil-Mohapel, J; Brocardo, PS; Christie, BR. *Curr Drug Targets.* **2014**, *15,*454-468.
5. Valko, MM; Cronon, MTD. *Curr. Med Chem.* **2005**, *12,*1161-1208.
6. Xing, SSD; Chen, C; Wang, J; Yu, Z. *Mol Med Rep.* **2014**, *10,*599-604.
7. Finkel, TJ. *J Leukocyte Biol.* **1999**, *65,*337-340.
8. Messner, K.R; Imla, J.A. *J Biol Chem.* **1999**, *277,*42563-42571.
9. Nakamura, Y; Makino, R; Tanaka, T; Isimura, Y; Ohtaki, S. *Biochemistry.* **1991**, *30,*4880-4886.
10. Cadet, JD; Pouget, JP; Ravanat, JL; Sauviago, S. *Curr Probl Dermatol.* **2001**, *29,*62-73.
11. Cook, JA; Gius, D; Wink, DA; Krishna, MC; Russo, A; Mitchell, JB. **2004**, *14,*259-266.
12. Schmidt-Ullrich, RK; Dent, P; Grant, S; Mikkelsen, RB; Valerie, K. *Radiat. Res.***2000**,*153,*245-257.
13. Evans, MD; Dizdaroglu, M; Cooke, MS. *Mutat Res.* **2004**, *567,*1-61.
14. Okada, S *DNA as target molecule responsible for cell killing.*, 1970.
15. von Sonntag, C *The Chemical Basis of Radiation Biology*; Taylor & Francis: London–New York–Philadelphia, 1987.

16. Ishii, T; Yasuda, K; Akatsuka, A; Hino, O; Hatman, PS; Ishii, A. *N Cancer Res.* **2005**, *65,*203-209.

17. Xu, YJ; Kim, EY; Demple, B. *J Biol Chem.* **1998**, *273,*28837-28834.

18. Crespo-Hernandez, CE; Close, DM; Gorb, L; Lexzczynski, J. *J Phys Chem.* **2007**, *111,*5386-5395.

19. Fukuzumi, K; Miyao, H; Ohkubo, K; Suenobu, T. *J Phys Chem.* **2005**, *109,*3285-3294.

20. Symons, MCR. *J Chem Soc, Faraday Trans I.* **1987**,*83,*1.

21. Candeias, LP; Steenken, S. *J Am Chem Soc.* **1993**, *115,*2437.

22. Melvin, T; Botchway, A; Parker, W; O'Neill, P. *J Chem Soc.* **1995**, *653,*

23. Moore, TJ. *Electronic Theses and Dissertations.* **2014**, *2445,*

24. Roginskaya, M; Bernhard, WA; Marion, RT; Razskazovskiy, Y. *Radiat Res.* **2005**, *163,*85-89.

25. Price, CS; Razskazovskiy, Y; Bernhard, WA. *Radiat Res.* **2010**, *174,*645-649.

26. Cai, Z; Sevilla, MD. *Radiat. Res.* **2003**, *159,*411-419.

27. Saito, I; Nakamura, T; Nakatani, K; Yoshioka, Y; Uamaguchi, K; Sugiyama, H. *J Am Chem Soc.***1998**, *120,*12686-12687.

28. Cadet, J; Douki, T; Gasparutto, D; Ravanat, J-L. *Mutat. Res.***2003**,*531,*5-23.

29. Douki, T; Matini, R; Ravamat, J; Turesky, J; Cadet, J. *Carcinogenesis.* **1997**, *18,*2385-2391.

30. Cadet, J; Douki, T; Ravanat, J-L. *Int J Biol Med.* **2010**, *49,*9-21.

31. Raoul, S; Berger, M; Buchko, GW; Joshi, PC; Morin, B; Weinfeld, M; Cadet, J. *J Chem Soc Perkin Trans.* **1996**, *2,*371-381.

32. von Sonntag, C *Free-radical-induced DNA Damage and its repair. A chemical perspective*; Springer-Verlag: Berlin Heidelberg New York, 2010.

33. Candeias, LP; Steenken, S. *J Am Chem Soc.* **1989**, *111,*1094-1099.

34. Shafirovich, V; Dourandin, A; Huang, W; Geacintov, NE. *J Biol Chem.* **2001**, *276,*24621-6.

35. Steenken, S. *Free Radic Res Commun.* **1992**, *16,*349-379.

36. Close, DM; Nelson, WH; Bernhard, WA. *J Phys Chem A.* **2013**, *117,*12608-12615.

37. Cadet, J; Wagner, JR; Shavirovich, V; Geacintov, NE. *Int J Radiat Biol.* **2014**, *90,*423–432.

38. Jackson, JH; Schraufstatter, IU; Hyslop, PA; Vosbeck, K; Sauerheber, R; Weitzman, SA; Cochrane, CG. *J Clin Invest.* **1987**, *80,*1090-1095.

39. Chen, Q; Marsh, J; Ames, B; Mossman, B. *Carcinogenesis.* **1996**, *17,*2525-2527.

40. Valavanidis, A; Vlachogianni, T; Fiotakis, C. *J Environ Sci Health C Environ Carcinog Ecotoxicol Rev.* **2009**, *27,*120-139.

41. Pope III, CA; Burnett, RT; Thun, MJ; Calle, EE; Krewski, D; Ito, K; Thurston, GD. *J Am Med Assoc.* **2002**, *287,*1132-1141.

42. Misiaszek, R; Crean, C; Joffe, A; Geacintov, NE; Shafirovich, V. *J Biol Chem.* **2004**, *279,*32106-32115.

43. Fridovich, I. *Annu Rev Biochem.* **1995**, *64,*97-112.

44. Fridovich, I. *J Biol Chem.* **1997**, *272,*18515-18517.

45. Valentine, J; Hart, P; Gralla, E. *Adv Exp Med Biol.* **1999**, *448,*193-203.

46. Buxton, GV; Greenstock, CL; Helman, WP; Ross, AB. *J Phys Chem Ref. Data.* **1988**, *17,*513-886.

47. Cadet, J; Douki, T; Ravanat, J; Di Mascio, P. *Photochem Photobiol Sci.* **2009**, *8,*903-311.

48. Cadet, J; Di Mascio, P. *Peroxides in biological systems. Functional Groups in Organic Chemistry - The Chemistry of Peroxides*; Wiley and Sons: New York, 2006; Vol. 2.

49. Cadet, J; Douki, T; Sage, E. *Mutat Res.* **2005**, *571,*3-17.

50. Cadet, J; Ravanat, J; Martinez, G; Medeiros, M; Di Mascio, P. *Photochem Photobiol.* **2006**, *82,*1219-1225.

51. Neeley, WL; Essigmann, JM. *Chem Res Toxicol.* **2006**, *19,*491–450.

52. Suzuki, T; Friesen, MD; Oshima, H. *Bioorg Med Chem.* **2003**, *11,*2157-2162.

53. Vialas, C; Pratviel, G; Claparols, C; Meunier, B. *J Am Chem Soc.* **1998**, *120,*11548-11553.

54. Cadet, J; Berger, M; Buchko, GW; Joshi, PC; Raoul, S; Ravanat, J-L. *J Am Chem Soc.* **1994**, *116,*7403-7404.

55. Raoul, S; Cadet, J. *J Am Chem Soc.* **1996**, *118,*1892–1898.

56. Yu, H; Venkatarangan, L; Wishnok, JS; Tannenbaum, SR. *Chem Res Toxicol.* **2005**, *18,*1849–1857.

57. Matter, B; Malejka-Giganti, D; Csallani, AS; Tretyakova, N. *Nuc Acids Res.* **2006**, *34,*5449–5460.

58. Kino, K; Sugiyama, H. *Chem Biol.* **2001**, *8,*369-378.

59. Roginskaya, M; Mohseni, R; Ampadu-Boateng, D; Razskazovskiy, Y. *Free Rad Res.* **2016**, *50,*756-766.

60. Giaretti, W; Rapallo, A; Geido, E; Scuitto, A; Merlo, F; Risio, M; Rossini, FP. *Am J Pathol.* **1998**, *153,*1201-1209.

61. Moerkerk, P; Arend, JW; van Driel, M; de Brune, A; de Geoji, A; ten Kate, J. *Cancer Res.* **1994**, *54,*3376-3378.

62. Grollman, AP; Moriya, M. *Trends Genet.* **1993**, *9,*246-249.

63. Henderson, PT; Delaney, JC; Gu, F; Tannenbaum, SR; Essigmann, JM. *Biochem.* **2002**, *41,*914–921.

64. Duarte, V; Gasparutto, D; Jaquinod, M; Cadet, J. *Nuc Acids Res.* **2000**, *28,*1555–1563.

65. Kino, K; Sugasawa, K; Mizuno, T; Bando, T; Sugiyama, H; Akita, M; Miyazawa, H; Hanaoka, F. *Chem Bio Chem.* **2009**, *10,*

66. Pilger, A; Ivancsits, S; Germadnik, D; Rudiger, HW. *J Chromatogr B Analyt Technol Biomed Life Sci.* **2002**, *778,*393-401.

67. Chiou, CC; Chang, PY; Chan, EC; Wu, TL; Tsao, KC; Wu, JT. *Clin Chim Acta.* **2003**, *334,*87-94.

68. Cooke, MS; Evans, MD; Dove, R; Rozalski, R; Gackowski, D; Siomek, A; Lunec, J; Olinski, R. *Mutat Res.* **2005**, *574,*58-66.

69. Weimann, A; Belling, D; Poulsen, HE. *Nucleic Acids Res.* **2002**, *30,*E7.

70. Holmberg, I; Stal, P; Hamberg, M. *Free Radic Biol Med.* **1999**, *26,*129-135.

71. Dizdaroglu, M; von Sonntag, C; Schulte-Frohlinde, D. *J Am Chem Soc.* **1975**, *97,*2277-2278.

72. Roginskaya, M; Mohseni, R; Moore, TJ; Bernhard, WA; Razskazovskiy, Y. *Radiat Res.* **2014**, *181,*131-134.

73. Aso, M; Kondo, M; Suemune, H; Hecht, SM. *J Am Chem Soc.* **1999**, *121,*9023-9033.

74. Scheffold, R; Dubs, P. *Helv Chim Acta.* **1967**, *50,*798-808.

75. Kasai, H. *J Rad Res.* **2003**, *44,*185-189.

76. Cooke, MJ; Evan, SM. *Free Rad Biol Med.* **2002**, *33,*1601-1614.

77. Dizdaroglu, M; Jaruga, P; Birincioglu, M; Rogrinquez, H. *Free Rad Biol Med.* **2002**, *32,*1102-1115.

78. Serrano, J; Palmeria, C; Wallace, K; Kuehl, D. *Rapid Comm Mass Spect.* **1996**, *10,*1789-1791.

79. Ampadu Boateng, D. *Electronic Theses and Dessertations.* **2014**, *2314,*

80. Roginskaya, M; Janson, H; Seneviratne, D; Razskazovskiy, Y. *Res Chem Intermed.* **2017**, *43,*1543-1555.

81. Gligorovski, S; Strekowski, R; Barbati, S; Vione, D. *Am Chem Soc.* **2015**, *115,*13051-13092.

82. Zehavi, D; Rabani, J. *J Phys Chem.* **1972**, *76,*312-319.

83. Matthews, RW; Mahlman, HA; Sworski, TJ. *J Phys Chem.* **1970**, *74,*2475-2479.

84. Klaning, UK; Sehested, K. *J Phys Chem.* **1986**, *90,*5460-5464.

85. Motohashi, N; Saito, Y. *Chem and Pharm Bull.* **1993**, *41,*1842-1945.

86. Neta, P; Huie, R; Ross, A. *J Phys Chem.* **1988**, *17,*1027-1284.

87. Shafirovich, V; Young, A; Durandin, A; Dedon, P; Geacintov, N. *J Phys Chem B.* **2008**, *112,* 1834-1844.

88. Crean, C; Lee, YA; Yun, BH; Geacintov, NE; Shafirovich, V. *Chembiochem.* **2008**, *9,*1985-91.

89. Tam, T; Leung-Toung, R; Li, W; Wang, Y; Karimian, K; Spino, M. *Curr Med Chem.* **2003**, *10,*983-995.

90. Zastawny, T; Altmann, S; Randerseichhorn, L; Madurawe, R; Lumpkin, J; Dizdaroglu, M; Rao, G. *Free Rad Biol Med.* **1995**, *18,*1013-1022.

91. Brezova, V; Valko, M; Breza, M; Morris, H; Telser, J; Dvoranova, D; Kaiserova, K; Varecka, L; Mazur, M; Leibfritz, D. *J Phys Chem B.* **2003**, *107,*2415-2425.

92. Elliot, AJ; McCracken, DR; Buxton, GV; Wood, ND. *J Chem Soc.* **1990**, *86,*1539-1547.

93. Lee, PC; Rodgers, MA. *Photochem. Photobiol.* **1987**, *45,*76-86.

94. Redpath, J; Willson, R. *Int. J Radiat Bio Relat Stud Phys Chem Me.* **1975**, *27,*389-398.

95. Houston, P *Chemical Kinetics and Reaction Dynamics*; Dover Publications, 2012.

96. Hayon, E; Treinin, A; Wilf, J. *J Am Chem Soc.* **1972**, *94,*47-57.

97. Chulkov, V; Kartasheva, L; Pikaev, A. *High Energy Chem.* **1995**, *29,*11-14.

98. Tamba, M; Badiello, R. *Radiat Phys Chem.* **1977**, *10,*283-288.

99. Whillians, D; Adams, G. *Int J Radiat Biol Relat Stud Phys Chem Me.* **1975**, *28,*501-510.

100. Anbar, M; Hart, E. *J. Phys. Chem.***1965**, *69,*271-274.

101. Maruthamuthu, P; Padmaja, S; Huie, RE. *Int J Chem Kinet.* **1995**, *27,*605-612.

102. Roginskaya, M; Moore, TJ; Ampadu-Boateng, D; Razskazovskiy, Y. *Free Radic Res.* **2015**, *49,*1431-1437.

APPENDIX

Plotting Data and Statistical Analyses

Table A.1 LMP Data for X-Irradiated DNA Solutions

Dose (kGy)	[AIz], μM			Mean	SD	SEM
0	0	0	0	0	0	0
0.109	0.261491	0.1121719	0.0830362	0.152233033	0.078167341	0.045129935
0.218	0.3957354	0.2312653	0.3253214	0.3174407	0.08223505	0.047478428
0.327	0.7294062	0.3639074	0.4583232	0.517212267	0.154915643	0.089440588
0.4905	1.1040719	0.4513363	1.0305732	0.8619938	0.291924878	0.168542907
0.654	1.0547712	0.6783942	1.3704352	1.034533533	0.282886737	0.163324734

Dose (kGy)	[Lac], μM			Mean	SD	SEM
0	0	0	0	0	0	0
0.109	3.3652	2.00737	1.3661396	2.246236533	0.833408078	0.481168378
0.218	4.5962052	3.5148104	4.6314176	4.247477733	0.518273444	0.299225312
0.327	8.7094572	4.8182708	5.9995312	6.5090864	1.628919432	0.940457073
0.4905	10.1494432	5.5745572	11.544516	9.089505467	2.549863136	1.472164168
0.654	9.6293788	7.3662536	14.544056	10.51322947	2.996231614	1.729875129

Dose (kGy)	[FBR], μM			Mean	SD	SEM
0	0	0	0	0	0	0
0.109	6.726278	6.1939418	4.690213	5.870144267	0.862177013	0.497778131
0.218	9.6821832	10.7330768	9.0796304	9.831630133	0.92111194	0.531804226
0.327	17.935348	15.0713736	11.9367134	14.981145	2.577761314	1.488271189
0.4905	23.732985	18.4078746	21.376766	21.17254187	2.178758181	1.257906622
0.654	26.0597054	24.2190678	26.8995718	25.726115	1.1194455	0.646312161

Table A.2 LMP Data for X-Irradiated DNA Solutions Containing 100 mM NaBr

Dose (kGy)	[AIz],µM						Mean	SD	SEM
0	0	0	0			0	0	0	0
0.654	0.397196	0.3458243	ND	ND	ND	0.1453079	0.2961094	0.10867561	0.062743892
1.308	0.8501128	0.7085654	ND	ND	ND	0.4826193	0.6804325	0.151341695	0.087377169
1.962	1.1415025	ND	0.6733366	0.5823434	0.4470199	0.8235386	0.7335482	0.237954524	0.106416498
2.616	2.2984067	ND	ND	ND	ND	1.1150373	1.706722	0.5916847	0.418384264
3.924	ND	3.8692929	ND	ND	ND	2.051271	2.96028195	0.90901095	0.642767807

Dose (kGy)	[Lac], µM						Mean	SD	SEM
0	0	0	0	ND	ND	0	0	0	0
0.654	0.0879652	0.176908	ND	ND	ND	0	0.088291067	0.072222756	0.041697828
1.308	0.6139516	0.310764	ND	ND	ND	0	0.308238533	0.250651053	0.144713453
1.962	1.1635132	ND	0.246186	0.2221784	0.178882	0.2326124	0.4086744	0.378091848	0.169087815
2.616	1.2064712	ND	ND	ND	ND	0.4264968	0.816484	0.3899872	0.275762594
3.924	ND	1.2367768	ND	ND	ND	1.9421904	1.5894836	0.650606559	0.290960098

Dose (kGy)	[FBR], µM					Mean	SD	SEM
0	0	0	0	ND	0	0	0	0
0.654	0.9122418	0.6662928	ND	ND	0.1891624	0.589232333	0.36764751	0.259966047
1.308	2.179455	1.461152	ND	ND	0.519302	1.386636333	0.679799693	0.480690973
1.962	4.0735174	ND	1.0884294	0.9909734	1.2139864	1.84172665	1.29094787	0.645473935
2.616	4.1546932	ND	ND	ND	1.2284716	2.6915824	1.4631108	1.034575568
3.924	ND	3.9291102	ND	ND	6.7071684	5.3181393	1.3890291	0.982191896

Table A.3 LMP Data for X-Irradiated DNA Solutions Containing 100 mM NaBr and 10 mM $K_2S_2O_8$

Dose	[AIz], μM		Mean	SD	SEM
0	0	ND	0	0	0
0.109	0.0618248	ND	0.0618248	0	0
0.218	0.1374817	0.167141	0.15231135	0.01482965	0.010486146
0.327	0.243179	0.237424	0.2403015	0.0028775	0.0020347
0.4905	0.3296923	0.404455	0.36707365	0.03738135	0.026432606
0.654	0.7673273	0.847028	0.80717765	0.03985035	0.028178453
0.872	1.0698786	1.2304465	1.15016255	0.08028395	0.056769325
1.09	2.3685046	2.2533788	2.3109417	0.0575629	0.040703117
1.308	3.0231041	3.140617	3.08186055	0.05875645	0.041547084
2.616	ND	7.7880173	7.7880173	0	0

Dose	[FBR], μM		Mean	SD	SEM
0	0	ND	0	0	0
0.109	0.0516528	ND	0.0516528	0	0
0.218	0.1061616	0.079002	0.0925818	0.0135798	0.009602369
0.327	0.1534896	0.099226	0.1263578	0.0271318	0.01918508
0.4905	0.1611328	0.128112	0.1446224	0.0165104	0.011674616
0.654	0.2128672	0.202286	0.2075766	0.0052906	0.003741019
0.872	0.2403528	0.2700008	0.2551768	0.014824	0.010482151
1.09	0.3737824	0.3566464	0.3652144	0.008568	0.006058491
1.308	0.4068576	0.478856	0.4428568	0.0359992	0.025455278
2.616	ND	1.1735712	1.1735712	0	0

Table A.4 LMP Data for X-Irradiated DNA Solutions Containing 100 mM SeO_4^{2-}

Dose	[AIz], µM		Mean	SD	SEM
0	0	0	0	0	0
0.109	0.2337287	0.1783894	0.20605905	0.02766965	0.019565397
0.218	0.5079618	0.6178883	0.56292505	0.05496325	0.038864887
0.327	1.1708671	0.8366404	1.00375375	0.16711335	0.118166983
0.436	1.4498962	1.350837	1.4003666	0.0495296	0.035022716
0.545	1.649933	1.7310944	1.6905137	0.0405807	0.028694888
0.654	1.9953104	1.7845698	1.8899401	0.1053703	0.074508054
0.8175	2.4244652	2.3610708	2.392768	0.0316972	0.022413305
0.981	3.7797385	3.117291	3.44851475	0.33122375	0.23421056

Dose	[Lac], µM		Mean	SD	SEM
0	0	0	0	0	0
0.109	0.8101296	0.9480464	0.879088	0.0689584	0.048760952
0.218	2.65362	3.1303128	2.8919664	0.2383464	0.168536356
0.327	5.2408948	4.1981528	4.7195238	0.521371	0.36866497
0.436	6.860214	5.685684	6.272949	0.587265	0.415259064
0.545	7.661376	8.1000176	7.8806968	0.2193208	0.155083225
0.654	9.1026592	7.3882308	8.245445	0.8572142	0.606141974
0.8175	10.4380044	9.6579736	10.047989	0.3900154	0.275782534
0.981	14.9123856	10.9909124	12.951649	1.9607366	1.386450146

Dose	[FBR], µM		Mean	SD	SEM
0	0	0	0	0	0
0.109	3.1633366	3.0466502	3.1049934	0.0583432	0.041254872
0.218	7.1873856	8.3096566	7.7485211	0.5611355	0.396782717
0.327	13.2849538	10.4645494	11.8747516	1.4102022	0.997163538
0.436	16.7927296	14.9725346	15.8826321	0.9100975	0.643536114
0.545	19.5952728	18.9145548	19.2549138	0.340359	0.240670157
0.654	20.7318072	19.2383258	19.9850665	0.7467407	0.528025413
0.8175	23.8827592	22.1688206	23.0257899	0.8569693	0.605968803
0.981	34.2711942	36.2269156	35.2490549	0.9778607	0.691451932

Table A.5 LMP Data for X-Irradiated DNA Solutions Containing 100 mM $HSeO_3^-$

Dose	[AIz], µM		Mean	SD	SEM
0	0	0	0	0	0
0.327	0.0920505	0.2915205	0.1917855	0.099735	0.070523295
0.654	0.4586829	0.5766972	0.51769005	0.05900715	0.041724356
0.981	0.8918925	0.9357105	0.9138015	0.021909	0.015492002
1.308	1.35814	1.4564907	1.40731535	0.04917535	0.034772223
1.635	1.6144862	1.4061436	1.5103149	0.1041713	0.073660233
1.962	2.6026584	1.9315345	2.26709645	0.33556195	0.23727813

Dose	[Lac], µM		Mean	SD	SEM
0	0	0	0	0	0
0.327	0.1789572	0.4276624	0.3033098	0.1243526	0.087930567
0.654	0.6339924	0.7480896	0.691041	0.0570486	0.040339452
0.981	1.0493784	1.1482476	1.098813	0.0494346	0.034955541
1.308	1.7112136	1.693504	1.7023588	0.0088548	0.006261289
1.635	2.1037952	1.5911192	1.8474572	0.256338	0.181258338
1.962	3.3092888	2.0287832	2.669036	0.6402528	0.452727097

Dose	[FBR], µM		Mean	SD	SEM
0	0	0	0	0	0
0.327	0.5436226	0.9488448	0.7462337	0.2026111	0.143267683
0.654	1.4566514	1.6814962	1.5690738	0.1124224	0.079494641
0.981	2.6570382	2.7452212	2.7011297	0.0440915	0.031177399
1.308	4.0124378	3.8875138	3.9499758	0.062462	0.044167304
1.635	4.845477	4.1361174	4.4907972	0.3546798	0.250796492
1.962	7.123186	5.0379056	6.0805458	1.0426402	0.737257956

Table A.6 LMP Data for X-Irradiated DNA Solutions Containing 200 mM $HSeO_3^-$

Dose	[AIz], µM		Mean	SD	SEM
0	0	0	0	0	0
0.327	0.0342369	0.0433166	0.03877675	0.00453985	0.003210159
0.654	0.1564368	0.1008795	0.12865815	0.02777865	0.019642472
0.981	0.2054432	0.2281261	0.21678465	0.01134145	0.008019616
1.308	0.5979304	0.4810824	0.5395064	0.058424	0.041312007
1.635	0.5335332	0.4872191	0.51037615	0.02315705	0.016374507
1.962	0.7826418	0.8816901	0.83216595	0.04952415	0.035018862

Dose	[Lac], µM		Mean	SD	SEM
0	0	0	0	0	0
0.327	0.19646	0.2059916	0.2012258	0.0047658	0.003369929
0.654	0.4021884	0.2707952	0.3364918	0.0656966	0.046454511
0.981	0.411814	0.4419692	0.4268916	0.0150776	0.010661473
1.308	0.8682968	0.7295528	0.7989248	0.069372	0.049053412
1.635	0.736772	0.7167876	0.7267798	0.0099922	0.007065552
1.962	0.9475952	1.0693816	1.0084884	0.0608932	0.043057995

Dose	[FBR], µM		Mean	SD	SEM
0	0	0	0	0	0
0.327	0.4965444	0.55014	0.5233422	0.0267978	0.018948906
0.654	1.1371404	0.803313	0.9702267	0.1669137	0.118025809
0.981	1.3887846	1.5649136	1.4768491	0.0880645	0.062271005
1.308	3.1048136	2.7019192	2.9033664	0.2014472	0.142444681
1.635	2.9723156	2.9123832	2.9423494	0.0299662	0.021189303
1.962	4.0778986	4.7918832	4.4348909	0.3569923	0.252431676

Table A.7 LMP Data for X-Irradiated DNA Solutions Containing 10 mM $K_2S_2O_9$

Dose	[AIz], µM		Mean	SD	SEM
0	0	0	0	0	0
0.109	ND	0.683267	0.683267	0	0
0.218	ND	1.280325	1.280325	0	0
0.327	2.034845	1.640417	1.837631	0.197214	0.139451
0.491	ND	2.517726	2.517726	0	0
0.654	3.601665	2.817312	3.209489	0.392177	0.277311

Dose	[Lac], µM		Mean	SD	SEM
0	0	0	0	0	0
0.109	ND	1.912261	1.912261	0	0
0.218	ND	3.676904	3.676904	0	0
0.327	5.193124	5.482437	5.337781	0.144657	0.102288
0.491	ND	9.147873	9.147873	0	0
0.654	10.11002	11.10625	10.60814	0.498115	0.352221

Dose	[FBR], µM		Mean	SD	SEM
0	0	0	0	0	0
0.109	ND	4.706322	4.706322	0	0
0.218	ND	9.028298	9.028298	0	0
0.327	12.36959	12.56704	12.46832	0.098726	0.069809
0.491	ND	19.78376	19.78376	0	0
0.654	22.67931	24.997	23.83815	1.158847	0.819428

Table A.8 LMP Data for X-Irradiated DNA Solutions Containing 100 mM NaN_3

Dose	[AIz], µM	[Lac], µM	[FBR], µM
0	0	0	0
0.1308	0	0.202852	0.8945182
0.327	0	0.83472	3.652328

Table A.9 LMP Data for X-Irradiated DNA Solutions Containing 100 mM NaBr, Deoxygenated

Dose	[AIz], µM		Mean	SD	SEM
0	0	0	0	0	0
0.654	0.1177418	0.1070816	0.1124117	0.0053301	0.00376895
1.308	0.2607498	0.327	0.2938749	0.0331251	0.023422983
1.962	0.7404479	0.5139786	0.62721325	0.11323465	0.080068989
2.616	0.879521	0.7263215	0.80292125	0.07659975	0.054164203
3.27	0.8508213	0.6588832	0.75485225	0.6364292	0.450023403
3.924	1.6484833	1.2652938	1.45688855	0.19159475	0.135477947

Dose	[Lac], µM		Mean	SD	SEM
0	0	0	0	0	0
0.654	0.7394416	0.8971924	0.818317	0.0788754	0.05577333
1.308	1.2798288	1.6671464	1.4734876	0.1936588	0.136937451
1.962	1.9000972	2.0231244	1.9616108	0.0615136	0.043496684
2.616	2.7109036	2.68464	2.6977718	0.0131318	0.009285585
3.27	2.515816	2.733144	2.62448	0.108664	0.076837051
3.924	4.8012004	3.7235656	4.262383	0.5388174	0.381001437

Dose	[FBR], µM		Mean	SD	SEM
0	0	0	0	0	0
0.654	1.9348312	1.9279538	1.9313925	0.0034387	0.002431528
1.308	3.7979326	4.6319572	4.2149449	0.4170123	0.294872225
1.962	5.2289244	6.045948	5.6374362	0.4085118	0.288861464
2.616	7.4516812	7.2634746	7.3575779	0.0941033	0.066541082
3.27	7.281299	8.4734572	7.8773781	0.5960791	0.421491574
3.924	12.4092398	11.0657588	11.7374993	0.6717405	0.474992263

Table A.10 LMP Data for X-Irradiated DNA Solutions Containing 100 mM NaBr, Oxygenated

Dose	[AIz], µM		Mean	SD	SEM
0.654	0.3290601	0.4403273	0.3846937	0.0556336	0.039338896
1.308	0.6881061	0.7955256	0.74181585	0.05370975	0.037978528
1.962	1.2044827	1.2634408	1.23396175	0.02947905	0.020844836
2.616	2.0938137	1.7249141	1.9093639	0.1844498	0.130425704
3.27	1.9317416	2.3444483	2.13809495	0.20635335	0.145913853
3.924	3.1011481	2.6236191	2.8623836	0.2387645	0.168831997

Dose	[Lac], µM		Mean	SD	SEM
0.654	0.1588036	0.6727956	0.4157996	0.256996	0.181723614
1.308	0.25004	0.7447244	0.4973822	0.2473422	0.174897347
1.962	0.5650716	0.8447404	0.704906	0.1398344	0.098877852
2.616	0.9745356	0.9519756	0.9632556	0.01128	0.007976164
3.27	1.0042772	1.4856888	1.244983	0.2407058	0.170204703
3.924	1.562374	1.0194864	1.2909302	0.2714438	0.191939752

Dose	[FBR], µM		Mean	SD	SEM
0.654	0.4219614	1.352864	0.8874127	0.4654513	0.329123771
1.308	0.6011834	1.4195884	1.0103859	0.4092025	0.289349863
1.962	1.4289852	1.8819872	1.6554862	0.226501	0.160160393
2.616	2.6655832	2.4008516	2.5332174	0.1323658	0.093596755
3.27	2.959865	3.6724004	3.3161327	0.3562677	0.251919307
3.924	4.2017038	2.8406456	3.5211747	0.6805291	0.481206741

Table A.11 LMP Data for X-Irradiated DNA Solutions Containing 100 mM NaBr and 10 mM $K_2S_2O_8$, Deoxygenated

Dose	[AIz], μM		Mean	SD	SEM
0	0	0	0	0	0
0.218	0.1872075	0.1508778	0.16904265	0.01816485	0.012844489
0.327	0.2955862	0.2992159	0.29740105	0.00181485	0.001283293
0.4905	0.6032932	0.6448658	0.6240795	0.0207863	0.014698134
0.654	1.3931726	1.3024301	1.34780135	0.04537125	0.032082319
0.872	1.3108558	1.652549	1.652549	0.1708466	0.120806789
1.09	2.4841645	2.3985559	2.4413602	0.0428043	0.030267211
1.308	3.4581558	3.0928968	3.2755263	0.1826295	0.129138558
2.616	9.5516482	8.9428069	9.24722755	0.30442065	0.215257906

Dose	[FBR], μM		Mean	SD	SEM
0	0	0	0	0	0
0.218	0.3573944	0.1984648	0.2779296	0.0794648	0.056190099
0.327	0.217192	0.2182936	0.2177428	0.0005508	0.000389474
0.4905	0.4005608	0.3005056	0.3505332	0.0500276	0.035374855
0.654	0.4245376	0.4437952	0.4341664	0.0096288	0.00680859
0.872	0.4812224	0.5390768	0.5101496	0.0289272	0.020454619
1.09	0.7442872	0.7829656	0.7636264	0.0193392	0.013674879
1.308	1.0150632	0.7777432	0.8964032	0.11866	0.083905291
2.616	3.1408248	2.70606	2.9234424	0.2173824	0.153712569

Table A.12 LMP Data for X-Irradiated DNA Solutions Containing 100 mM NaBr and 10 mM $K_2S_2O_8$, Oxygenated

Dose	[AIz], µM		Mean	SD	SEM
0.218	0.0932277	0.1343861	0.1138069	0.0205792	0.014551692
0.327	0.1860085	0.2188066	0.20240755	0.01639905	0.011595879
0.4905	0.3390772	0.2836398	0.3113585	0.0277187	0.019600081
0.654	0.6377699	0.4931051	0.5654375	0.0723324	0.051146731
0.872	1.0214935	0.9785257	1.0000096	0.0214839	0.015191411
1.09	1.3722882	1.1441185	1.25820335	0.11408485	0.080670171
1.308	1.153591	1.6347711	1.6347711	0.24059025	0.170122997
2.616	4.6782473	4.6839807	4.681114	0.0028667	0.002027063

Dose	[FBR], µM		Mean	SD	SEM
0.218	0.2459288	0.2495872	0.247758	0.0018292	0.00129344
0.327	1.8525512	0.1785272	0.1785272	0	0
0.4905	0.2074408	0.332316	0.2698784	0.0624376	0.04415005
0.654	0.2247672	0.2721632	0.2484652	0.023698	0.016757017
0.872	0.3787056	0.3751424	0.376924	0.0017816	0.001259781
1.09	1.2244488	0.4136712	0.4136712	0	0
1.308	1.2674114	0.99467	1.1310407	0.1363707	0.096428647
2.616	2.0473308	1.899316	1.9733234	0.0740074	0.052331134

Table A.13 LMP Data for X-Irradiated DNA Solutions, Deoxygenated

Dose	[AIz], µM		Mean	SD	SEM
0	0	0	0	0	0
0.218	0	0	0	0	0
0.327	0	0	0	0	0
0.4905	0	0	0	0	0
0.654	0.0877777	0.0558407	0.0718092	0.0159685	0.011291435
0.872	0.0454312	0.1074522	0.0764417	0.0310105	0.021927735
1.09	0.0747195	0.097337	0.08602825	0.01130875	0.007996494
1.308	0.0867313	0.112924	0.09982765	0.01309635	0.009260518

Dose	[Lac], µM		Mean	SD	SEM
0	0	0	0	0	0
0.218	1.5744436	0.7511916	1.1628176	0.411626	0.291063536
0.327	0.6536384	0.8208832	0.7372608	0.0836224	0.18095506
0.4905	0.9469748	0.9068556	0.9269152	0.0200596	0.227549154
0.654	1.304626	1.1179608	1.2112934	0.0933326	0.266055997
0.872	0.970268	1.5096964	1.2399822	0.2697142	1.075815521
1.09	1.5488568	1.8052512	1.677054	0.1281972	0.201238489
1.308	1.7571232	1.8779508	1.817537	0.0604138	0.042719008

Dose	[FBR], µM		Mean	SD	SEM
0	0	0	0	0	0
0.218	6.2194132	4.448653	5.3340331	0.8853801	0.626058273
0.327	5.7066244	6.2184426	5.9625335	0.2559091	0.18095506
0.4905	7.9675648	8.611171	8.2893679	0.3218031	0.227549154
0.654	10.4067364	9.6542164	10.0304764	0.37626	0.266055997
0.872	10.0021432	13.045009	11.5235761	1.5214329	1.075815521
1.09	14.481955	15.0511434	14.7665492	0.2845942	0.201238489
1.308	15.6045082	16.4543874	16.0294478	0.4249396	0.300477673

Table A.14 LMP Data for X-Irradiated DNA Solutions, Oxygenated

Dose	[AIz], μM		Mean	SD	SEM
0.218	0.503907	0.4850173	0.49446215	0.00944485	0.006678517
0.327	0.5857333	0.7980326	0.69188295	0.10614965	0.075059137
0.4905	1.0236735	1.1316489	1.0776612	0.0539877	0.038175069
0.654	1.5419358	1.4802854	1.5111106	0.0308252	0.021796708
0.872	1.9003496	2.6928668	2.2966082	0.3962586	0.280197143
1.09	2.7995233	2.7551494	2.77733635	0.02218695	0.015688543
1.308	3.5289077	2.9246553	3.2267815	0.3021262	0.213635485

Dose	[Lac], μM		Mean	SD	SEM
0.218	7.1195412	6.5603916	6.8399664	0.2795748	0.197689237
0.327	8.3869244	9.2912796	8.839102	0.4521776	0.319737847
0.4905	13.0263696	14.1719476	13.5991586	0.572789	0.405022986
0.654	18.0586408	15.2008152	16.629728	1.4289128	1.010393931
0.872	19.9708828	24.0444856	22.0076842	2.0368014	1.440236082
1.09	27.3238072	26.5058004	26.9148038	0.4090034	0.289209078
1.308	28.26815	24.7394088	26.5037794	1.7643706	1.247598416

Dose	[FBR], μM		Mean	SD	SEM
0.218	12.7877234	11.9902746	12.388999	0.3987244	0.281940727
0.327	14.819725	17.528096	16.1739105	1.3541855	0.95755375
0.4905	24.3441712	23.8542678	24.0992195	0.2449517	0.173207008
0.654	30.3056156	27.1243876	28.7150016	1.590614	1.124733946
0.872	33.6671362	41.7748254	37.7209808	4.0538446	2.866501007
1.09	43.1988822	44.2638924	43.7313873	0.5325051	0.376537967
1.308	48.7976968	41.1979496	44.9978232	3.7998736	2.68691639

Table A.15 LMP Data for X-Irradiated DNA Solutions, Not Pre-Oxidized

Dose	[AIz], µM		Mean	SD	SEM
0	0	0	0	0	0
0.109	0.0399376	ND	0.0399376	0	0
0.218	0.0604841	0.0417361	0.0511101	0.009374	0.006628419
0.327	0.109436	0.0674165	0.08842625	0.02100975	0.014856137
0.491	0.1835233	0.0979365	0.1407299	0.0427934	0.030259503
0.654	0.1842209	0.1673586	0.17578975	0.00843115	0.005961723
0.872	0.2917494	0.3159474	0.3038484	0.012099	0.008555285
1.09	0.5022284	0.3545443	0.42838635	0.07384205	0.052214214

Dose	[Lac], µM		Mean	SD	SEM
0	0	0	0	0	0
0.109	0.9837664	ND	0.9837664	0	0
0.218	1.3481856	1.3420756	1.3451306	0.003055	0.002160211
0.327	2.1542168	1.7271936	1.9407052	0.2135116	0.1509755
0.491	3.3249868	2.1165416	2.7207642	0.6042226	0.427249898
0.654	2.9393424	3.536186	3.2377642	0.2984218	0.211016078
0.872	3.8551468	5.5290612	4.692104	0.8369572	0.591818112
1.09	6.349606	5.5572988	5.9534524	0.3961536	0.280122897

Dose	[FBR], µM		Mean	SD	SEM
0	0	0	0	0	0
0.109	1.816824	ND	1.816824	0	0
0.218	2.4956952	2.4087854	2.4522403	0.0434549	0.030727254
0.327	4.0964494	3.4032964	3.7498729	0.3465765	0.245066593
0.491	6.0452248	4.2747112	5.159968	0.8852568	0.625971086
0.654	5.659472	6.4965122	6.0779921	0.4185201	0.295938401
0.872	7.990547	10.7254728	9.3580099	1.3674629	0.96694229
1.09	13.2121884	10.4425138	11.8273511	1.3848373	0.979227846

Table A.16 LMP Data for X-Irradiated DNA Solutions, Pre-Oxidized

Dose	[AIz], μM			Mean	SD	SEM
0	0.6798984	0.3268147	1.0177221	0.674811733	0.282084697	0.162861676
0.109	0.6927604	0.4100035	0.922467	0.675076967	0.209585683	0.12100435
0.218	0.8284545	0.4649504	0.8023708	0.6985919	0.165552313	0.095581673
0.327	0.853252	0.6149562	0.6435905	0.7039329	0.106229707	0.06133175
0.491	0.8154399	0.5917174	0.9205377	0.775898333	0.137121234	0.079166981
0.654	0.6819585	0.7814428	1.0698241	0.844408467	0.164485941	0.094966002
0.872	0.9763457	0.764635	0.8936038	0.878194833	0.087114608	0.050295642
1.09	0.9887172	1.2213341	0.8352452	1.015098833	0.1587202	0.09163715
1.308	1.222108	1.2042211	1.3066593	1.244329467	0.044674686	0.025792942

Dose	[Lac], μM			Mean	SD	SEM
0	0.3626144	0.3503756	0.4439996	0.3856632	0.041551564	0.023989807
0.109	1.0216108	1.0771084	1.0964724	1.065063867	0.031726623	0.018317374
0.218	1.7315552	1.2809004	1.41376	1.4754052	0.189072359	0.109160977
0.327	2.2311088	1.9915592	1.7647372	1.995801733	0.190419041	0.109938484
0.491	3.1374004	1.9177316	2.4054412	2.486857733	0.501244773	0.289393805
0.654	2.7008832	3.5942216	4.1652904	3.4867984	0.602648001	0.347938986
0.872	3.2529076	2.7135168	4.670014	3.545479467	0.825093549	0.476367982
1.09	4.277564	5.9886836	4.2331396	4.833129067	0.817301695	0.471869354
1.308	6.5177908	5.2401052	6.4186396	6.0588452	0.58034997	0.335065211

Dose	[FBR], μM			Mean	SD	SEM
0	0	0.342741	0.1708724	0.171204467	0.139923624	0.069961812
0.109	1.3554006	1.9516724	3.076337	2.127803333	0.713522764	0.41195256
0.218	2.5008196	2.7814338	2.712696	2.664983133	0.119424929	0.059712465
0.327	3.8026778	4.3351388	3.992652	4.043489533	0.220328573	0.110164287
0.491	5.7889322	4.5227372	5.5668776	5.292849	0.552045409	0.318723565
0.654	5.4030342	8.3191358	9.21268	7.64495	1.626703241	0.81335162
0.872	6.358817	7.3198434	11.603137	8.4272658	2.279694621	1.13984731
1.09	9.6096642	15.1733628	11.709704	12.16424367	2.293998003	1.146999002
1.308	13.7050372	14.7037946	15.8430454	14.75062573	0.873466134	0.504295908

Table A.17 LMP Data for X-Irradiated DNA Solutions Containing 100 mM NaBr, Not Pre-Oxidized

Dose	[AIz], μM		Mean	SD	SEM
0	0	0	0	0	0
0.654	0.3054834	ND	0.305483	0	0
1.308	1.0706634	0.9617942	1.0162288	0.0544346	0.038491075
1.962	1.4901281	2.1982466	2.1412069	0.35405925	0.250357697
2.616	2.0056218	2.7922857	2.39895375	0.39333195	0.278127689
3.27	2.9121421	3.2522657	3.0822039	0.1700618	0.120251852
3.924	ND	3.7742667	3.7742667	0	0

Dose	[Lac], μM		Mean	SD	SEM
0	0	0	0	0	0
0.654	0.1377664	ND	0.1377664	0	0
1.308	0.4045196	0.4398072	0.4221634	0.0176438	0.012476051
1.962	0.5092544	0.8623748	0.6858146	0.1765602	0.124846915
2.616	0.5855072	1.13646	0.8609836	0.2754764	0.19479123
3.27	0.8510948	1.2349344	1.0430146	0.1919198	0.135707792
3.924	ND	1.4300972	1.4300972	0	0

Dose	[FBR], μM		Mean	SD	SEM
0	0	0	0	0	0
0.654	0.2033832	ND	0.2033832	0	0
1.308	1.0047902	1.1814184	1.0931043	0.0883141	0.062447499
1.962	1.499815	2.3823148	1.9410649	0.4412499	0.312010796
2.616	1.0027616	2.9171922	1.9599769	1.2399521	0.876778538
3.27	2.2971132	3.4826658	2.8898895	0.5927763	0.419156141
3.924	ND	3.9355428	3.9355428	0	0

Table A.18 LMP Data for X-Irradiated DNA Solutions Containing 100 mM NaBr, Pre-Oxidized

Dose	[AIz], µM		Mean	SD	SEM
0	0.5015526	1.0792417	0.79039715	0.28884455	0.20424394
0.654	1.021112	ND	1.021112	0	0
1.308	1.6542058	2.3389329	1.99656935	0.34236355	0.242087588
1.962	2.2316333	3.4498173	2.8407253	0.609092	0.430693084
2.616	3.3034412	4.312912	3.8081766	0.5047354	0.356901824
3.27	3.576835	4.425727	4.001281	0.424446	0.300128645
3.924	3.798541	4.9776158	4.3880784	0.5895374	0.416865893

Dose	[Lac], µM		Mean	SD	SEM
0	0.4630628	0.7625092	0.612786	0.1497232	0.10587029
0.654	0.671348	ND	0.671348	0	0
1.308	0.6374892	1.1796248	0.908557	0.2710678	0.19167388
1.962	0.8023276	1.636916	1.2196218	0.4172942	0.295071559
2.616	1.277648	1.8889676	1.5833078	0.3056598	0.216134117
3.27	1.1629868	1.925402	1.5441944	0.3812076	0.269554479
3.924	1.3752012	1.9751656	1.6751834	0.2999822	0.212119448

Dose	[FBR], µM		Mean	SD	SEM
0	0	0.537547	0.2687735	0.2687735	0.190051564
0.654	0.8291758	ND	0.8291758	0	0
1.308	1.0375878	1.759446	1.3985169	0.3609291	0.255215414
1.962	1.4360986	2.7447526	2.0904256	0.654327	0.462679059
2.616	2.8203066	3.7036524	3.2619795	0.4416729	0.312309903
3.27	2.5509544	4.303427	3.4271907	0.8762363	0.61959263
3.924	3.73748	5.0425676	4.3900238	0.6525438	0.461418146

VITA

HANNAH CATHERINE JANSON POLLARD

Education	B.A. Chemistry, University of Virginia, Charlottesville, Virginia, 2011 M.S. Chemistry, East Tennessee State University, Johnson City, Tennessee, 2017
Professional Experience	Teacher, Washington County Public Schools, Abingdon, Virginia, 2014-Present Adjunct Faculty, Virginia Highlands Community College Abingdon, Virginia, 2012-Present Teacher, Russell County Public Schools Lebanon, Virginia, 2013-2014
Publication	Roginskaya, M.; Janson, H.; Seneviratne, D.; Razskazovskiy, Y. *Res Chem Intermed*. **2017**, 43: 1543-1555
Honors	Outstanding Graduate Student Award ETSU Chemistry Department, 2017